Supporting Information

Identification and quantification of lignin monomers and oligomers from reductive catalytic fractionation of pine wood with GC × GC - FID/MS

Hang Dao Thi[†,1], Korneel Van Aelst[†,2], Sander Van den Bosch[2], Rui Katahira [,3], Gregg T. Beckham[,3], Bert F. Sels[*,2], Kevin M. Van Geem[*,1]

[1]*Laboratory for Chemical Technology, Ghent University, Technologiepark 121, 9052 Ghent, Belgium.*

[2]*Center for Sustainable Catalysis and Engineering, KU Leuven, Celestijnenlaan 200F, Leuven 3001, Belgium.*

[3]*Renewable Resources and Enabling Sciences Center, National Renewable Energy Laboratory, Golden CO 80401, United States.*

[†]Both authors contributed equally to this manuscript

* Correspondence:

E-mail: kevin.vangeem@ugent.be

E-mail: bert.sels@kuleuven.be

Table of contents

S1. GPC chromatogram and GC × GC - FID color plot of the RCF lignin oil samples.

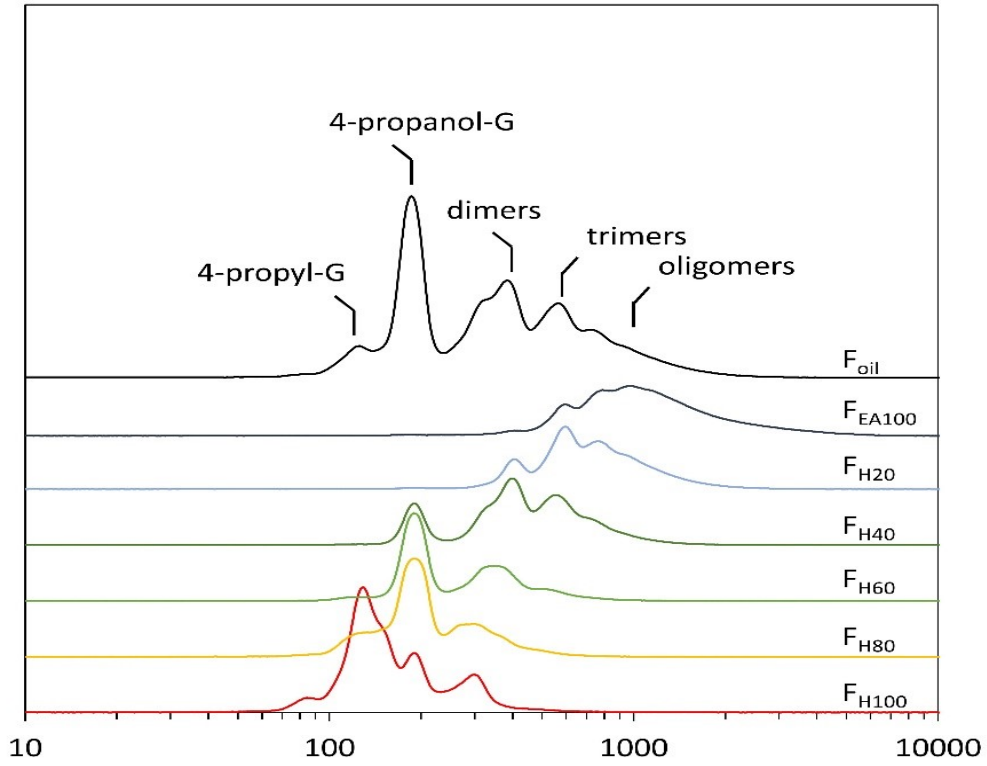

Figure S1.1. GPC chromatogram of the RCF lignin oil samples.

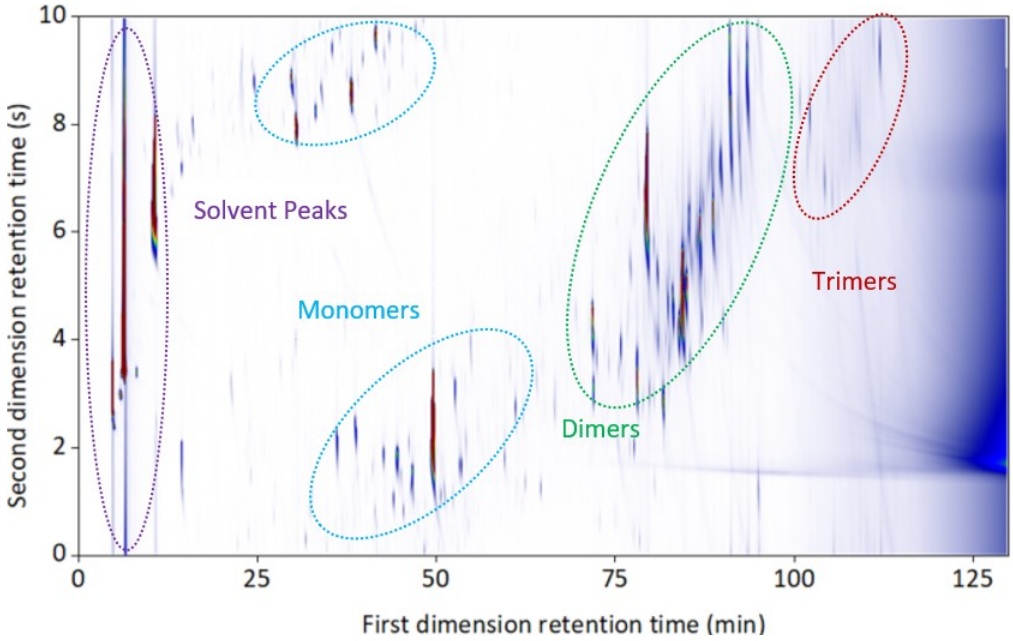

Figure S1.2. GC × GC - FID color plot of the non-derivatized entire lignin oil (Foil).

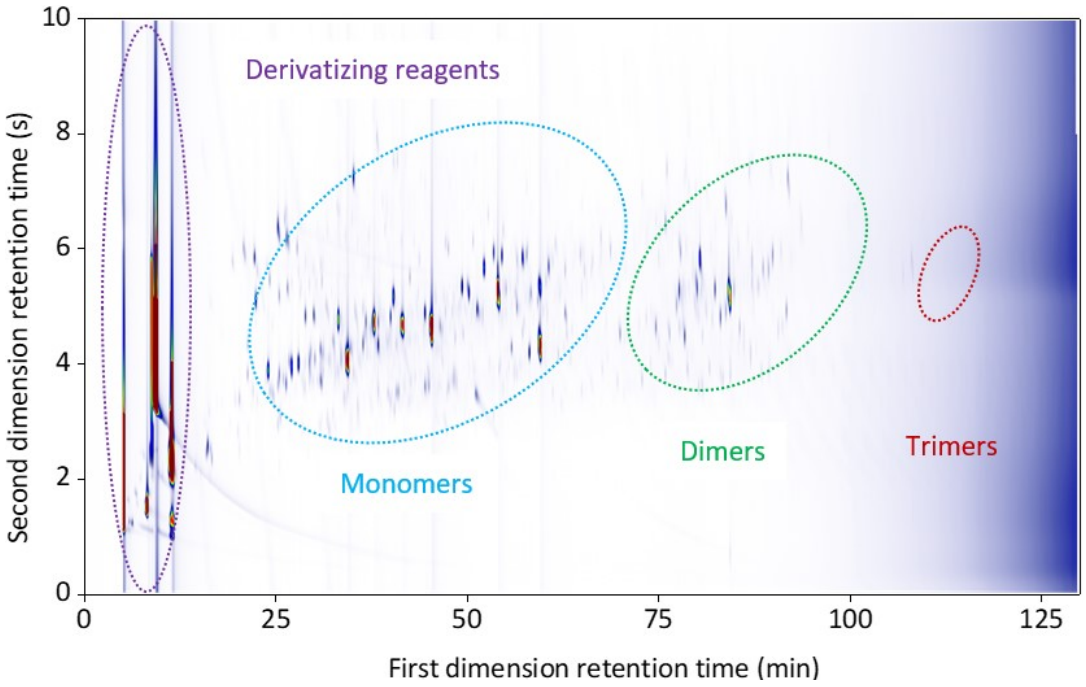

Figure S1.3. GC × GC - FID color plot of the derivatized F_{H100} fraction.

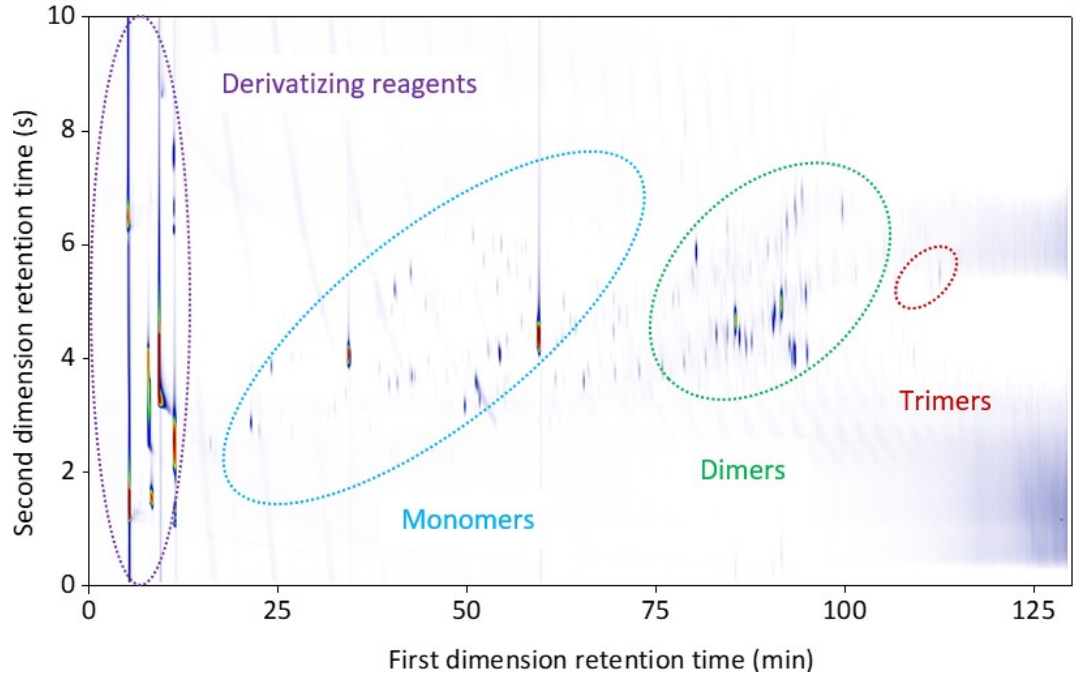

Figure S1.4. GC × GC - FID color plot of the derivatized F_{H60} fraction.

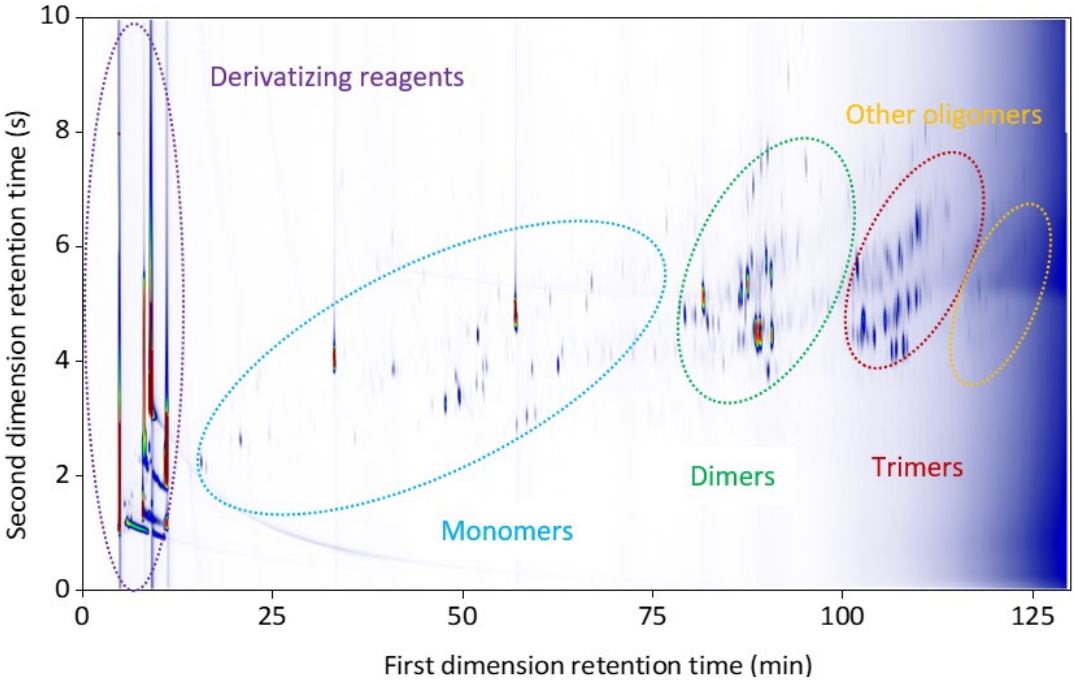

Figure S1.5. GC × GC - FID color plot of the derivatized F_{H20} fraction.

S2. Calculation of the GC-FID relative response factors and quantification of the assigned monomers, dimers, and trimers in the RCF lignin oils fractions

To quantify each of the identified compounds in the seven RCF lignin oil fractions, three known concentrations of calibration mixtures are prepared and analyzed on the GC × GC - FID/MS setup in the same way of actual lignin oil samples. The calibration mixtures consist of 2-phenoxy-1-phenyl ethanol, 1-(4-hydroxyphenyl)-2-phenoxy-1,3-propanediol, 2-(2,6-dimethoxyphenoxy)-1-(4-hydroxy-3-methoxyphenyl)propane-1,3-diol, 4-propanolguaiacol, 2-isopropyl phenol (internal standard), guaiacol, 4-ethylguaiacol, 4-*n*-propylguaiacol, syringol, and isoeugenol.

The relative response factor (RRF) of each component in the calibration mixtures were experimentally calculated as the following equation:

$$RRF = \frac{m_i \times A_{IS}}{m_{IS} \times A_i} \quad (1)$$

where m_i is the mass of the compound i, m_{IS} is the mass of the internal standard, A_i is the peak area of the compound i, and A_{IS} is the peak area of the internal standard.[1-3]

Subsequently, a relationship between experimental RRFs and the molecular weight of molecule i (MW_i), molecular weight of molecule i after derivatization ($MWSi_i$) and the number of carbon (n_C), hydrogen (n_H), oxygen (n_O) atoms, and number of aromatic rings (n_a) in their structure was established via multiple linear regression.

$$RRF_i = f(MW_i, MWSi_i, n_C, n_{Si}, n_H, n_O, n_a) \quad (2)$$

By performing the multiple linear regression, the response factors of the compounds present in the RCF lignin oil samples could be predicted using the following formula:

$$RRF_i = 1.293 - 12.6\ MW_i + 12.594\ MWSi_i + 0.2074\ n_C - 907.2\ n_{Si} - 0.088\ n_H + 0.23\ n_O - 0.492\ n_{Benz} \quad (3)$$

It should be noted that a strong linear relationship between the experimental response factors of the compounds in the calibration mixture and the predicted response factors exists (Equation 3) exemplified by the high coefficient of determination ($R^2 > 0.975$).

To the end, a weight fraction of each compound in the sample is calculated based on the known amount of internal standard using the following equation:

$$wt\%_i = \frac{f_i \times A_i}{f_{IS} \times A_{IS}} wt\%_{IS} \quad (4)$$

where $wt\%_i$ is the weight fraction of compound *i*, $wt\%_{IS}$ is the weight fraction of internal standard, f_i is the relative response factor of compound *i* which is calculated based on equation (3), f_{IS} is the response factor of the internal standard, A_i is peak area of compound *i,* A_{IS} *is* peak area of the internal standard.

Table S2.1. Detailed monomer compositions determined by 2D-GC and 1D-GC* in the RCF lignin oil samples.

	F_{H100}-2D	F_{H100}-1D	F_{H80}-2D	F_{H80}-1D	F_{H60}-2D	F_{H60}-1D	F_{H40}-2D	F_{H40}-1D	F_{H20}-2D	F_{H20}-1D	F_{EA100}-2D	F_{EA100}-1D	F_{oil}-2D	F_{oil}-1D
4-Propanolguaiacol	7,38	6,70	48,89	46,30	51,04	52,80	15,96	14,20	0,50	0,10	0,28	0,00	29,01	28,80
4-Propylguaiacol	19,53	21,10	0,59	0,46	0,00	0,00	0,00	0,00	0,00	0,00	0,00	0,00	2,08	2,50
4-(3-Methoxypropyl)guaiacol	8,02	10,10	2,14	2,80	0,13	0,30	0,30	0,30	0,00	0,00	0,00	0,00	1,19	1,70
4-Ethylguaiacol	3,49	3,80	0,29	0,40	0,06	0,10	0,00	0,00	0,00	0,00	0,00	0,00	0,39	0,50
Isoeugenol	0,34	0,20	0,05	0,20	0,00	0,50	0,02	0,70	0,00	0,00	0,00	0,00	0,04	0,30
4-Methylguaiacol	3,05	3,10	0,43	0,60	0,00	0,10	0,00	0,00	0,00	0,00	0,09	0,00	0,38	0,50
Guaiacol	1,24	0,00	0,19	0,00	0,00	0,00	0,00	0,00	0,00	0,00	0,00	0,00	0,13	0,00
4-Propylsyringol	0,45	0,00	0,30	0,00	0,06	0,00	0,14	0,00	0,00	0,00	0,00	0,00	0,13	0,00
4-Ethylsyringol	0,49	0,00	0,49	0,00	0,06	0,00	0,04	0,00	0,00	0,00	0,00	0,00	0,15	0,00
4-(2-Hydroxyethyl)-2-methoxyphenol	0,00	0,00	0,00	0,00	0,00	0,00	0,09	0,00	0,00	0,00	0,00	0,00	0,33	0,00
Methyl 3-(4-hydroxy-3-methoxyphenyl)propanoate	0,38	0,00	0,32	0,00	0,00	0,00	0,06	0,00	0,00	0,00	0,06	0,00	0,20	0,00
Total	44,37	45,00	53,69	50,76	51,35	53,80	16,61	15,20	0,50	0,10	0,43	0,00	34,03	34,30

* RFs have been determined based on external calibration of the authentic compounds on 1D-GC in our previous study.[4]

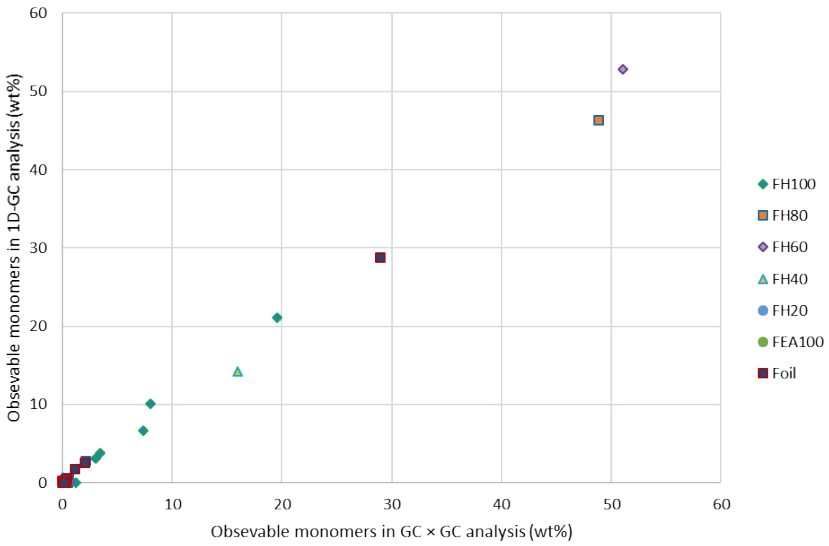

Figure S2.1. Comparison of monomers determined by 2D-GC and 1D-GC

Table S2.2. Composition of monomers, dimers, and trimers in seven RCF lignin oil samples.

	Monomers	**Dimers**	**Trimers**	**Total**
F_{H100}	44,37	5,28	0,46	50,11
F_{H80}	53,69	8,68	0,54	62,91
F_{H60}	51,35	15,68	1,20	68,23
F_{H40}	16,61	33,47	14,55	64,63
F_{H20}	0,50	9,87	22,78	33,15
F_{EA100}	0,43	0,95	8,26	9,64
F_{oil}	34,03	15,79	7,26	57.08
$F_{oil\ mass\ balance}$	34,15	16,50	8,33	58,98

S3. Mass spectrum and proposed fragmentation pathways of dimers

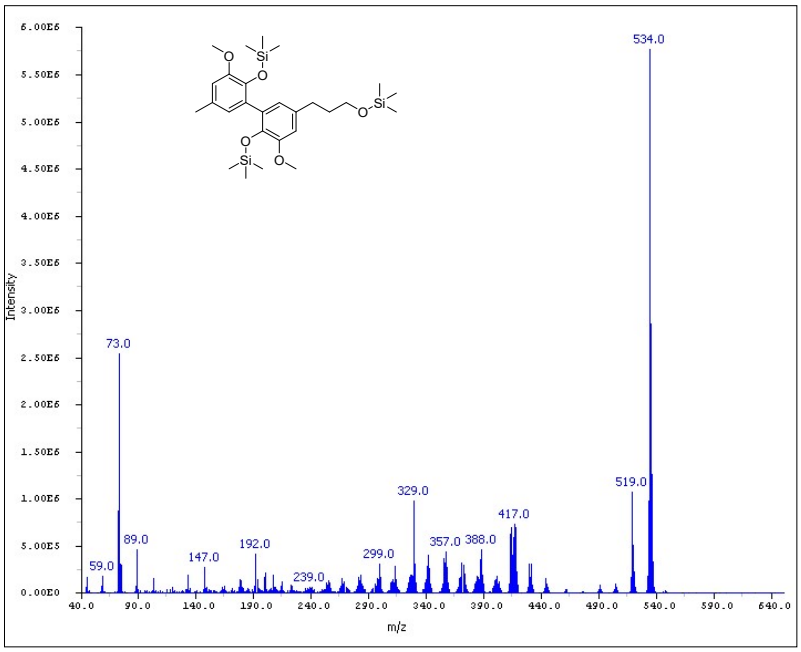

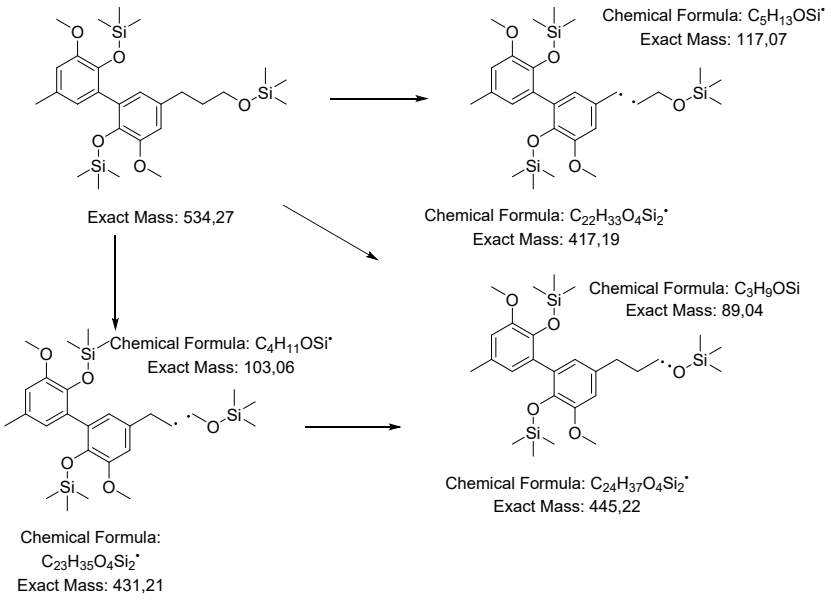

Figure S3.1. Mass spectrum and fragmentation pattern analysis of dimer **D1**.

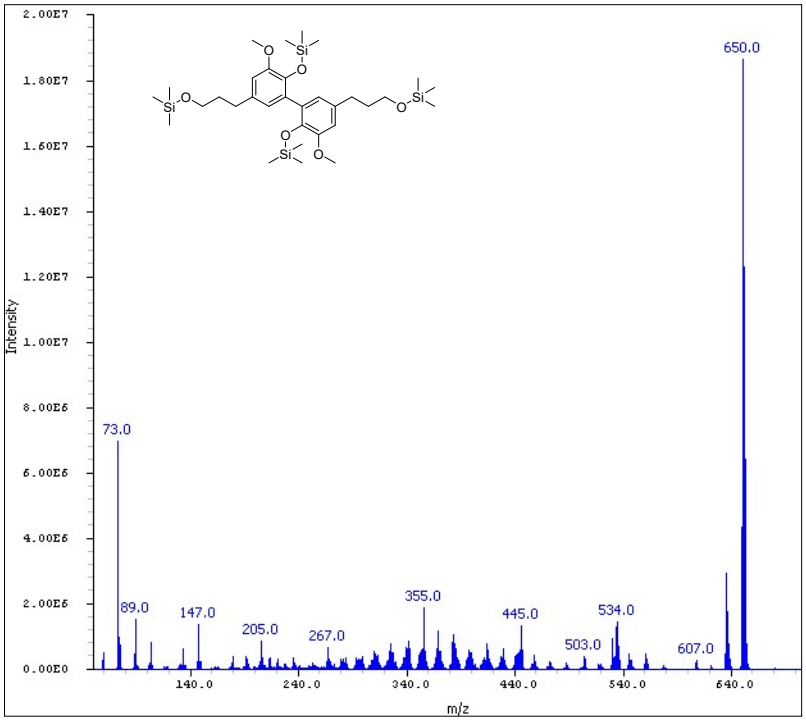

Figure S3.2. Mass spectrum of dimer **D2**.[4]

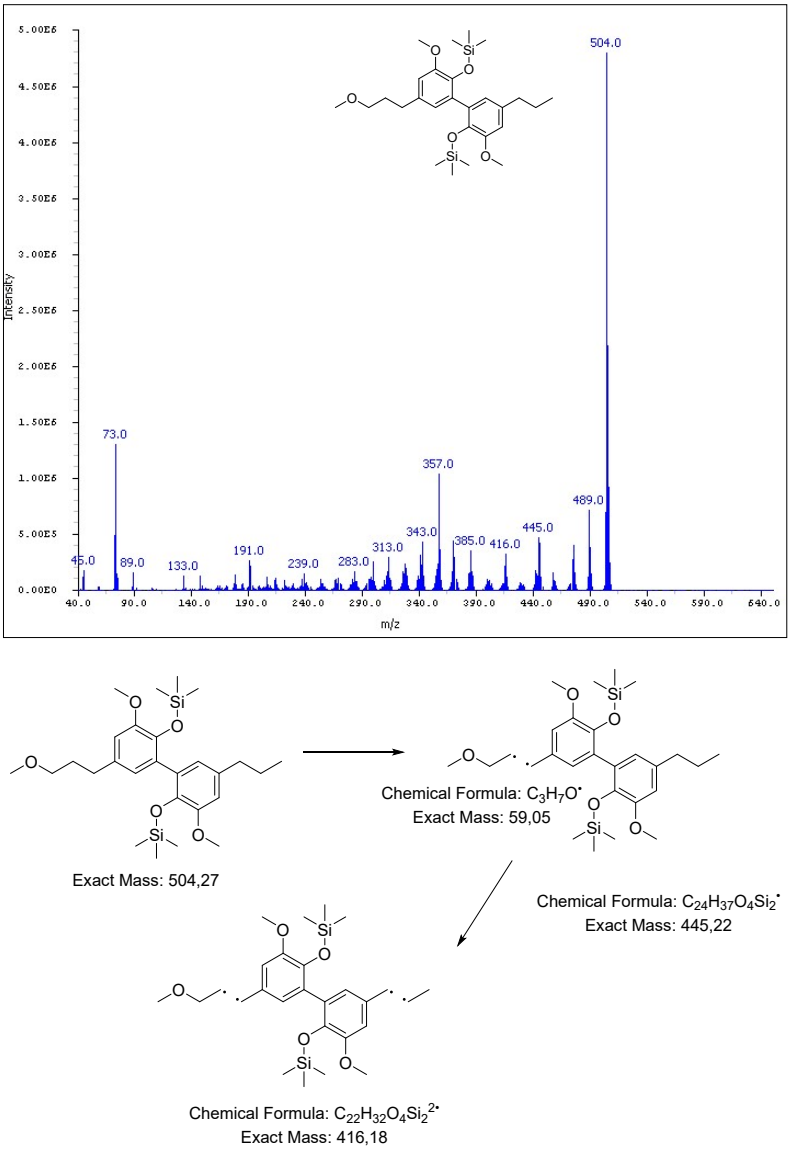

Figure S3.3. Mass spectrum and fragmentation pattern analysis of dimer **D3**.

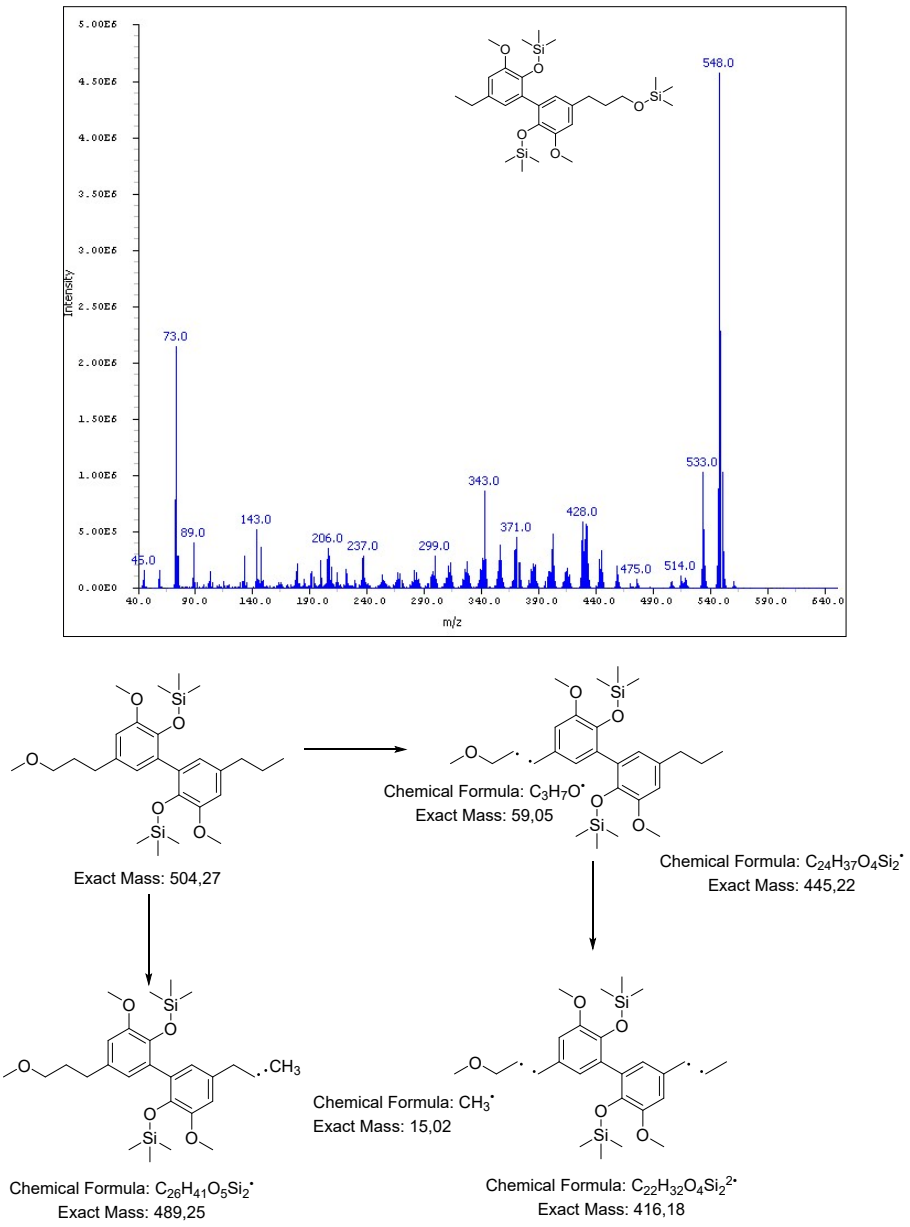

Figure S3.4. Mass spectrum and fragmentation pattern analysis of dimer **D4**.

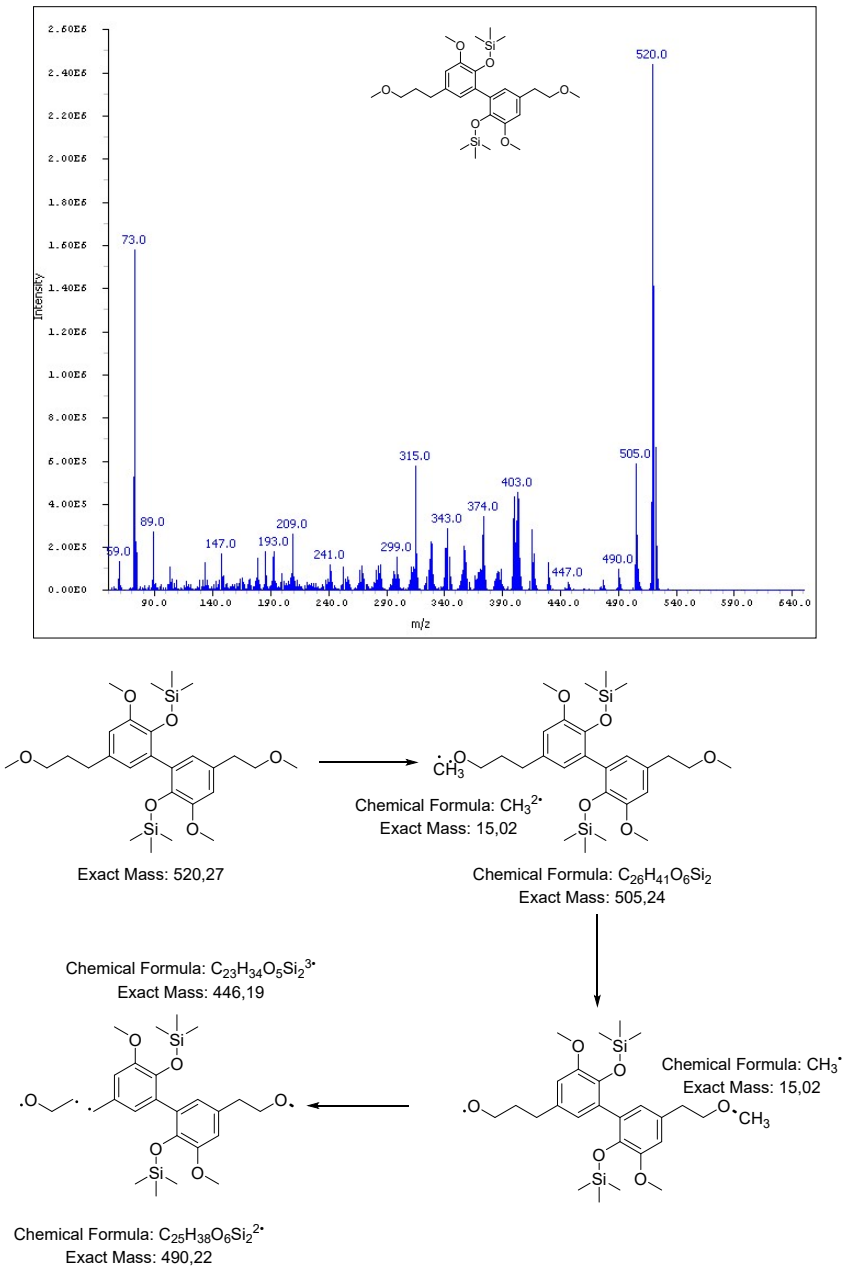

Figure S3.5. Mass spectrum and fragmentation pattern analysis of dimer **D5**.

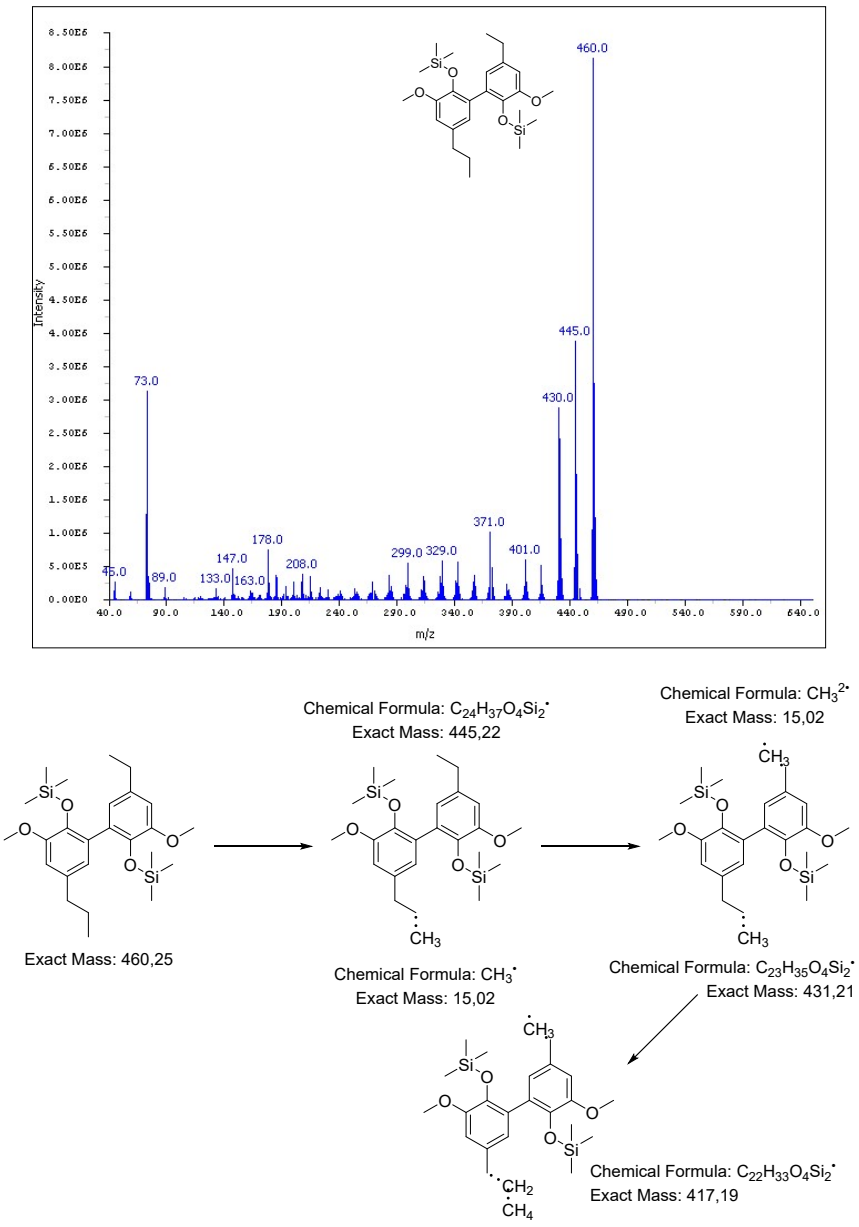

Figure S3.6. Mass spectrum and fragmentation pattern analysis of dimer **D6**.

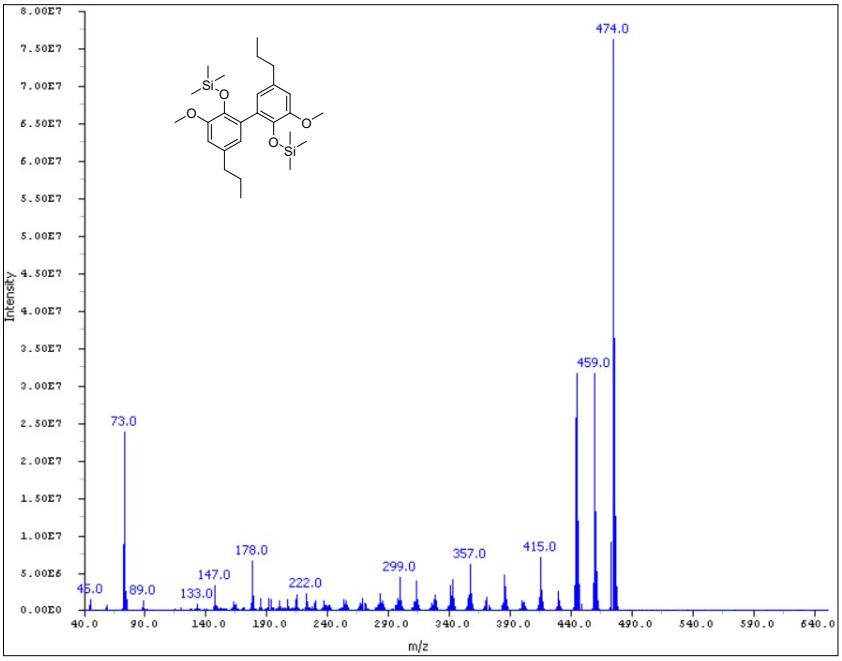

Figure S3.7. Mass spectrum of dimer **D7**.[5-6]

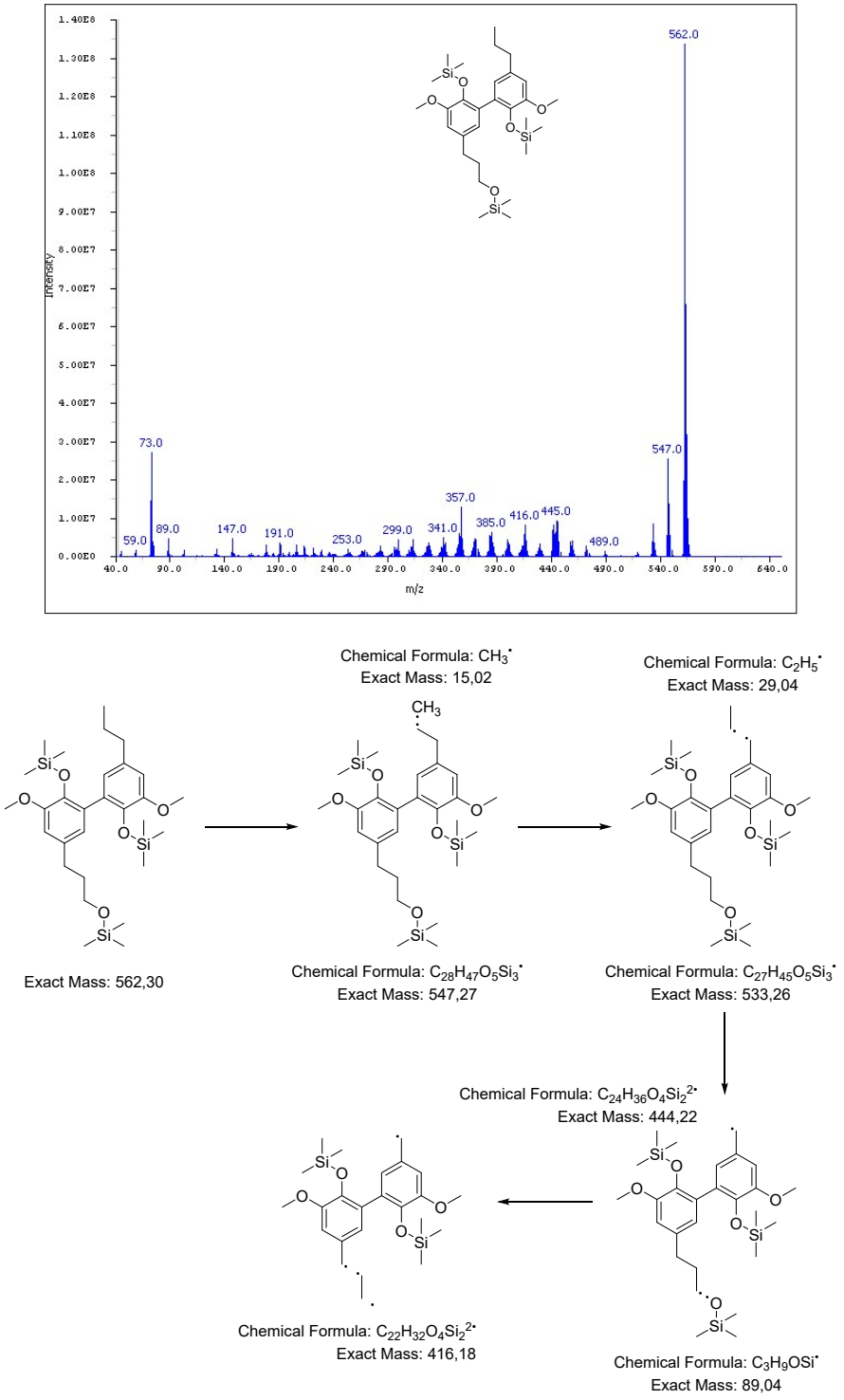

Figure S3.8. Mass spectrum and fragmentation pattern analysis of dimer **D8**.

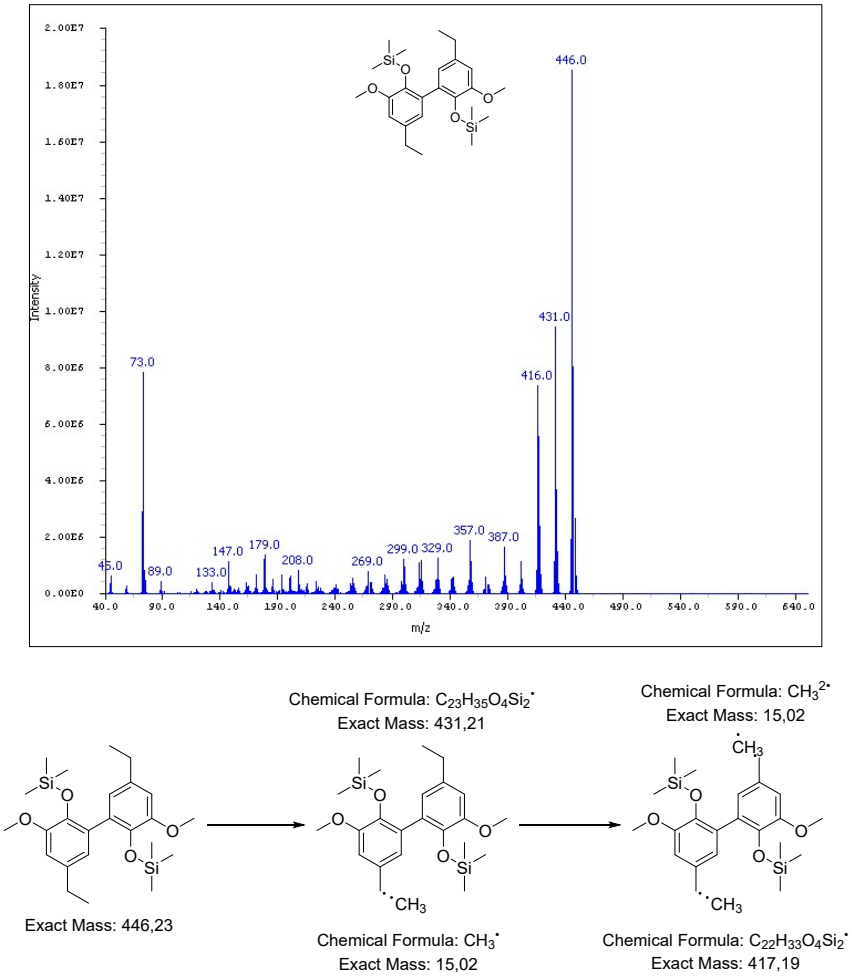

Figure S3.9. Mass spectrum and fragmentation pattern analysis of dimer **D9**.

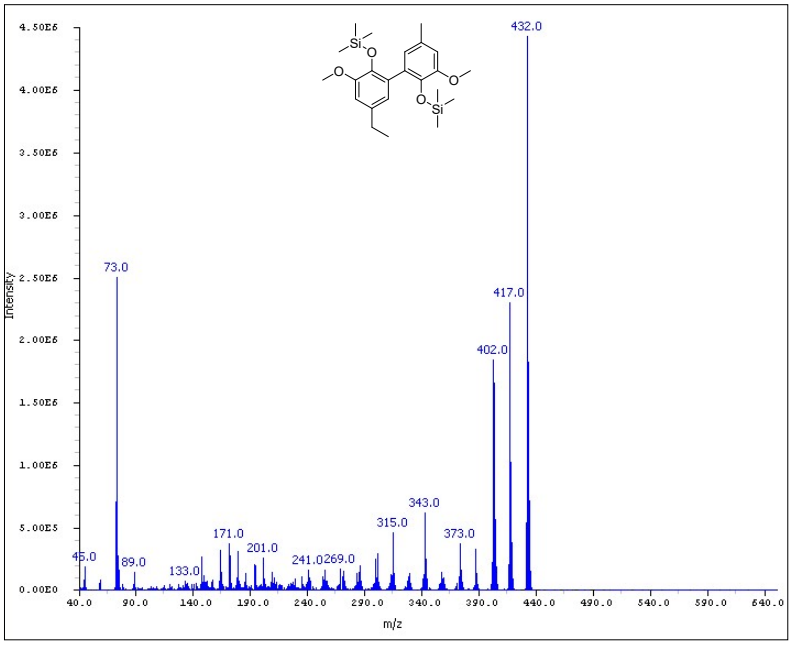

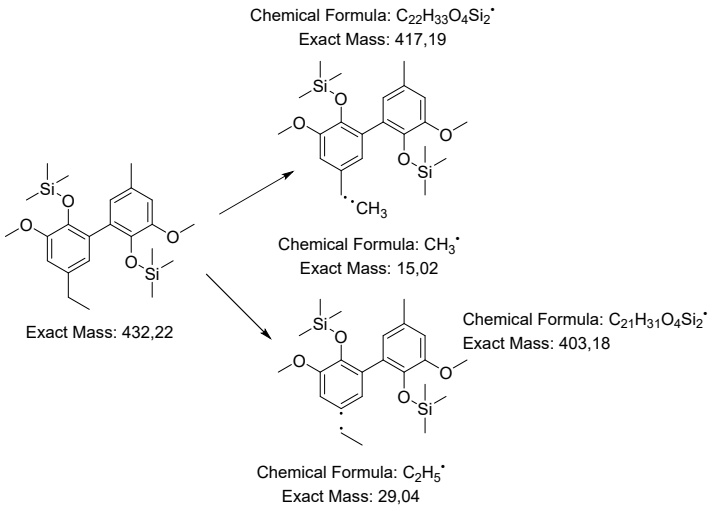

Figure S3.10. Mass spectrum and fragmentation pattern analysis of dimer **D10**.

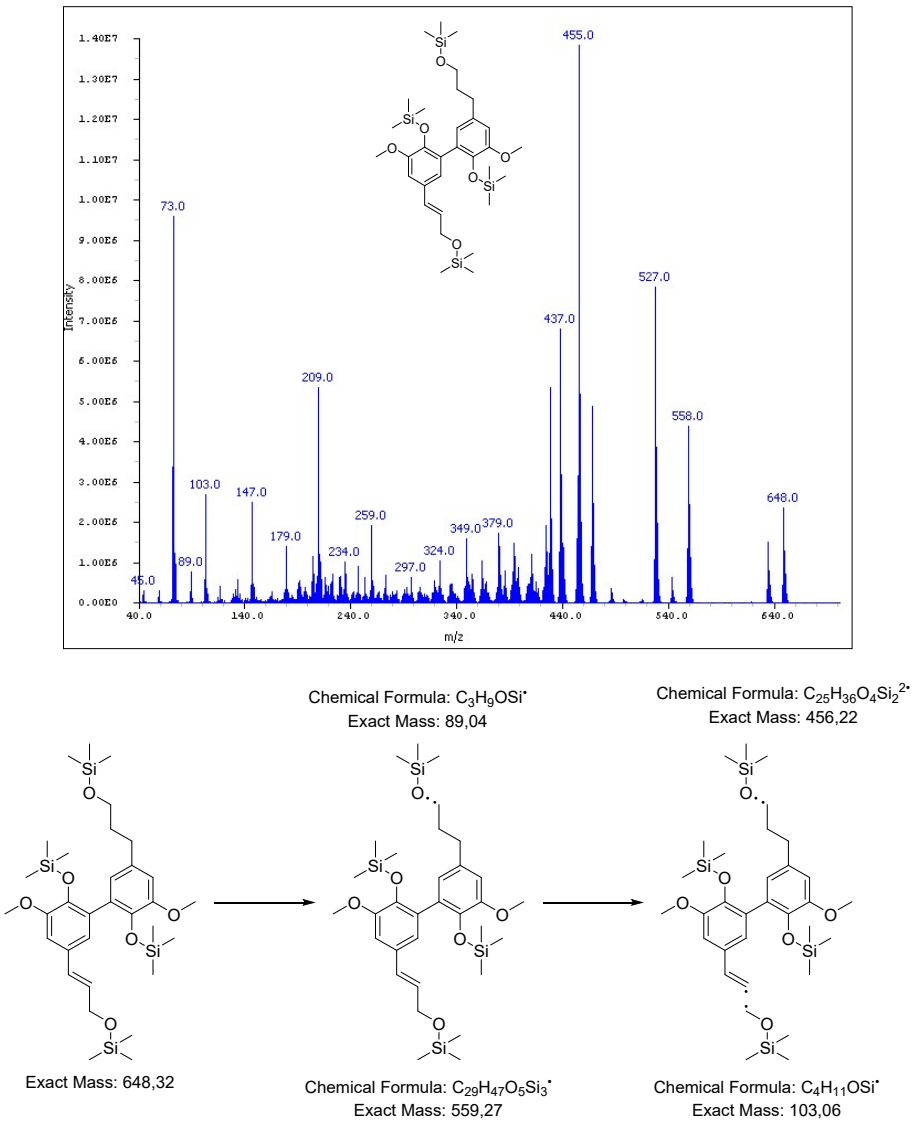

Figure S3.11. Mass spectrum and fragmentation pattern analysis of dimer **D11**.

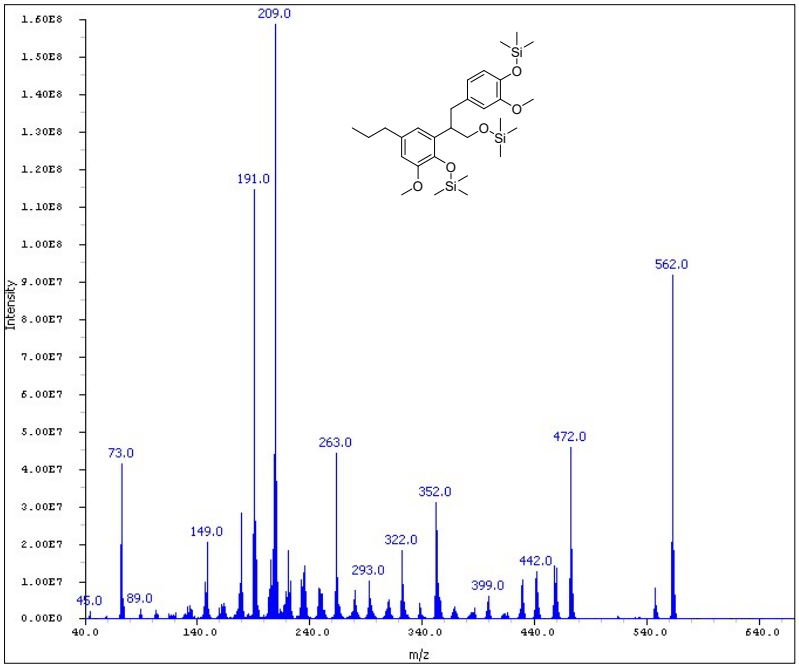

Figure S3.12. Mass spectrum of dimer **D12**.[6]

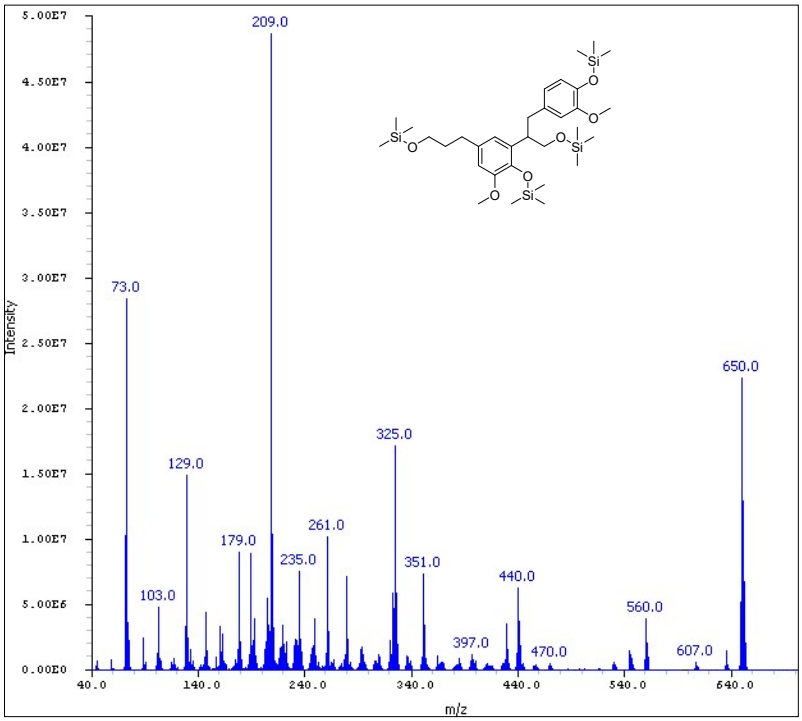

Figure S3.13. Mass spectrum of dimer **D13**.[5-6]

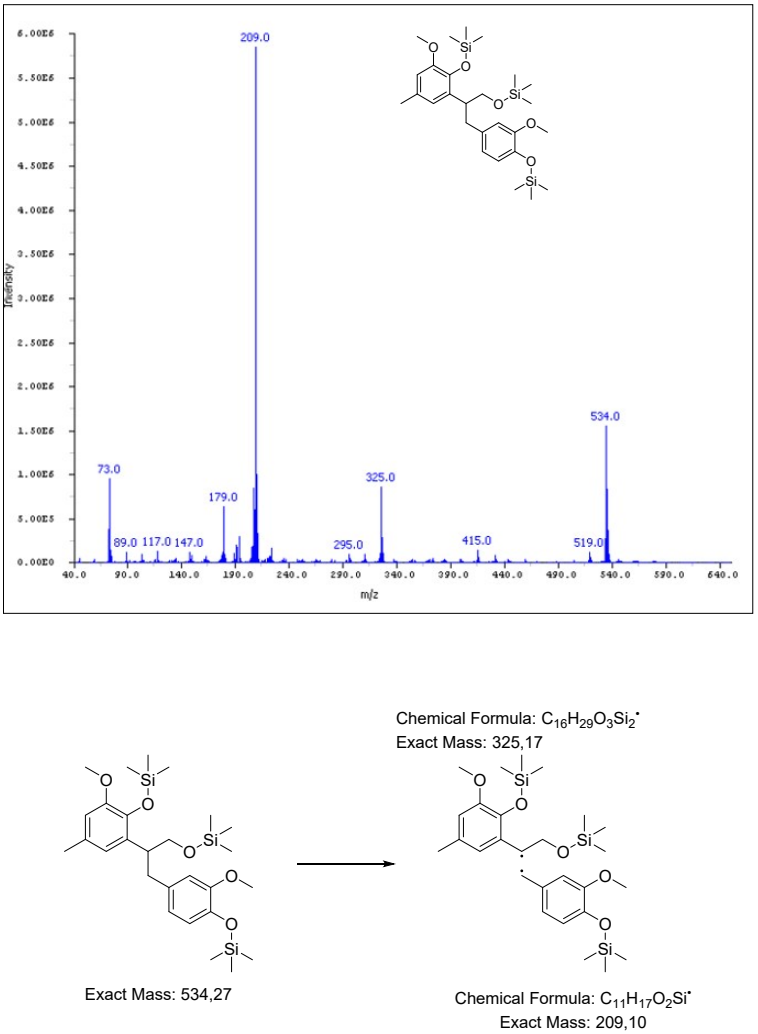

Figure S3.14. Mass spectrum and fragmentation pattern analysis of dimer **D14**.

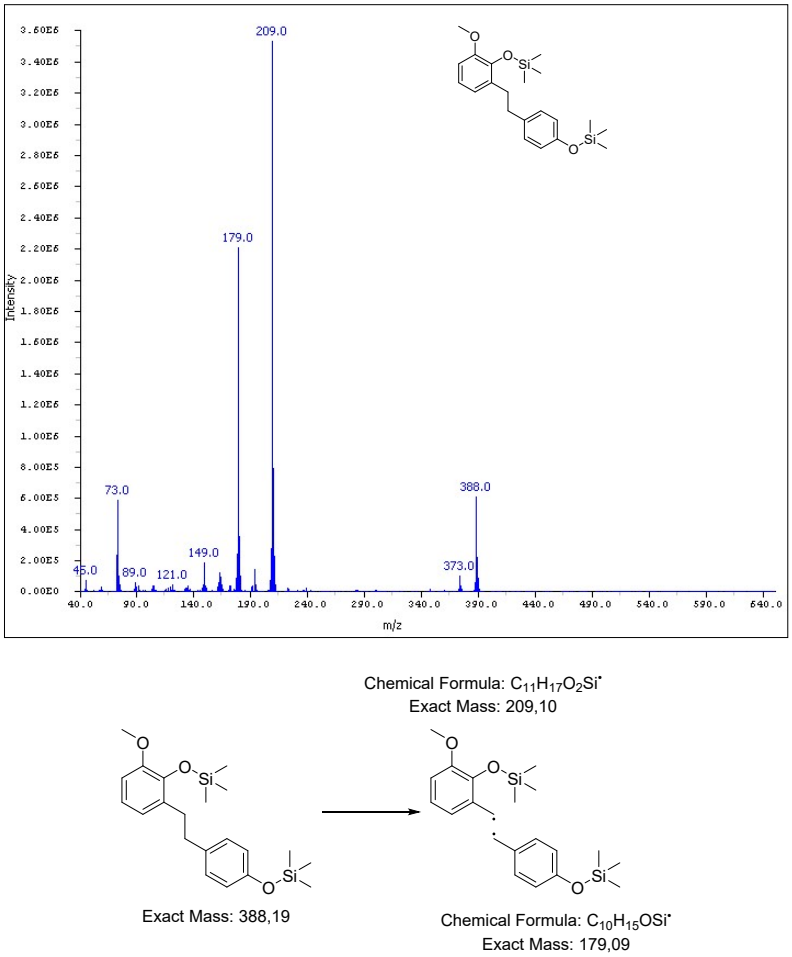

Figure S3.15. Mass spectrum and fragmentation pattern analysis of dimer **D15**.

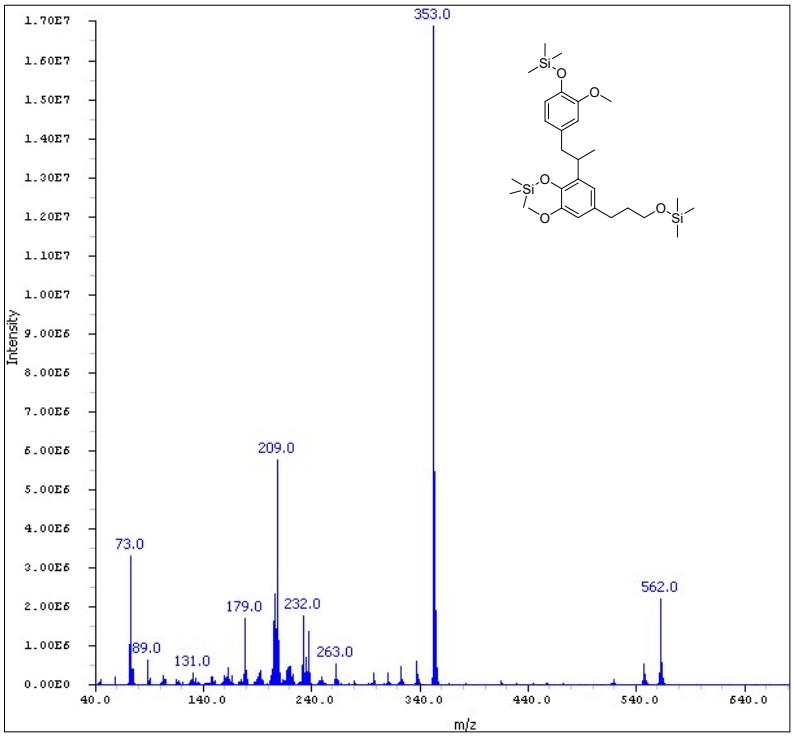

Figure S3.16. Mass spectrum of dimer **D16**.[6]

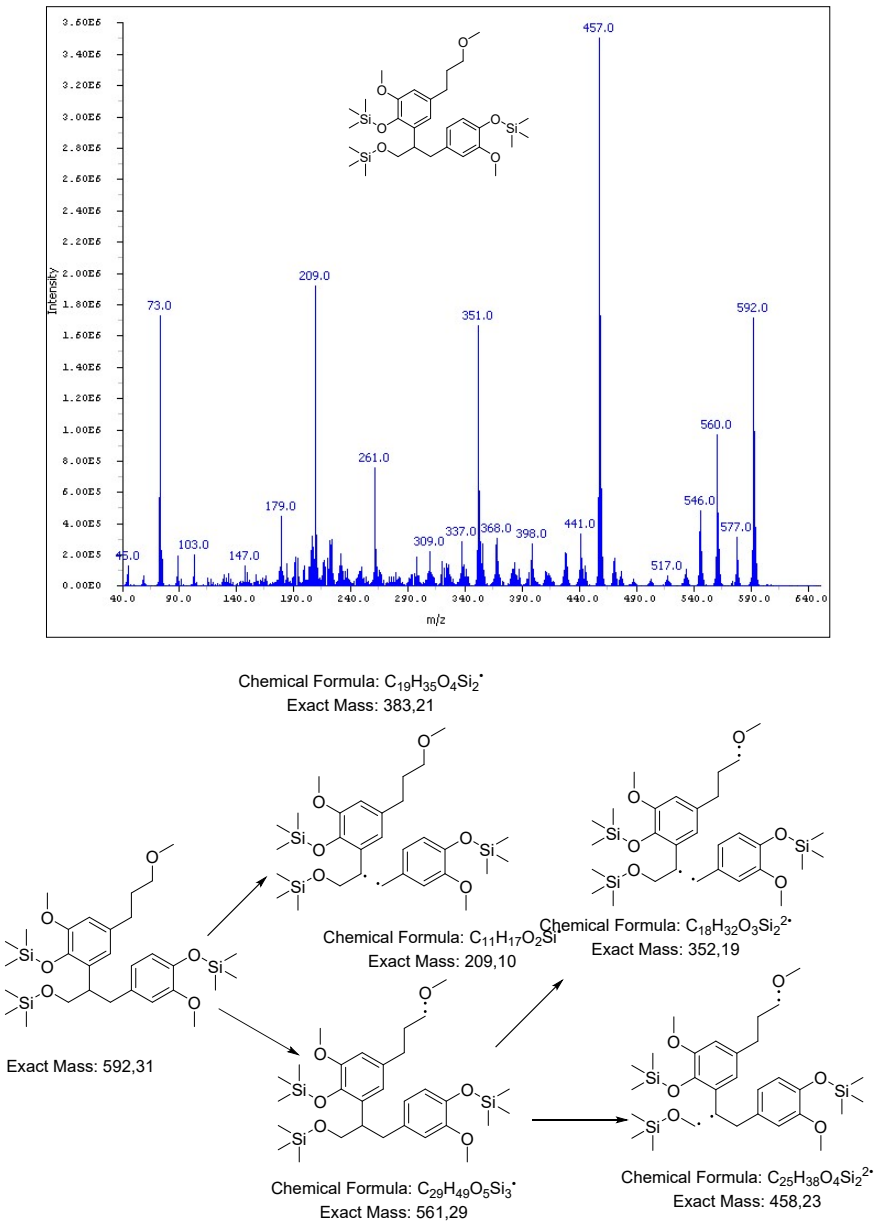

Figure S3.17. Mass spectrum and fragmentation pattern analysis of dimer **D17**.

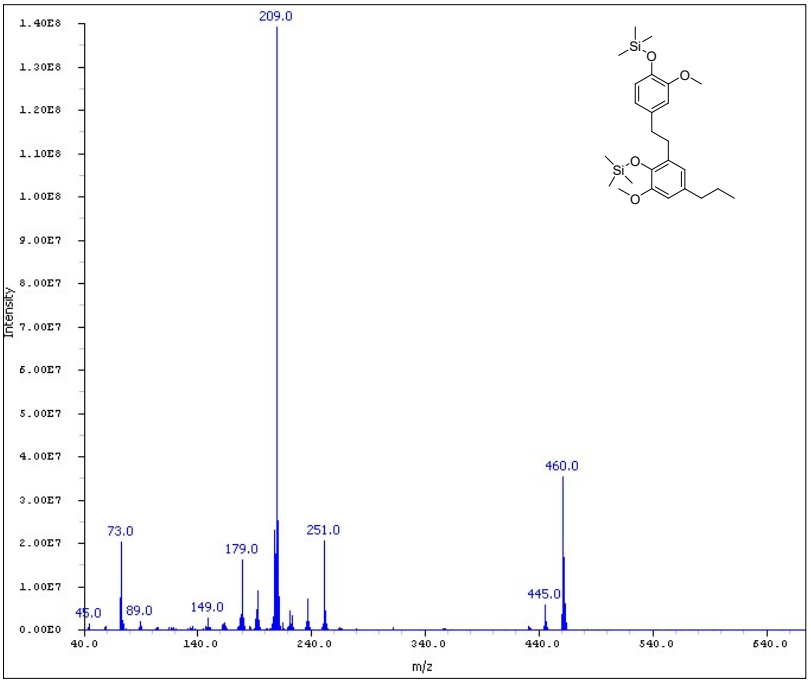

Figure S3.18. Mass spectrum of dimer **D18**.[4, 6]

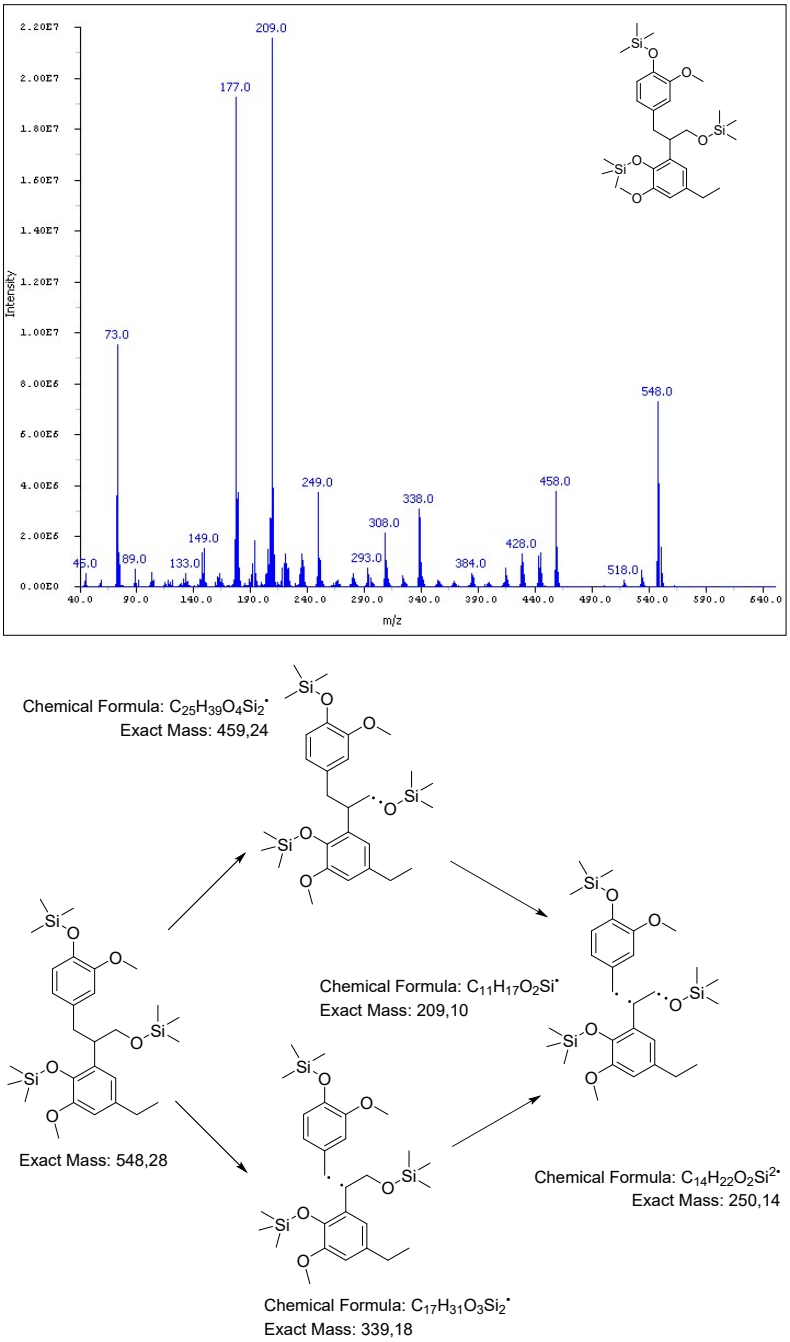

Figure S3.19. Mass spectrum and fragmentation pattern analysis of dimer **D19**.

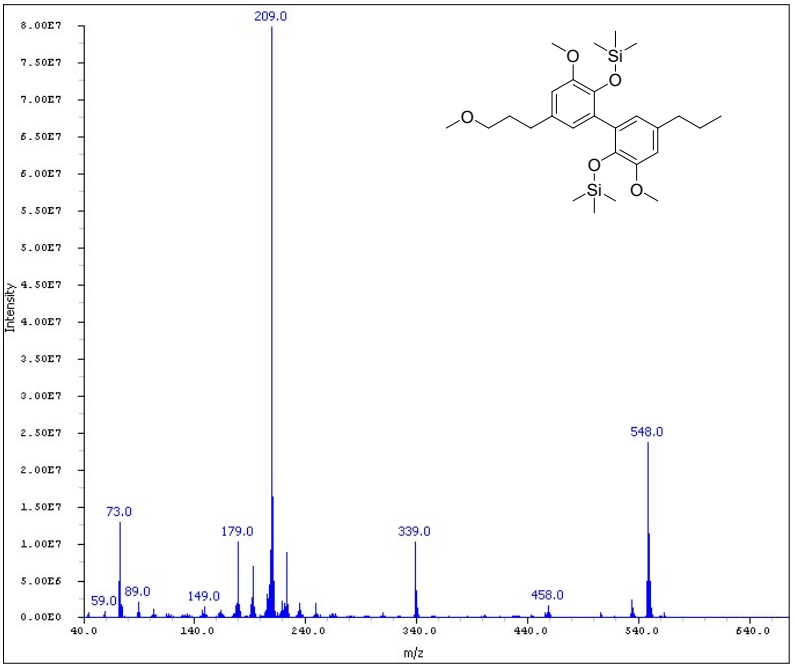

Figure S3.20. Mass spectrum of dimer **D20**.[4, 6]

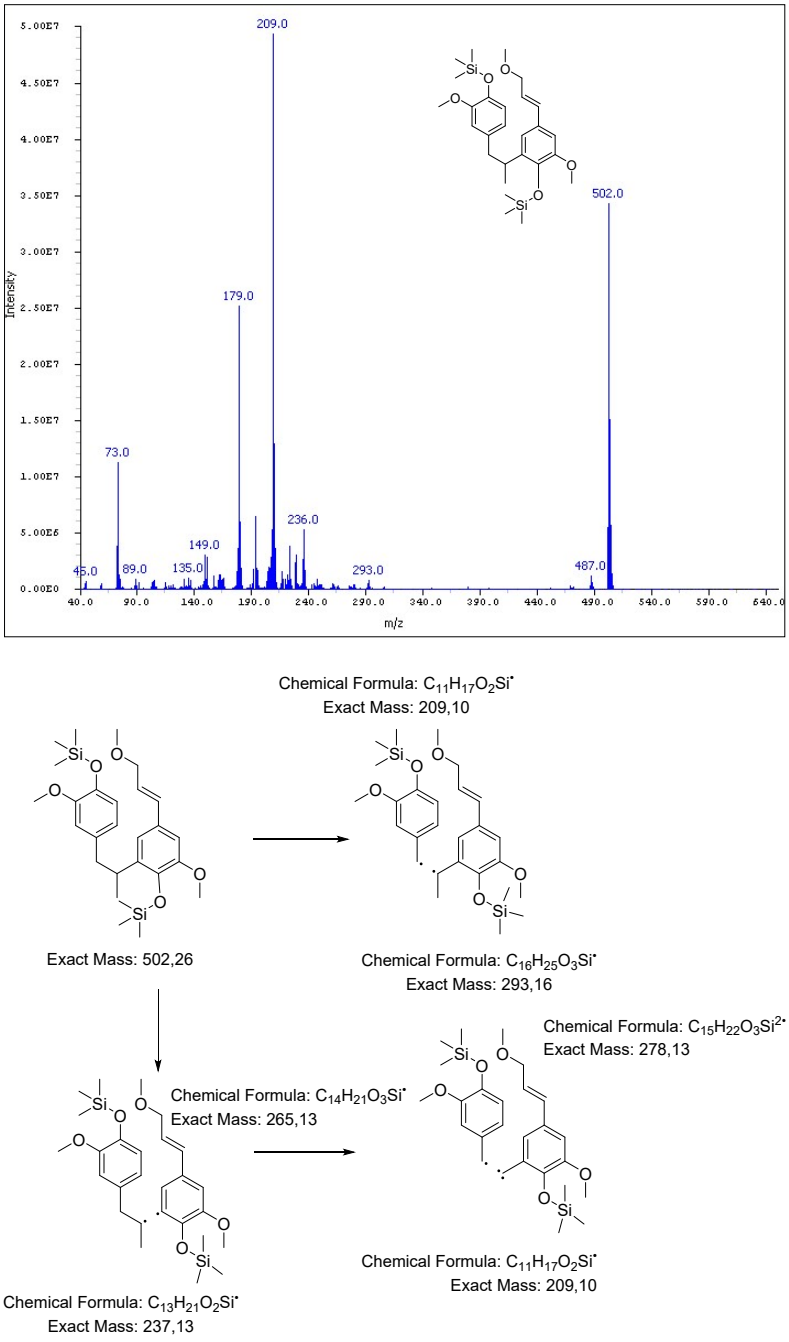

Figure S3.21. Mass spectrum and fragmentation pattern analysis of dimer **D21**.

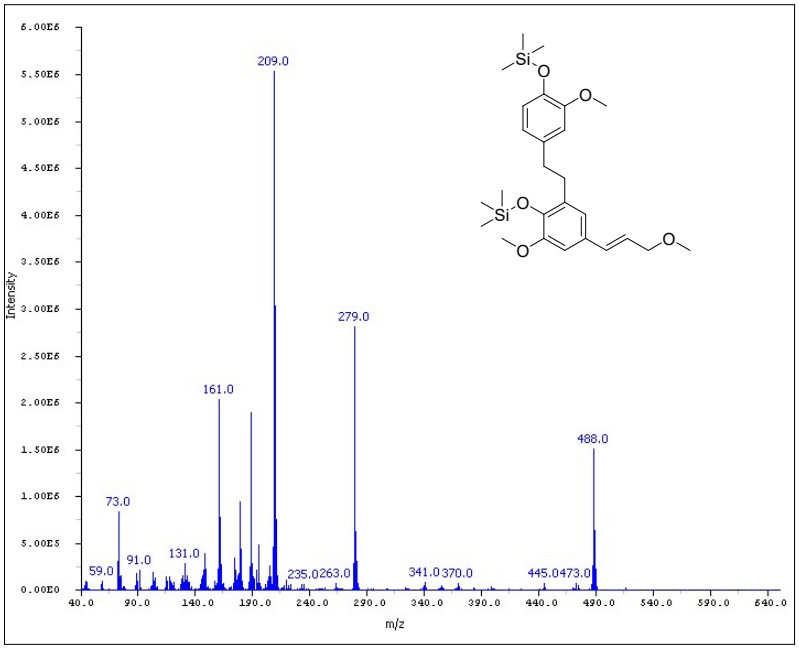

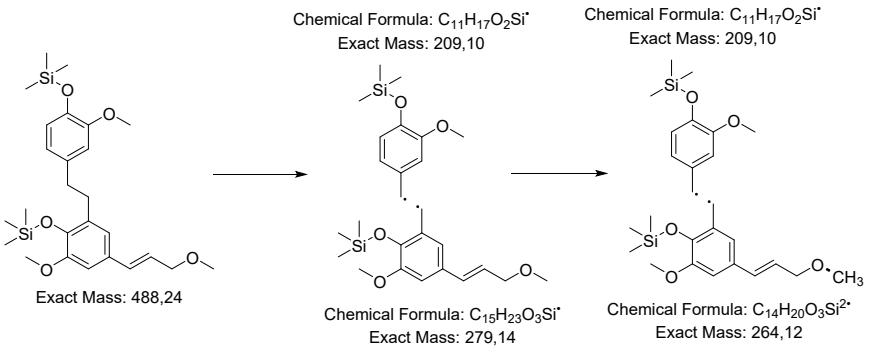

Figure S3.22. Mass spectrum and fragmentation pattern analysis of dimer **D22**.

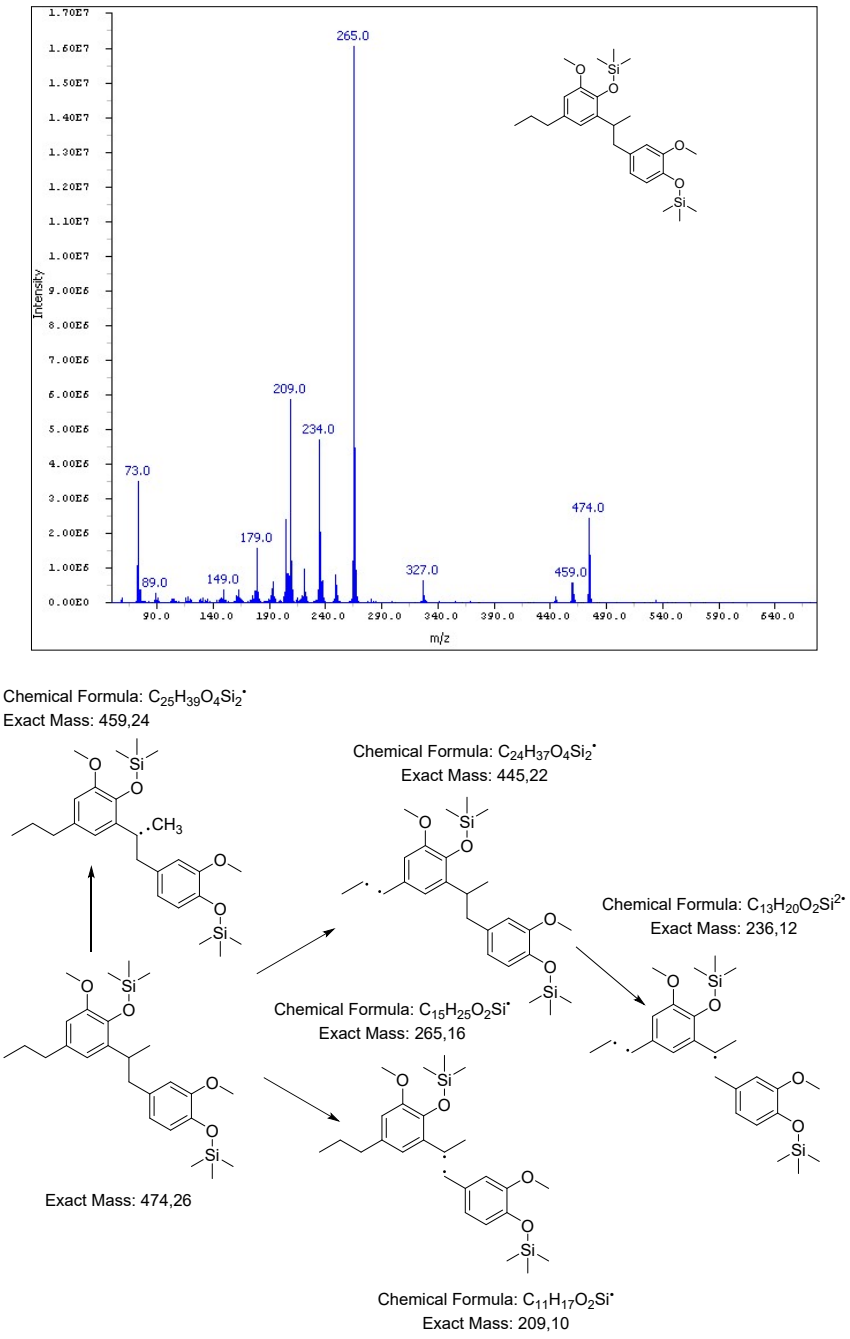

Figure S3.23. Mass spectrum and fragmentation pattern analysis of dimer **D23**.

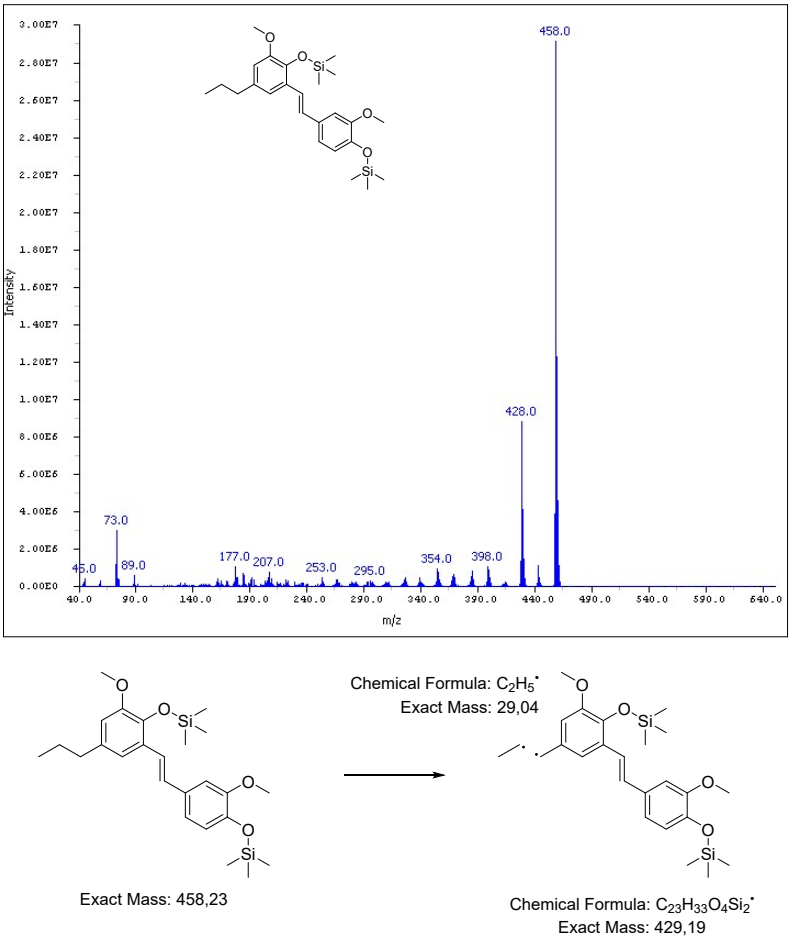

Figure S3.24. Mass spectrum and fragmentation pattern analysis of dimer **D24**.

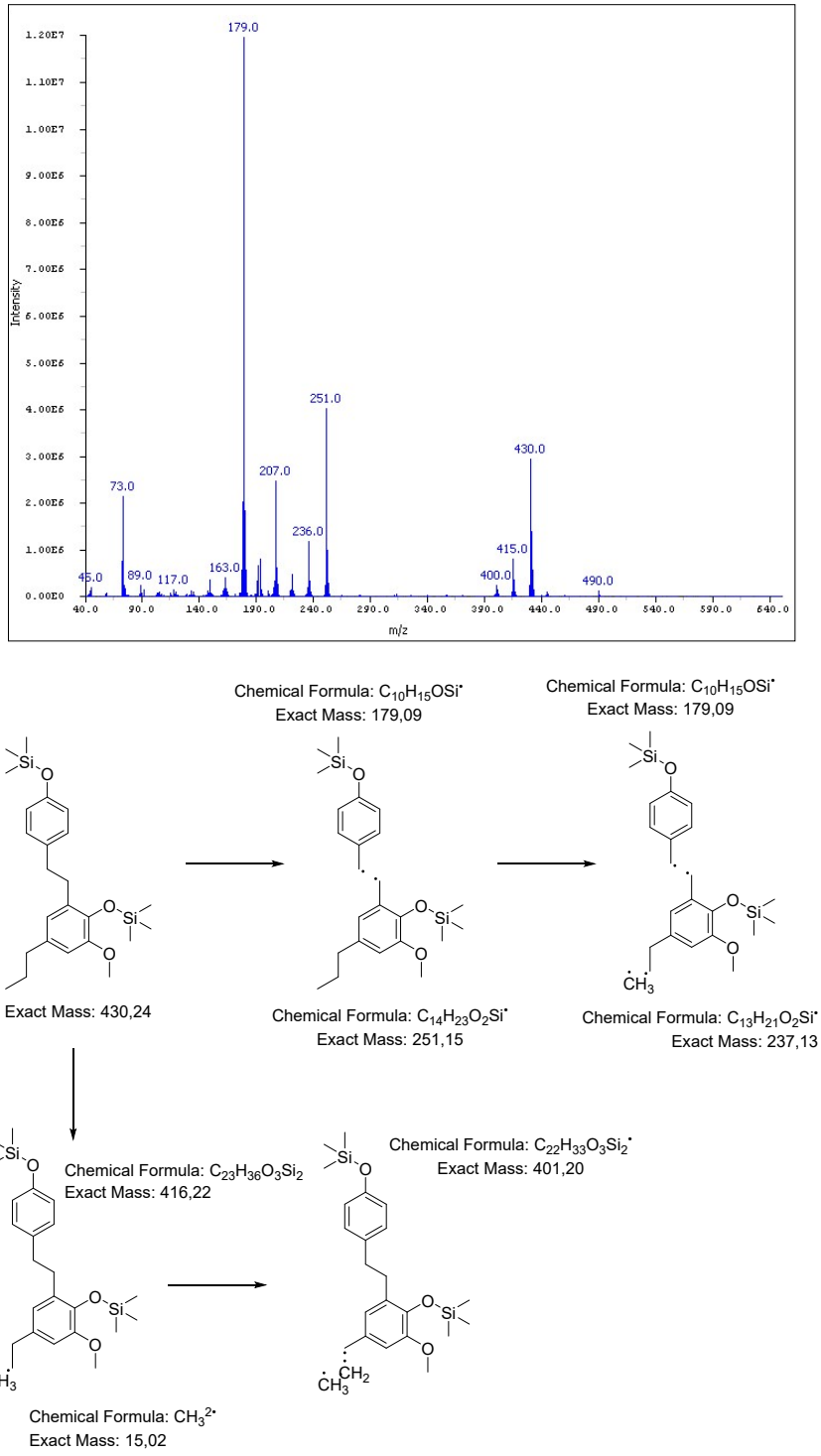

Figure S3.25. Mass spectrum and fragmentation pattern analysis of dimer **D25**.

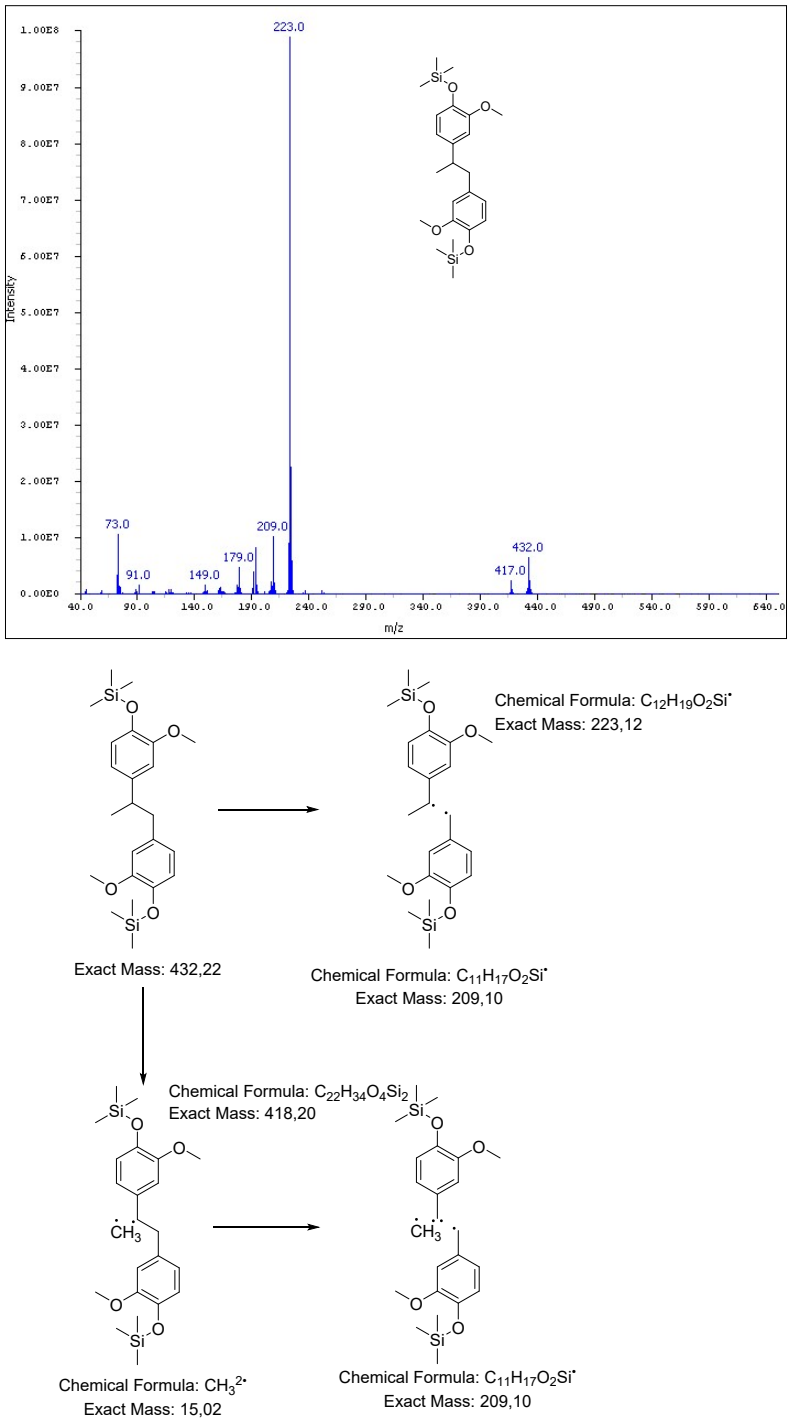

Figure S3.26. Mass spectrum and fragmentation pattern analysis of dimer **D26**.

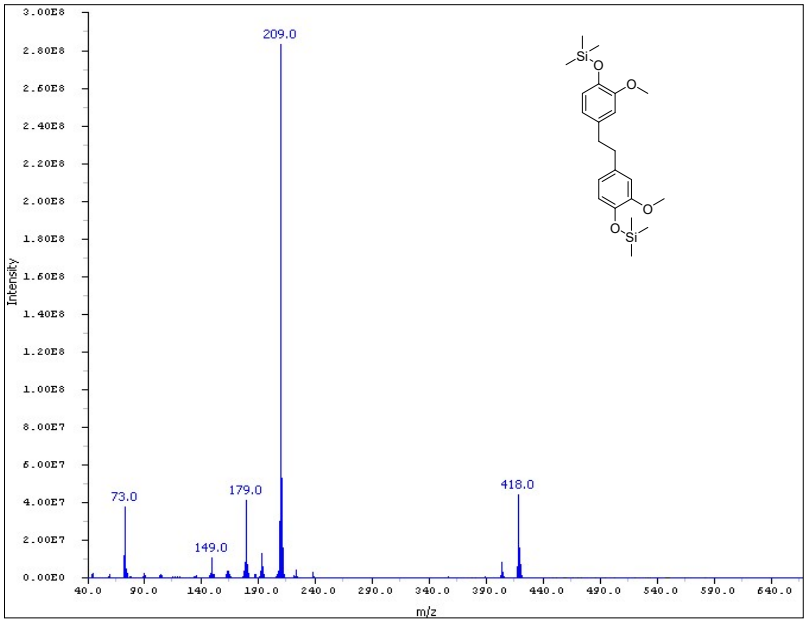

Figure S3.27. Mass spectrum of dimer **D27**.[5-6]

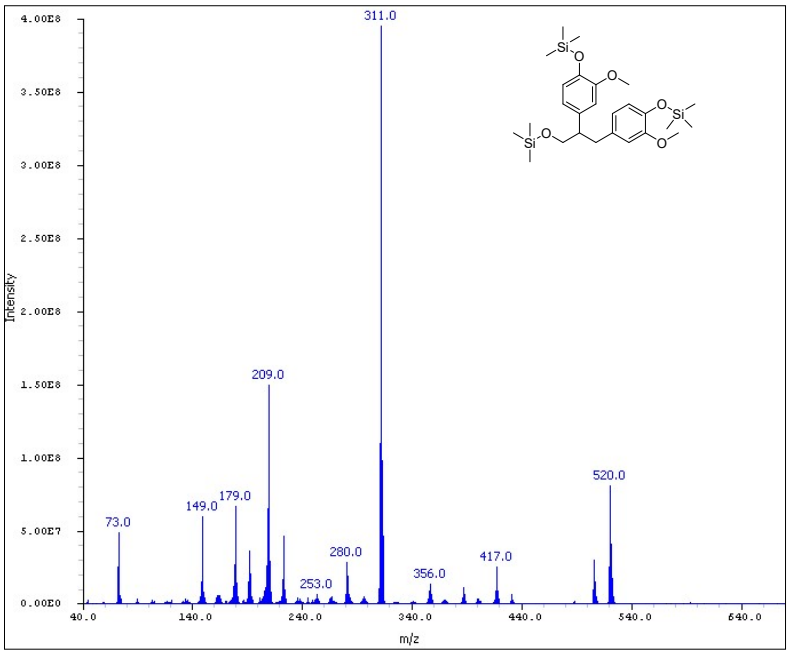

Figure S3.28. Mass spectrum of dimer **D28**.[4-6]

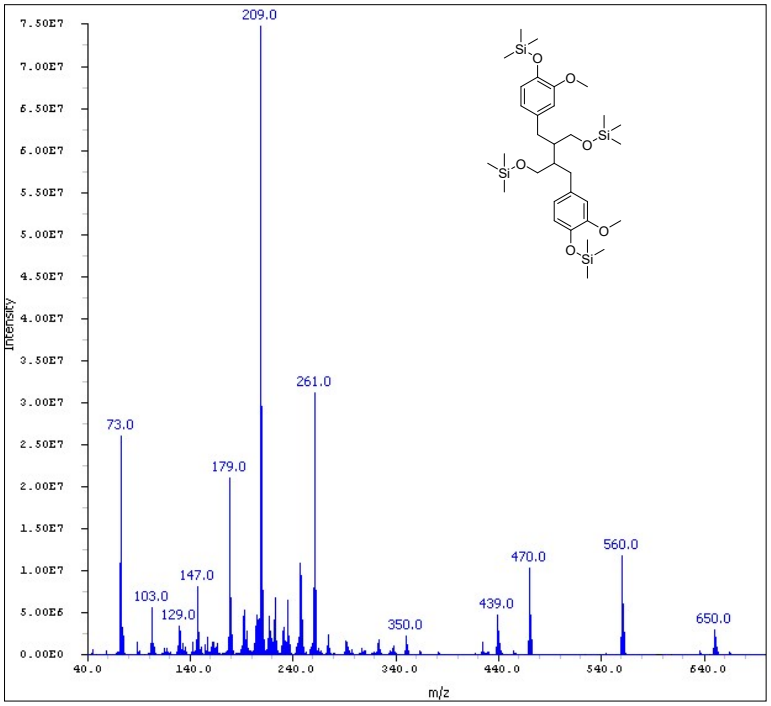

Figure S3.29. Mass spectrum of dimer **D29**.[6]

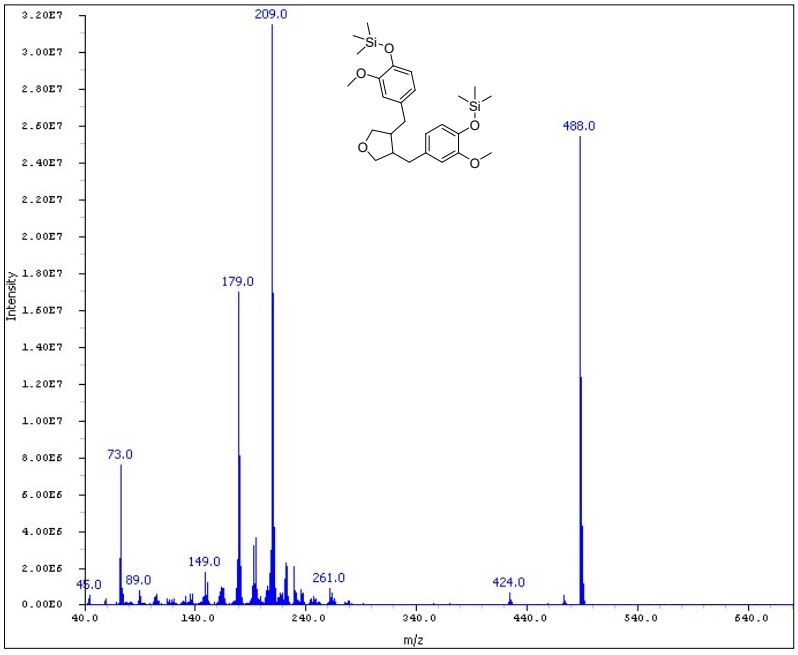

Figure S3.30. Mass spectrum of dimer **D30**.[4, 7]

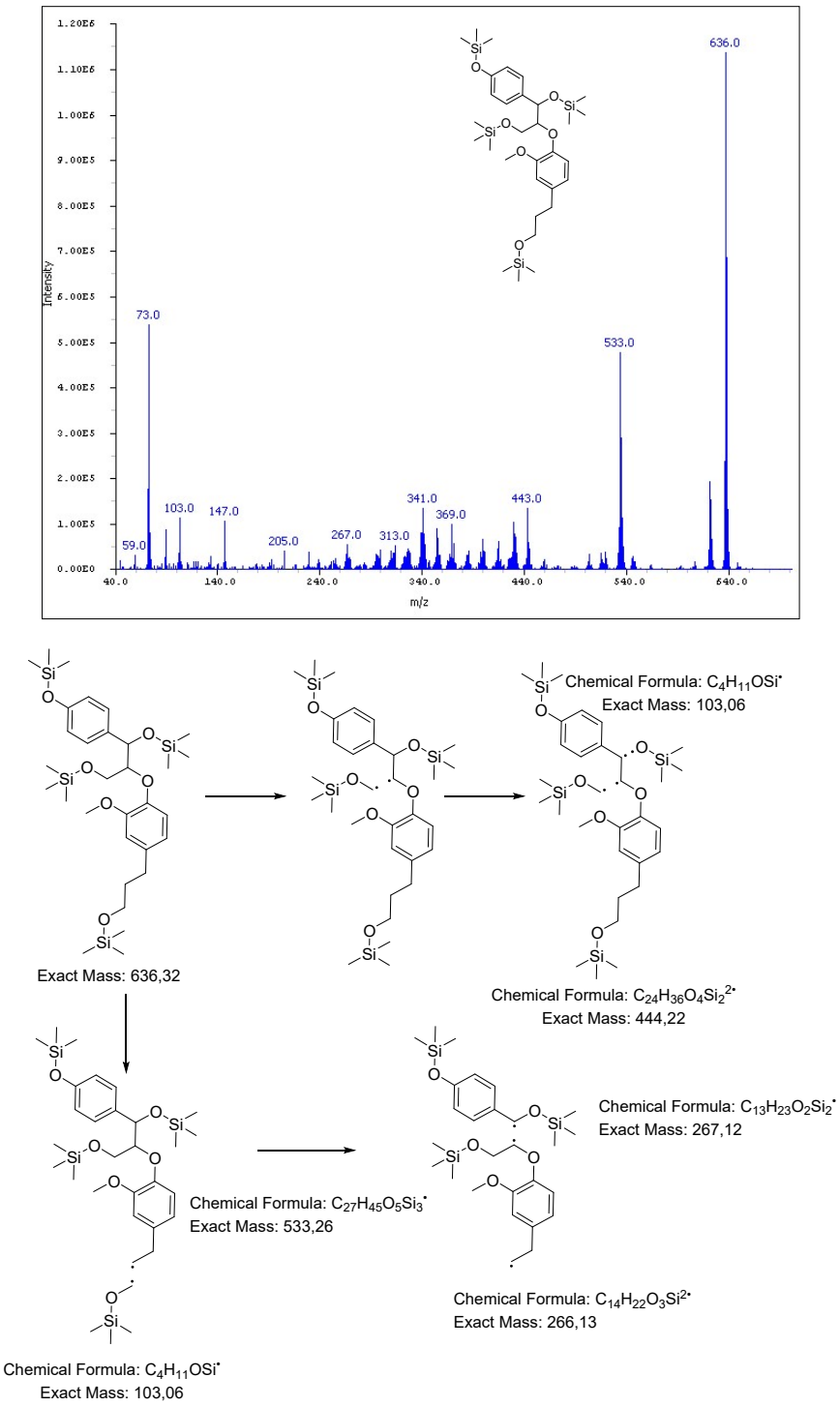

Figure S3.31. Mass spectrum and fragmentation pattern analysis of dimer **D31**.

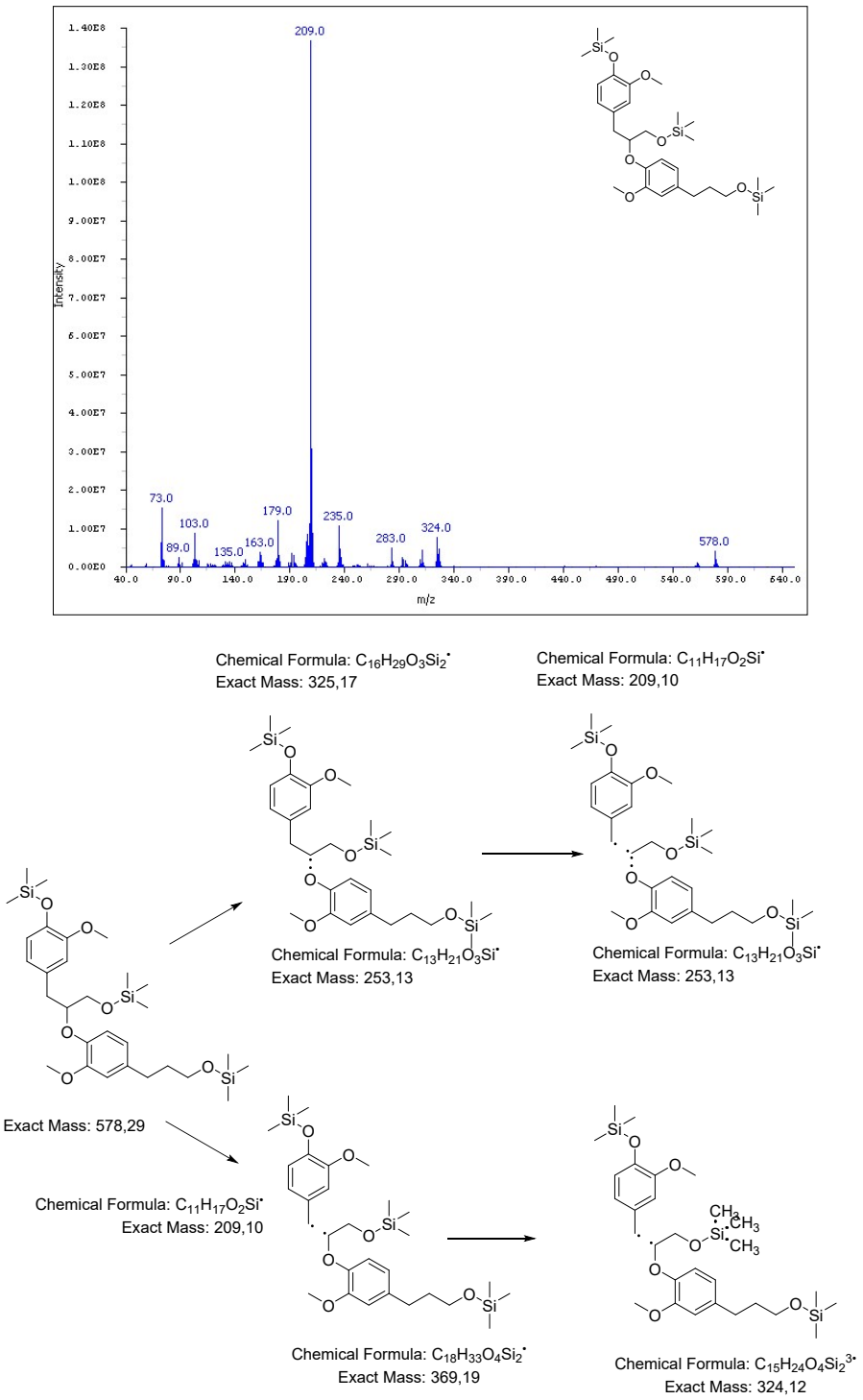

Figure S3.32. Mass spectrum and fragmentation pattern analysis of dimer **D32**.

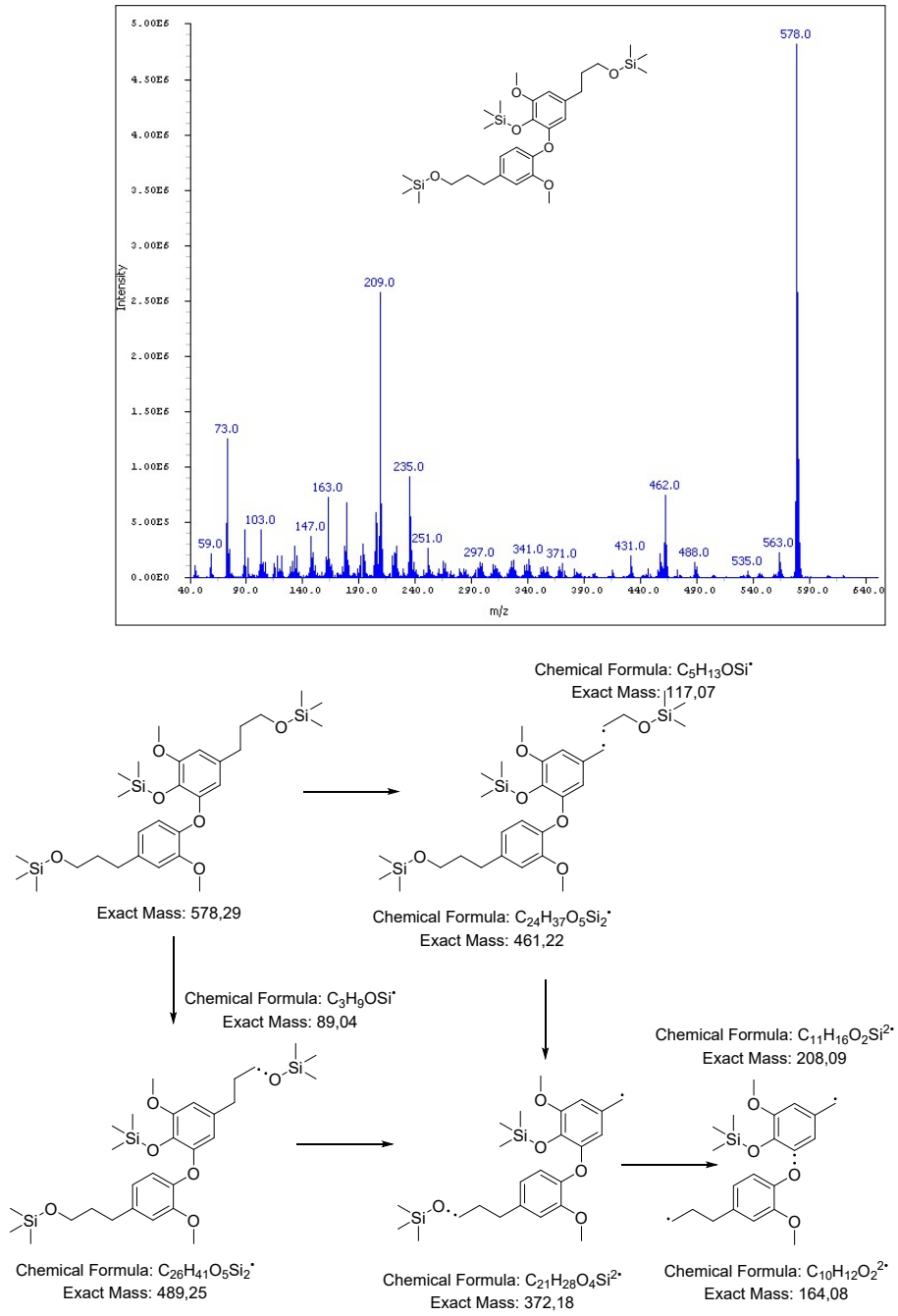

Figure S3.33. Mass spectrum and fragmentation pattern analysis of dimer **D33**.

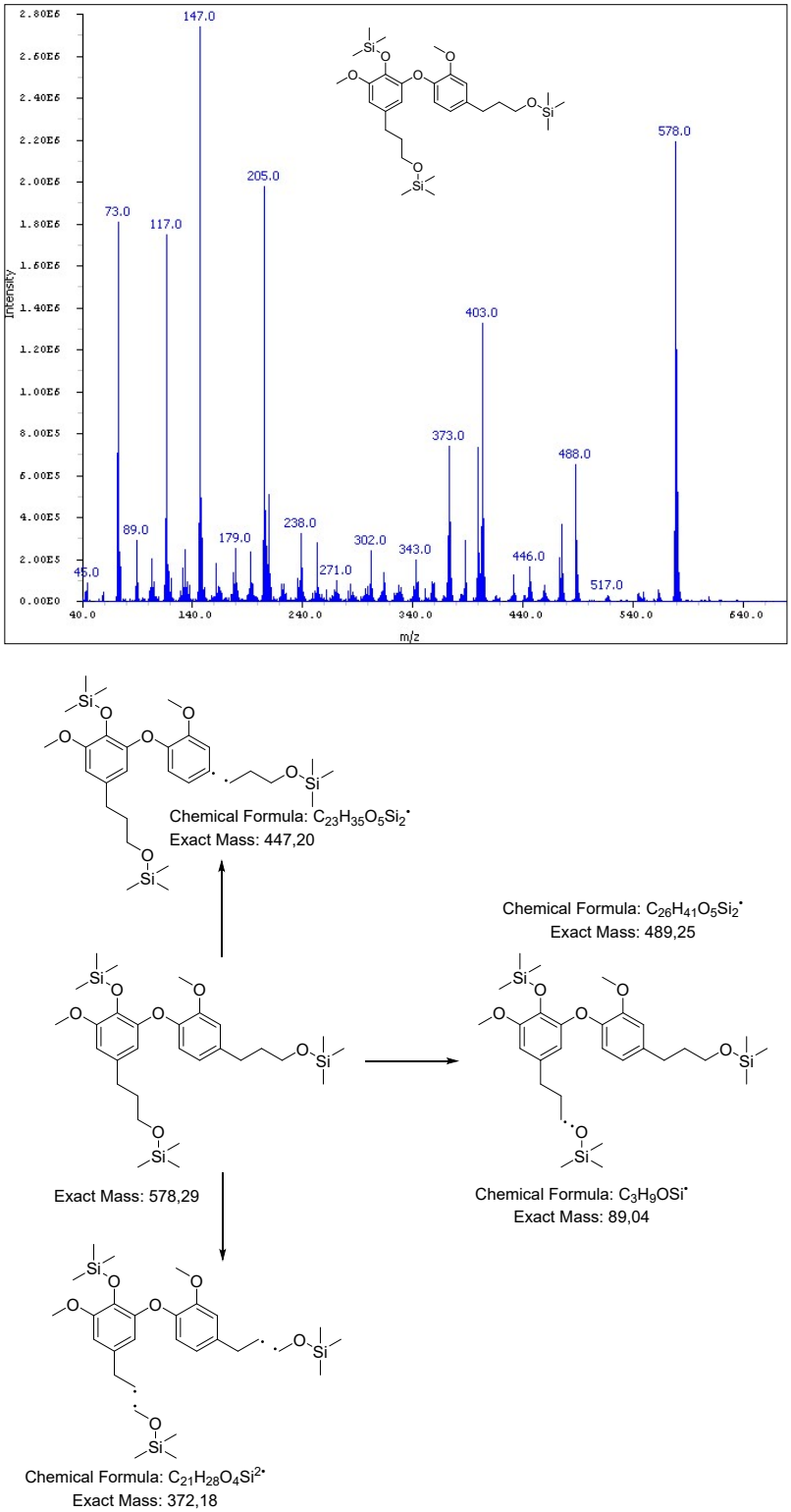

Figure S3.34. Mass spectrum and fragmentation pattern analysis of dimer **D34**.

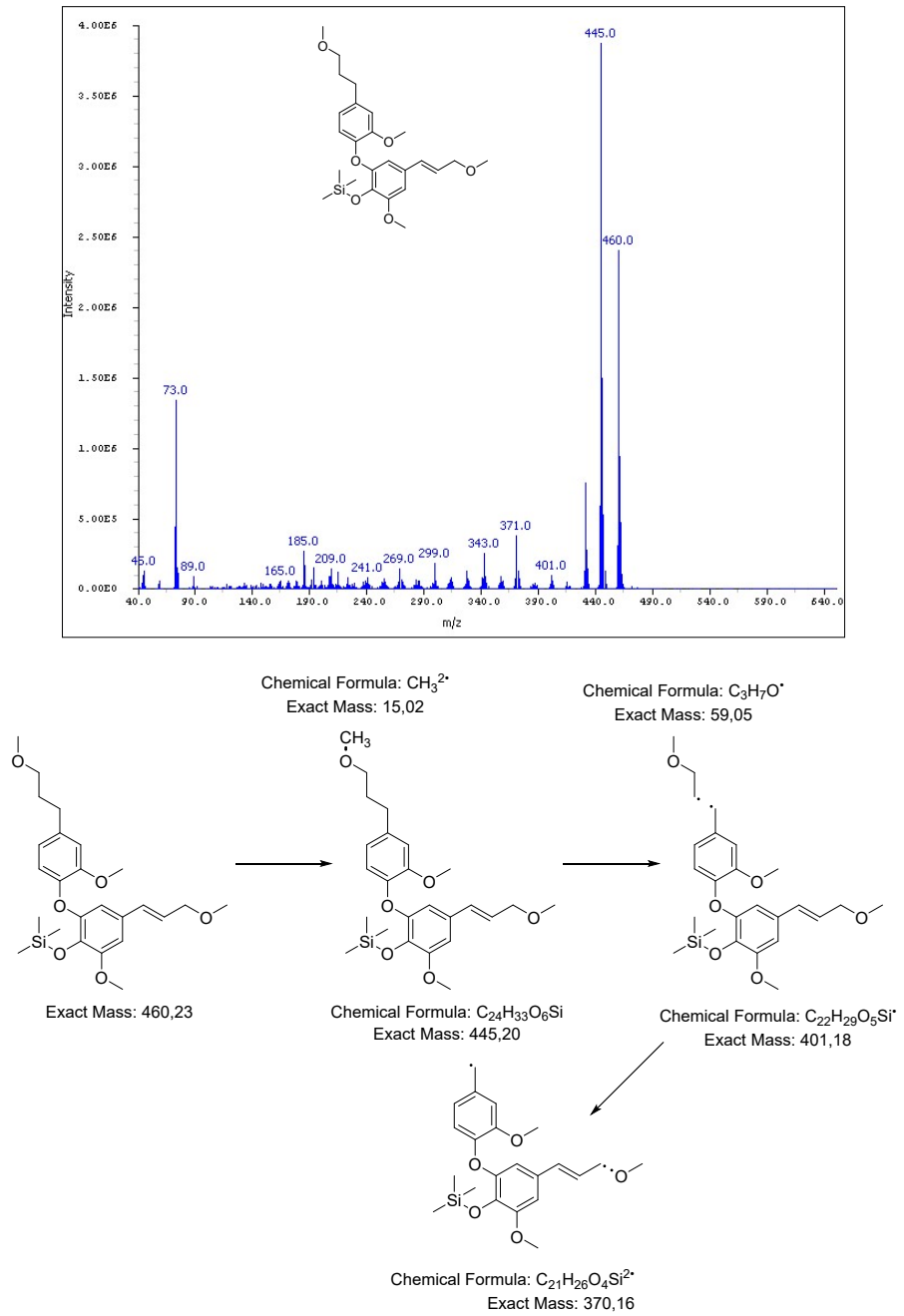

Figure S3.35. Mass spectrum and fragmentation pattern analysis of dimer **D35**.

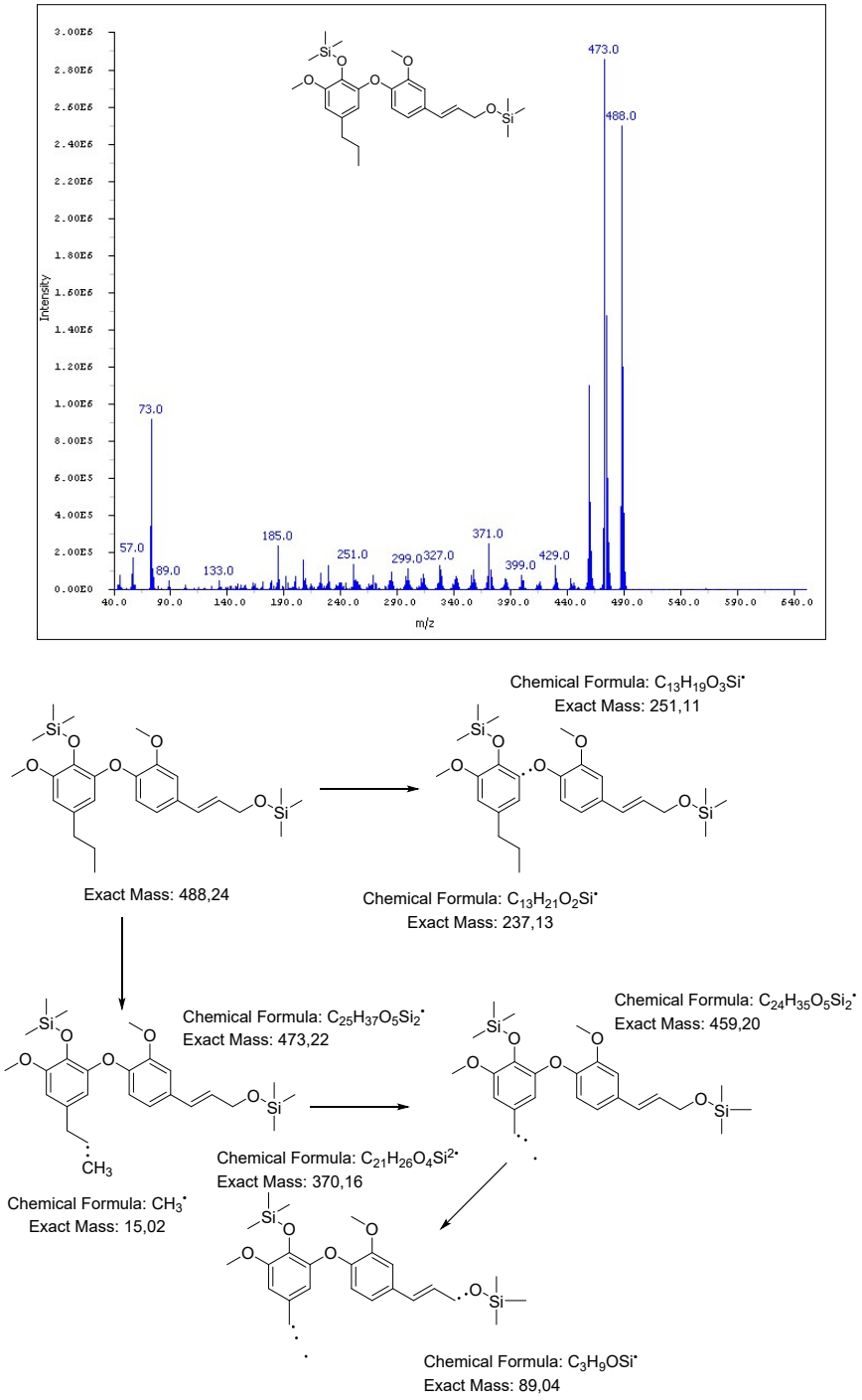

Figure S3.36. Mass spectrum and fragmentation pattern analysis of dimer **D36**.

S4. Mass spectrum and proposed fragmentation pathways of trimers

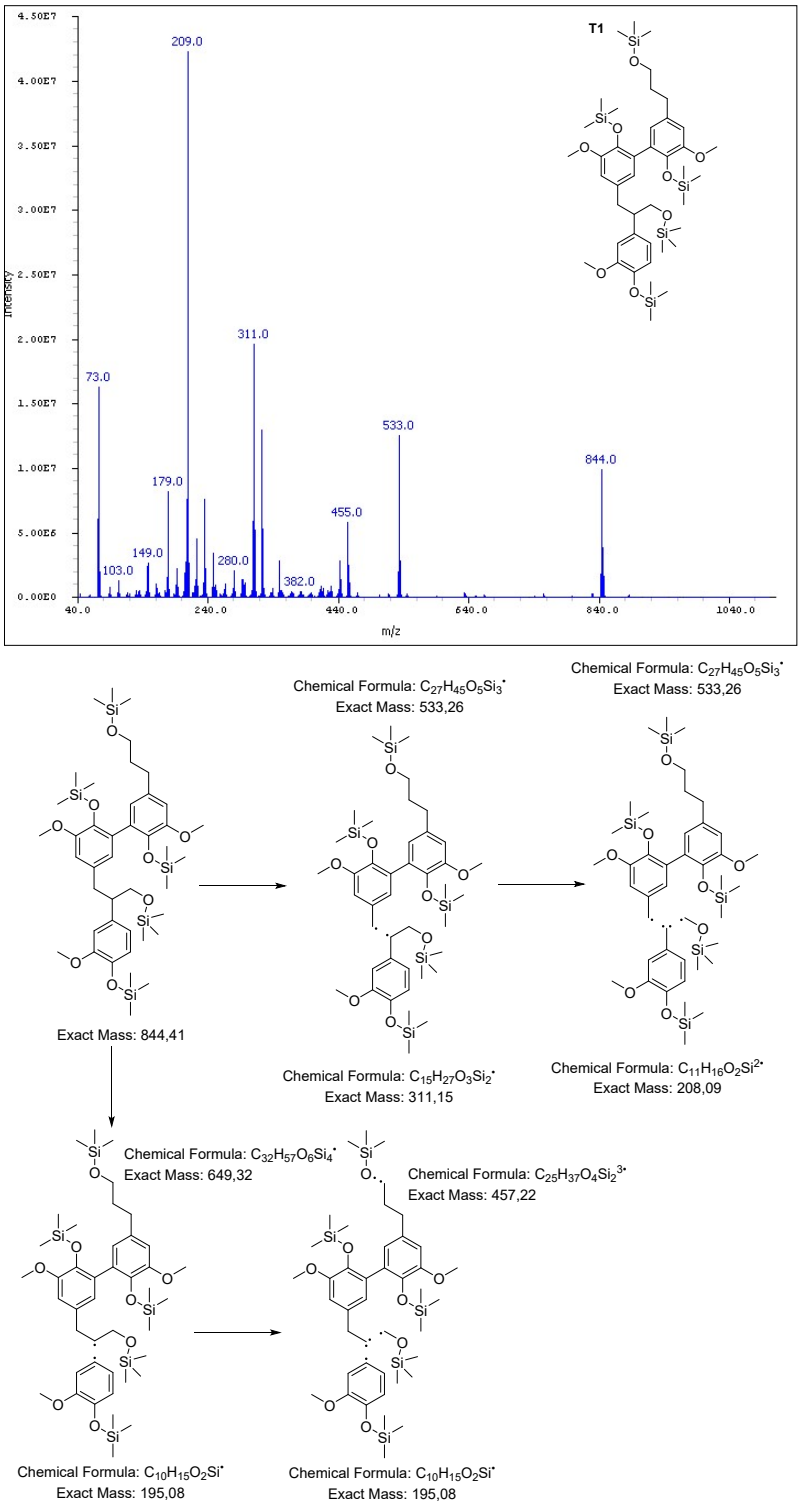

Figure S4.1. Mass spectrum and fragmentation pattern analysis of trimer **T1**.

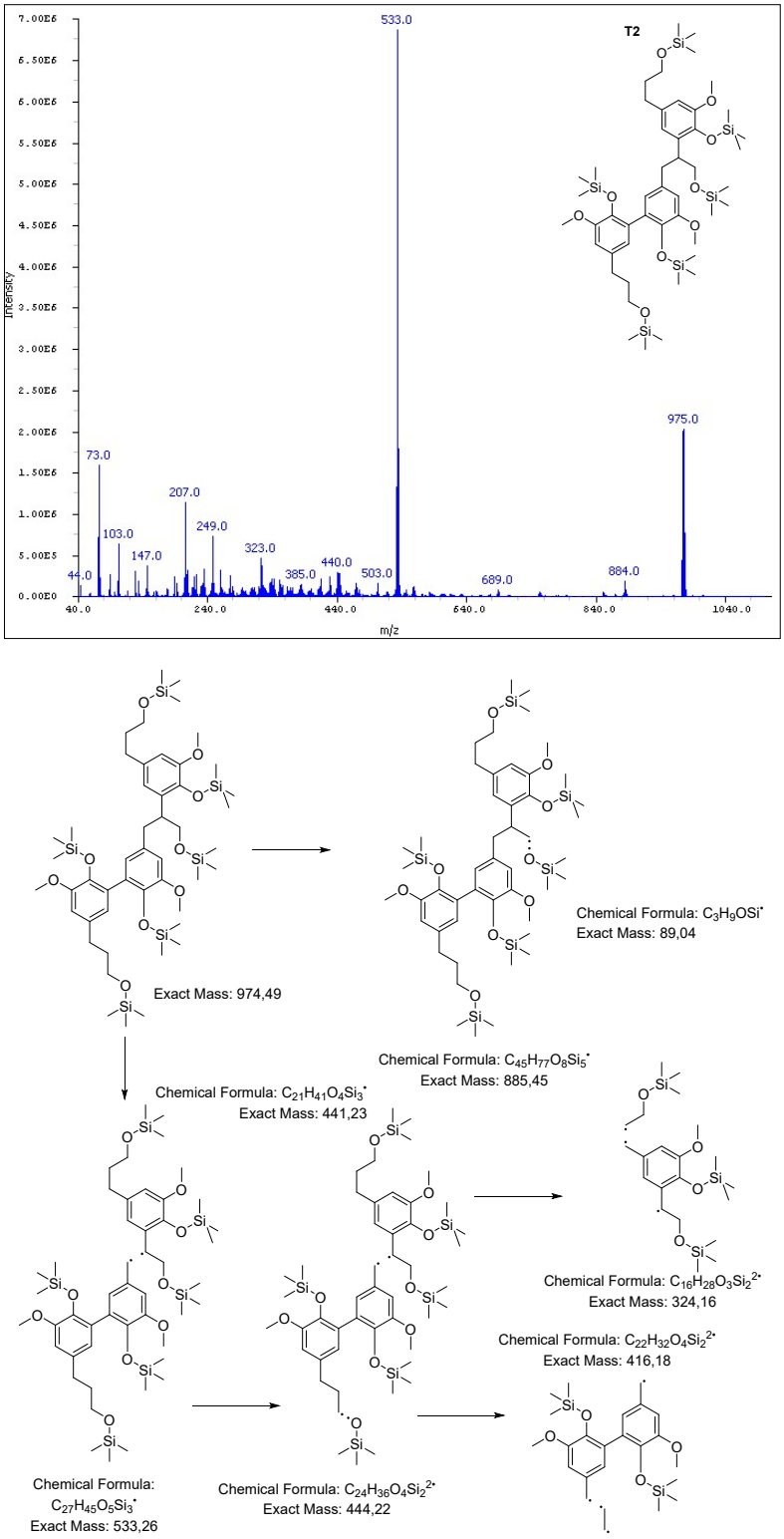

Figure S4.2. Mass spectrum and fragmentation pattern analysis of trimer **T2**.

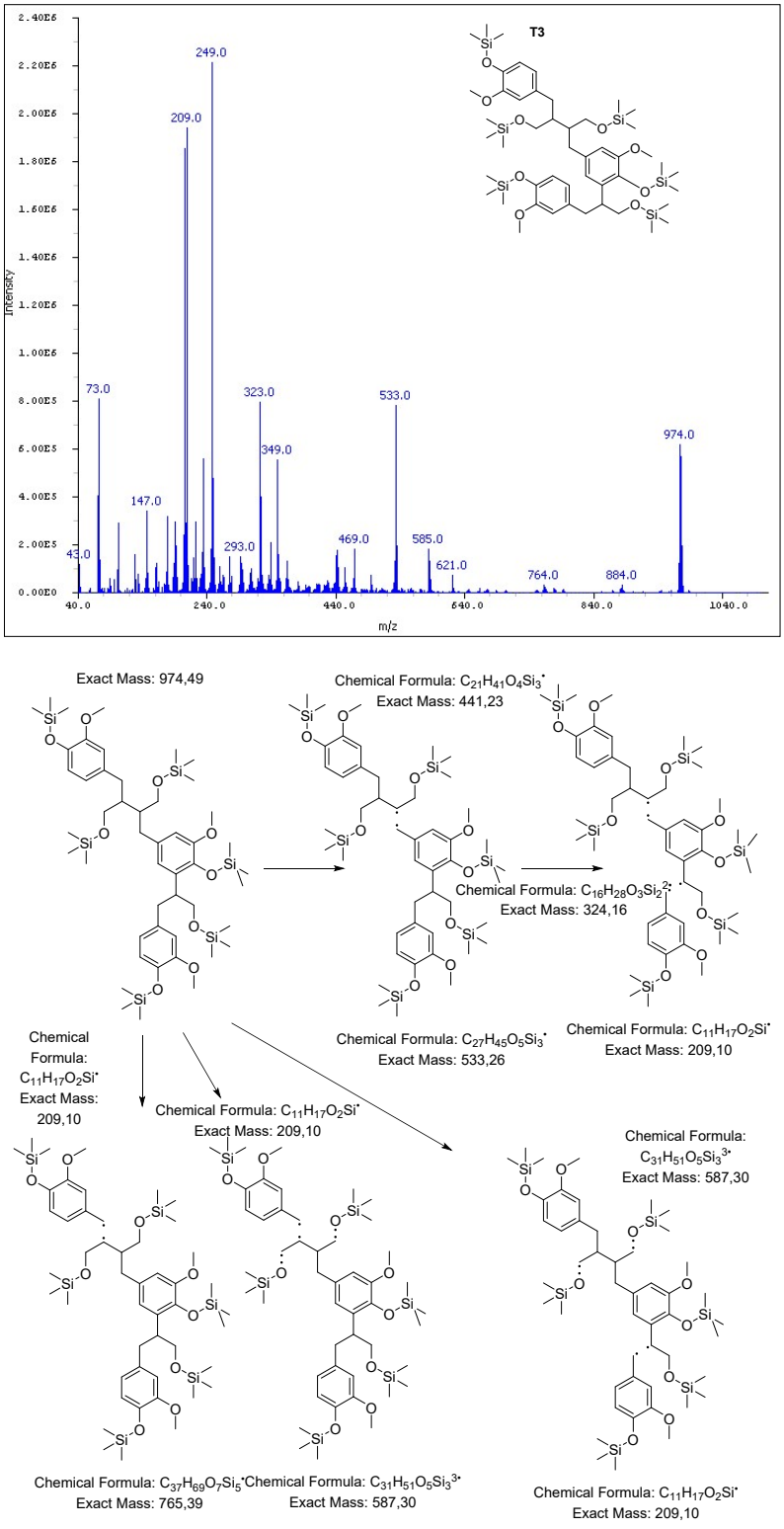

Figure S4.3. Mass spectrum and fragmentation pattern analysis of trimer **T3**.

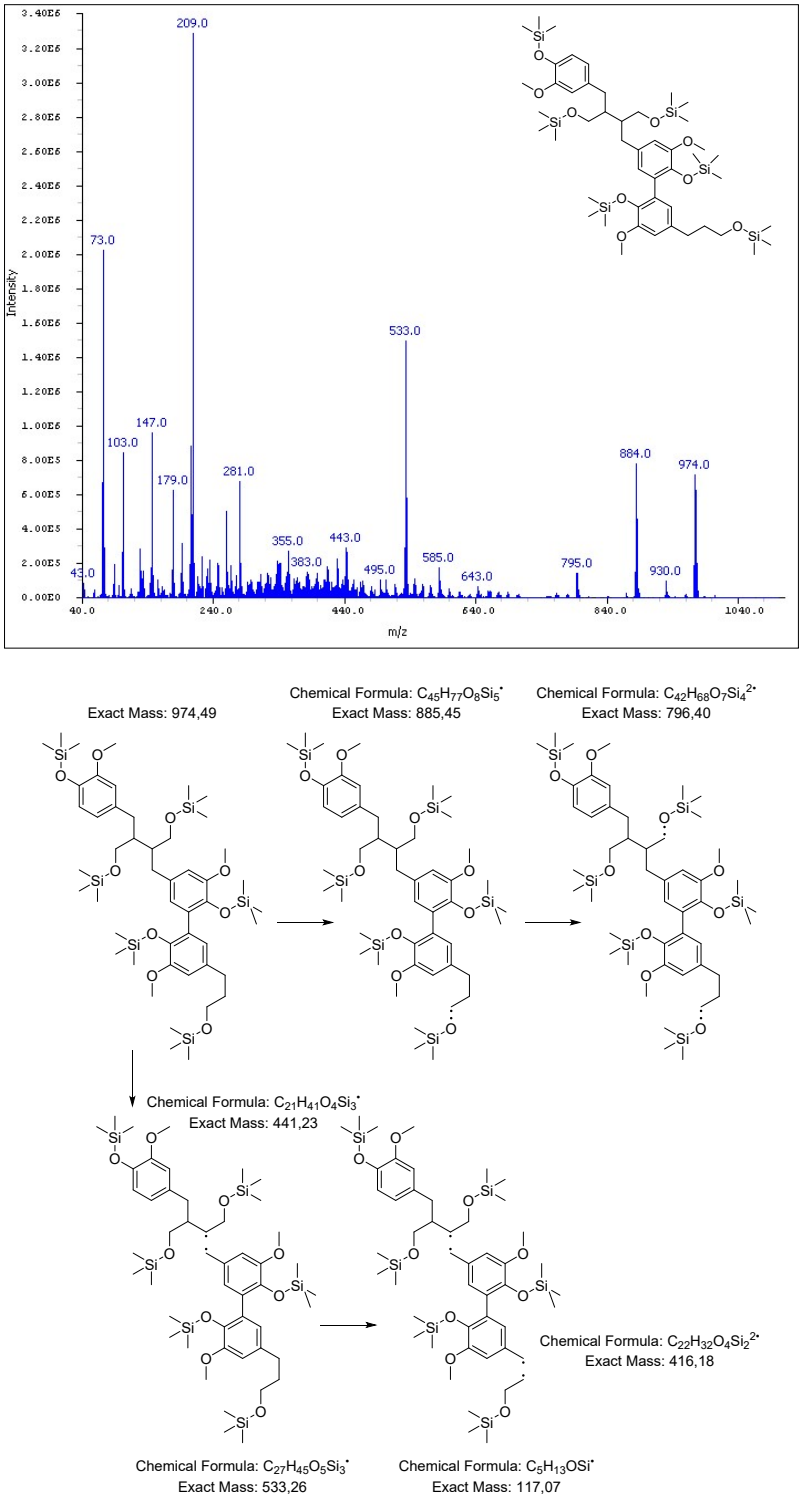

Figure S4.4. Mass spectrum and fragmentation pattern analysis of trimer **T4**.

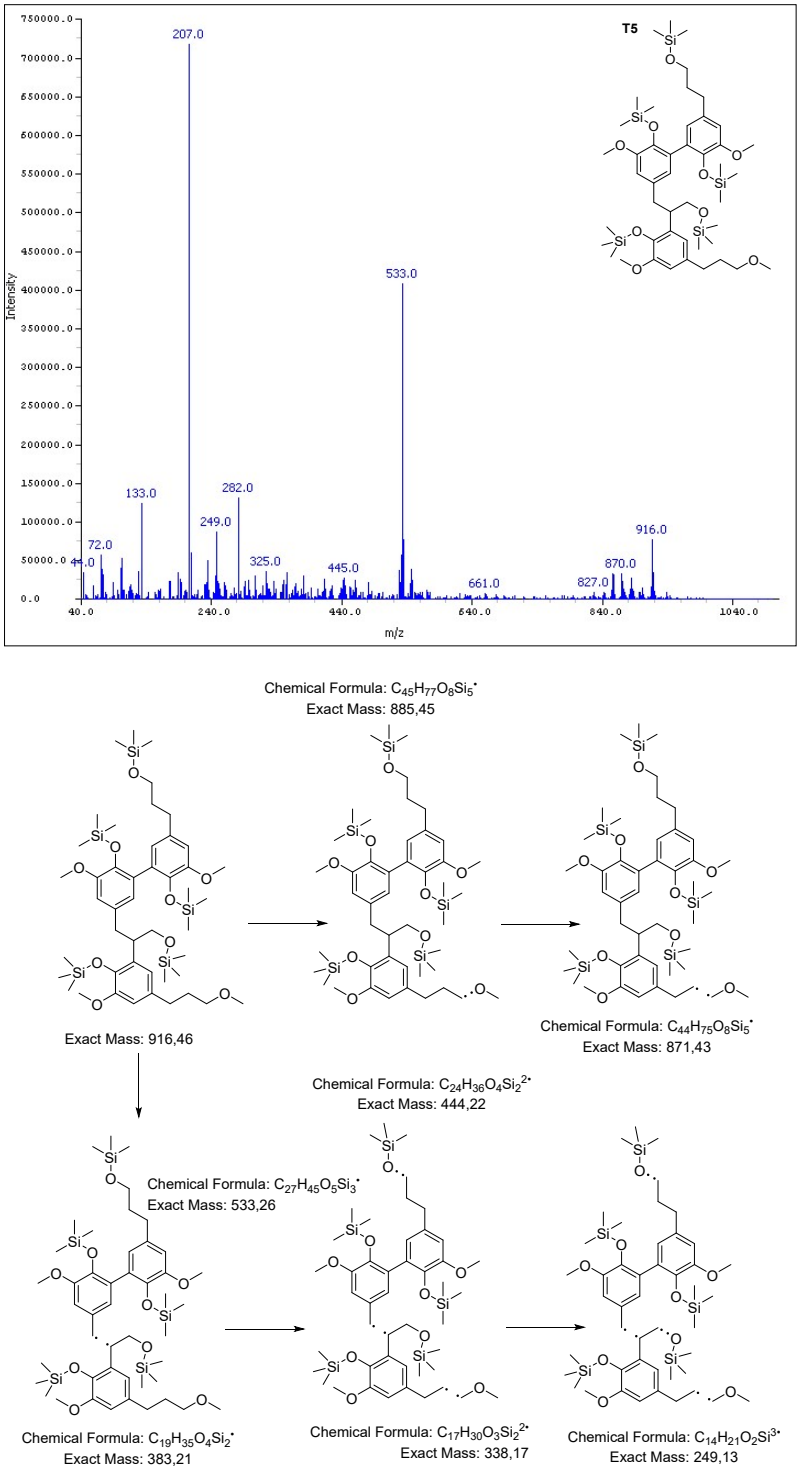

Figure S4.5. Mass spectrum and fragmentation pattern analysis of trimer **T5**.

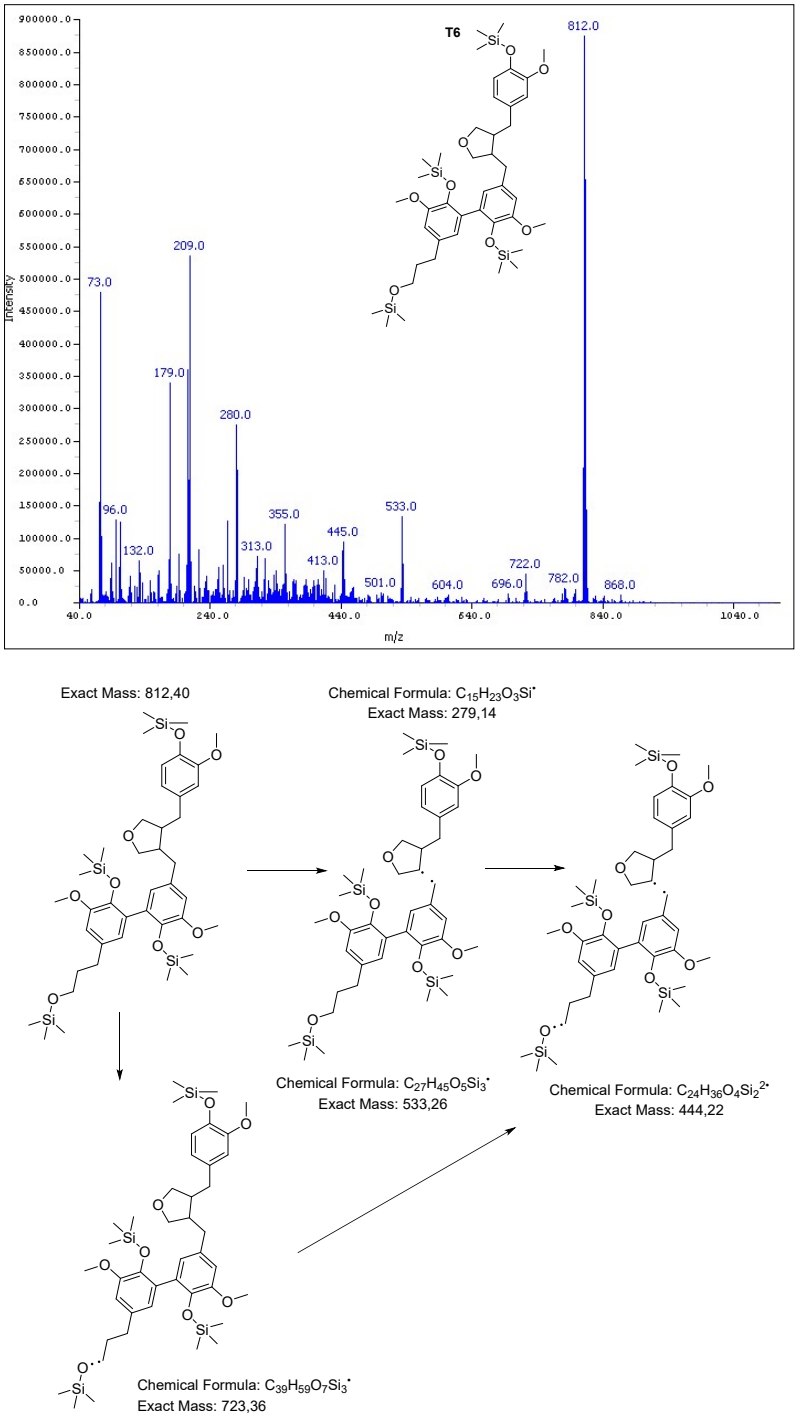

Figure S4.6. Mass spectrum and fragmentation pattern analysis of trimer **T6**.

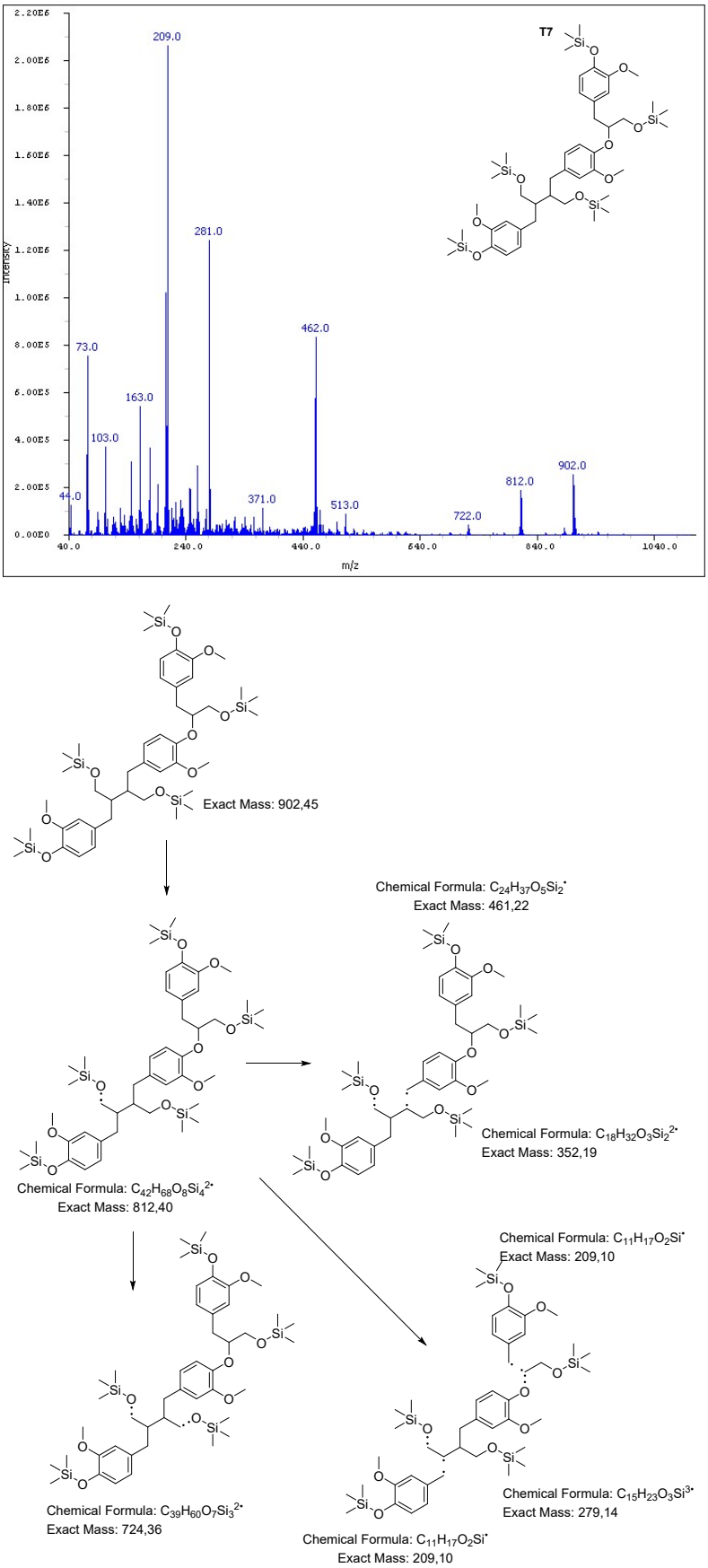

Figure S4.7. Mass spectrum and fragmentation pattern analysis of trimer **T7**.

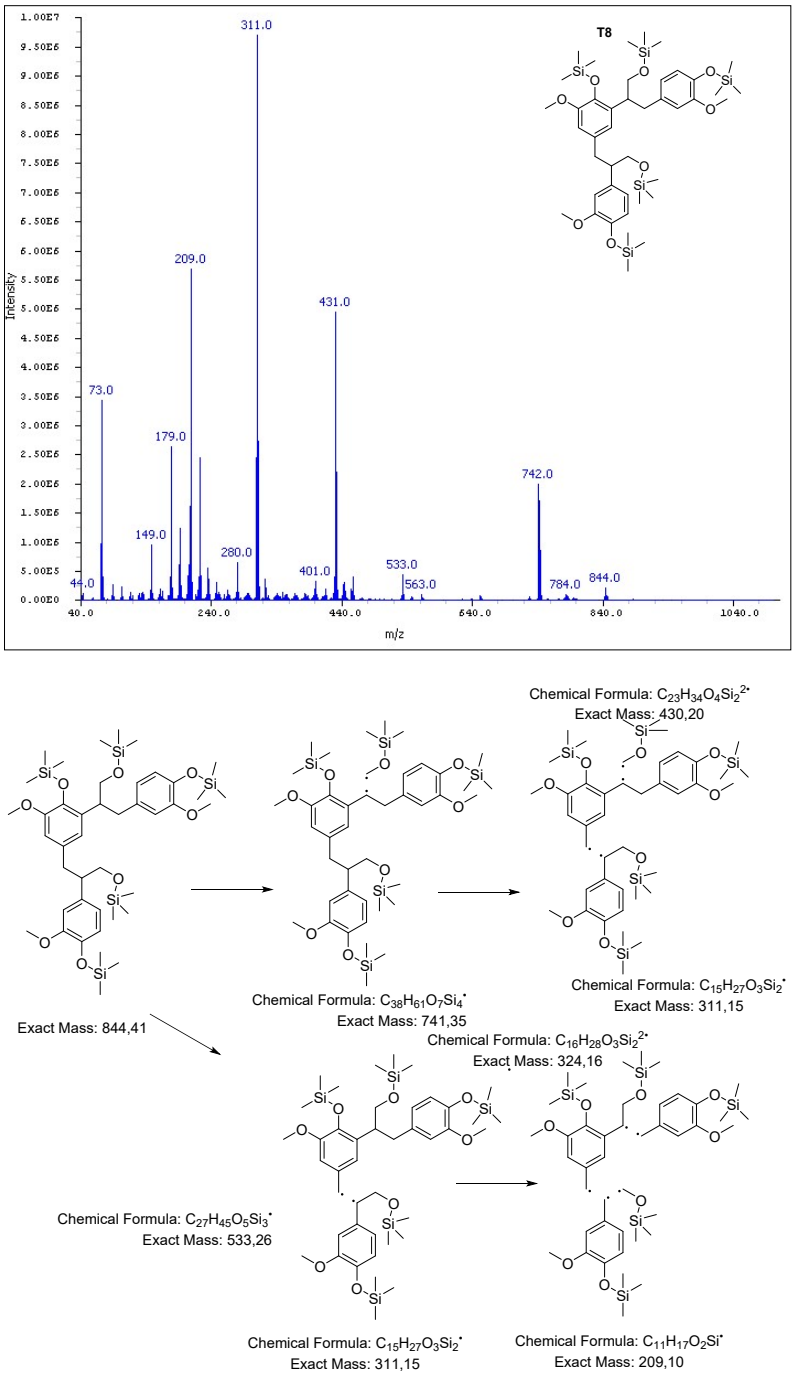

Figure S4.8. Mass spectrum and fragmentation pattern analysis of trimer **T8**.

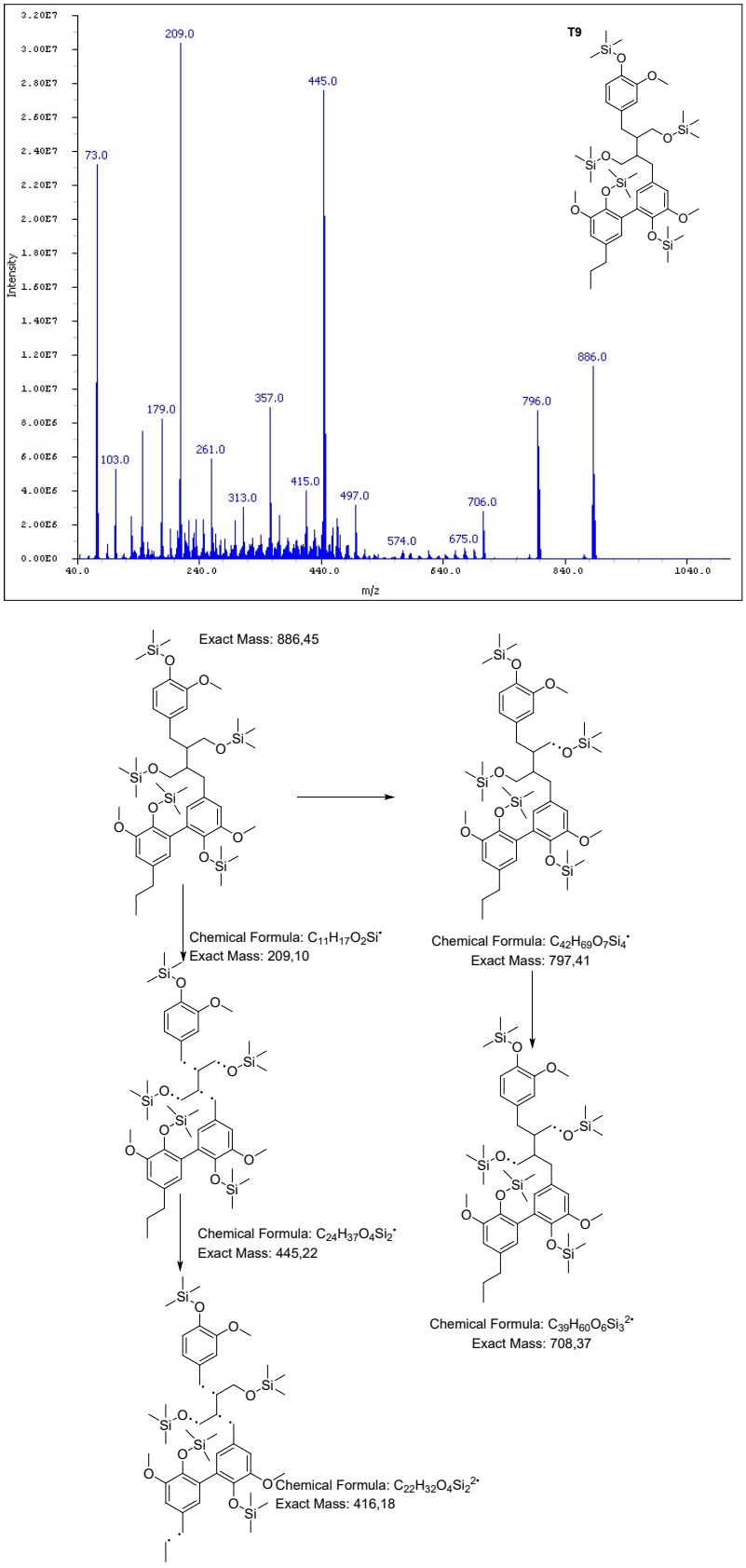

Figure S4.9. Mass spectrum and fragmentation pattern analysis of trimer **T9**

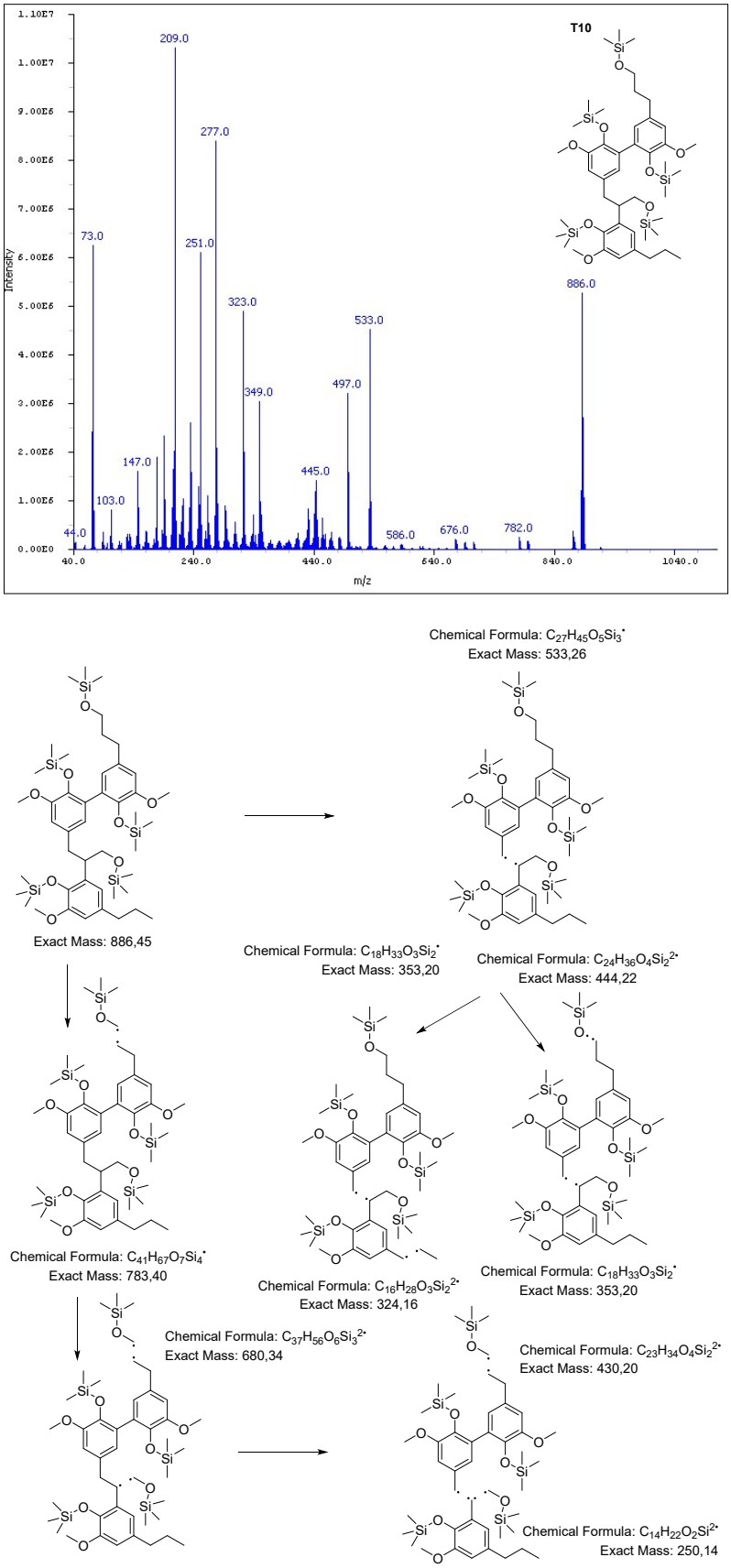

Figure S4.10. Mass spectrum and fragmentation pattern analysis of trimer **T10**.

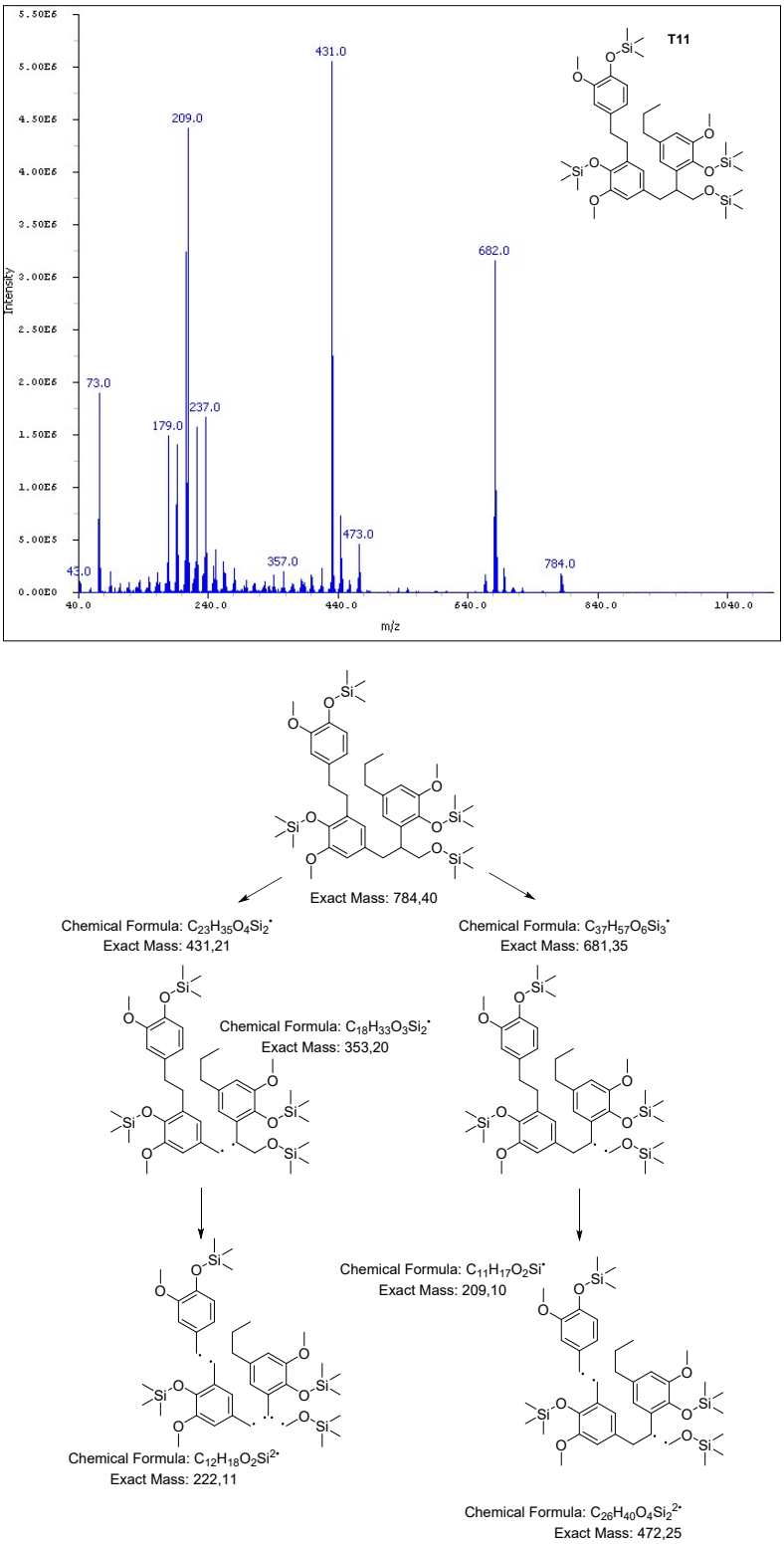

Figure S4.11. Mass spectrum and fragmentation pattern analysis of trimer **T11**.

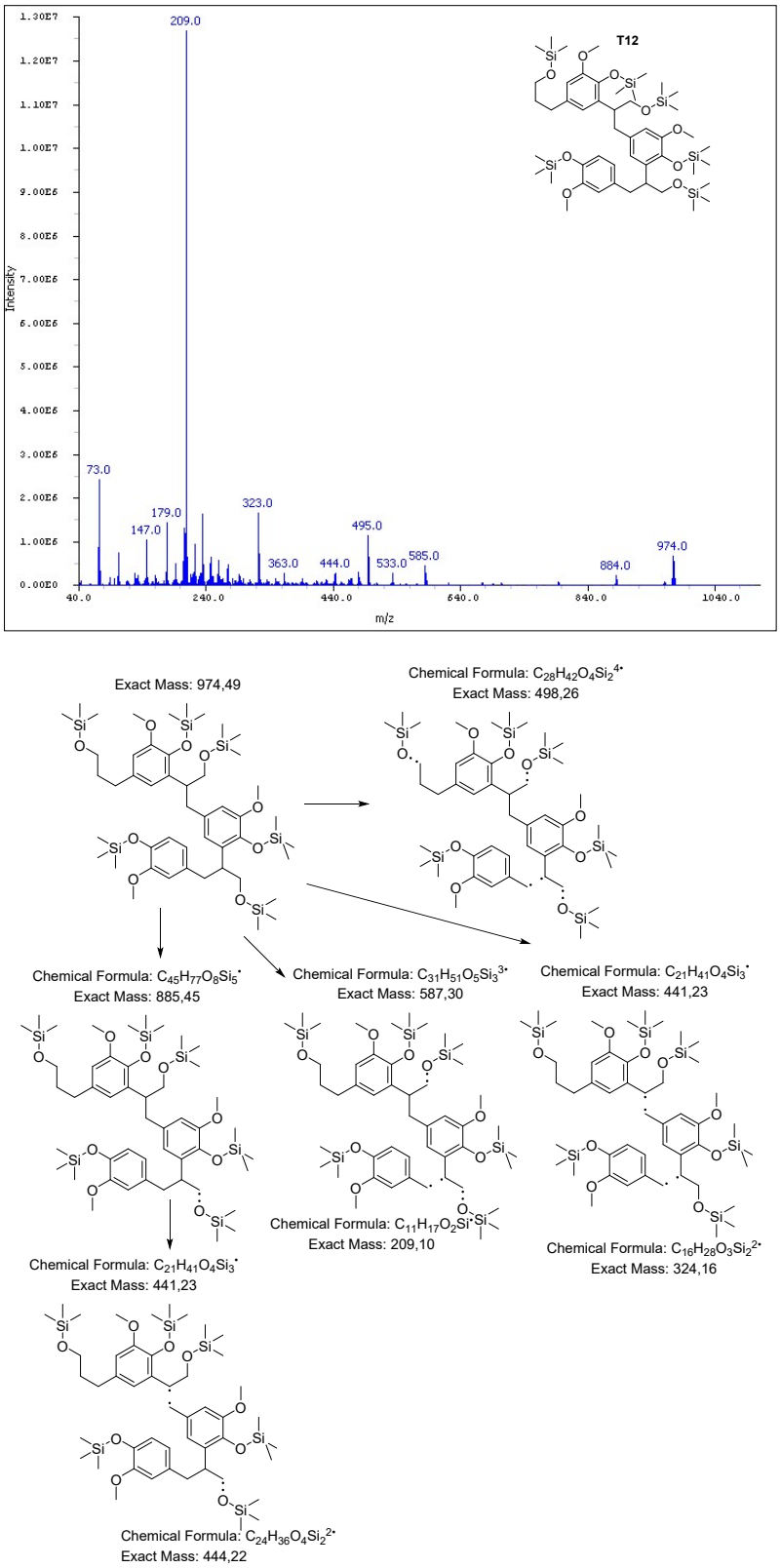

Figure S4.12. Mass spectrum and fragmentation pattern analysis of trimer **T12**.

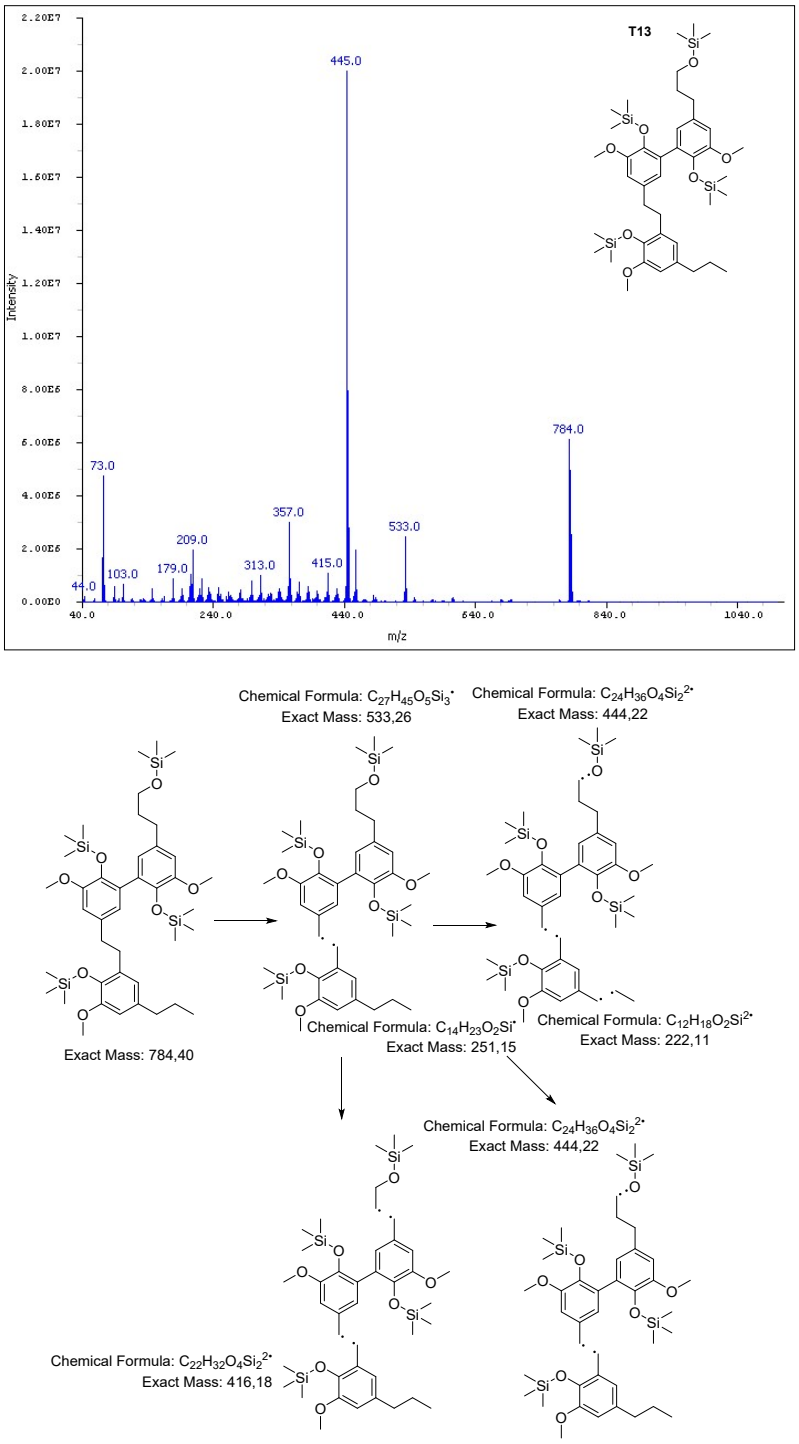

Figure S4.13. Mass spectrum and fragmentation pattern analysis of trimer **T13**.

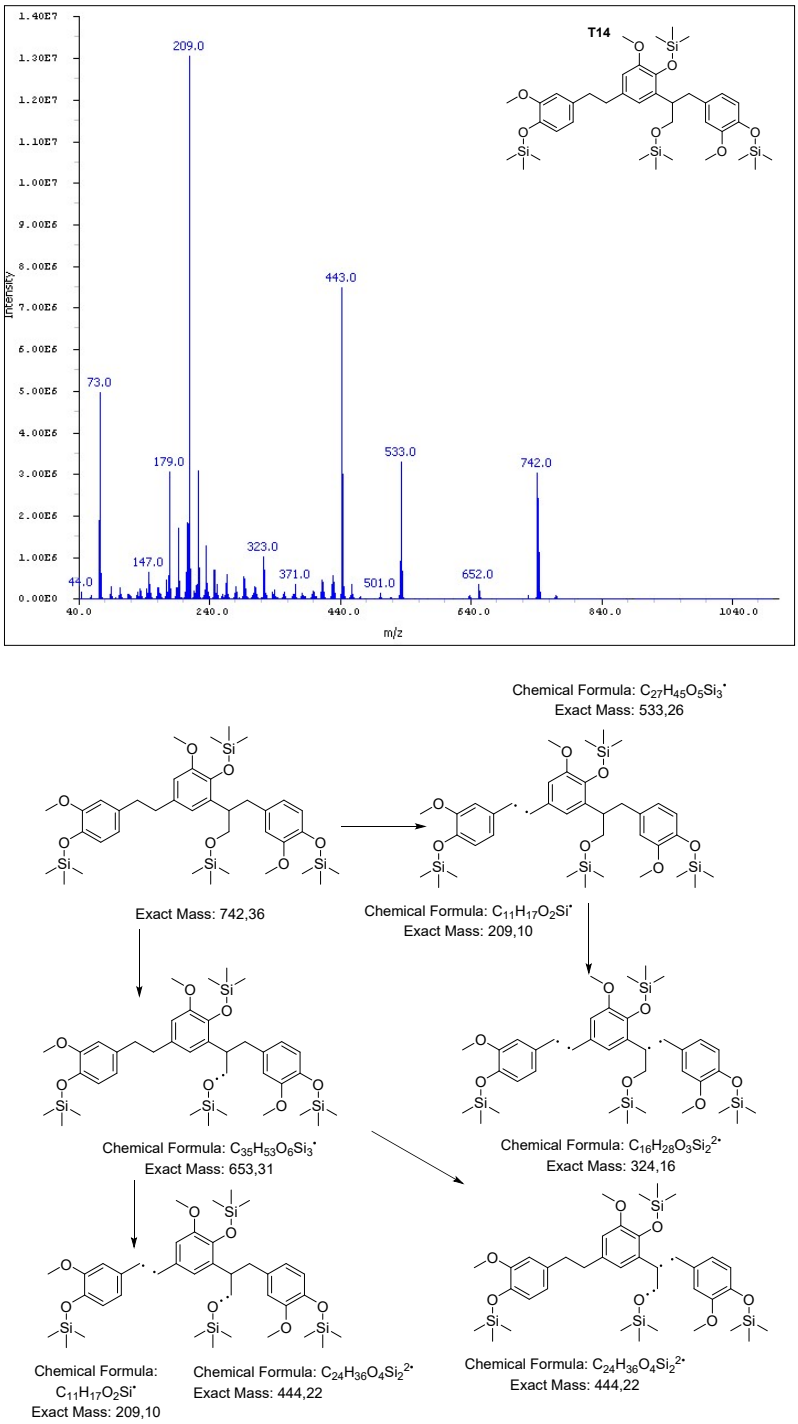

Figure S4.14. Mass spectrum and fragmentation pattern analysis of trimer **T14**.

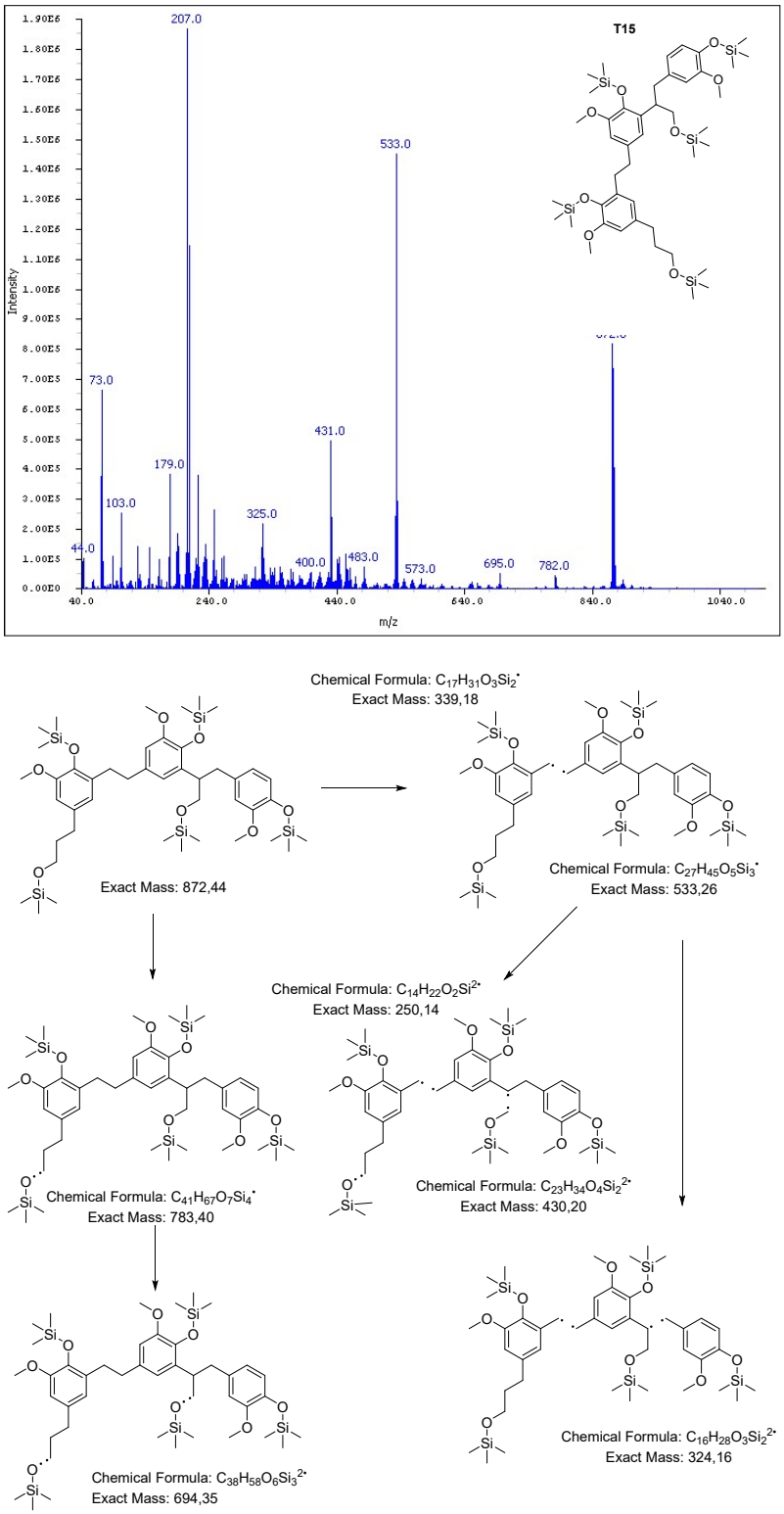

Figure S4.15. Mass spectrum and fragmentation pattern analysis of trimer **T15**.

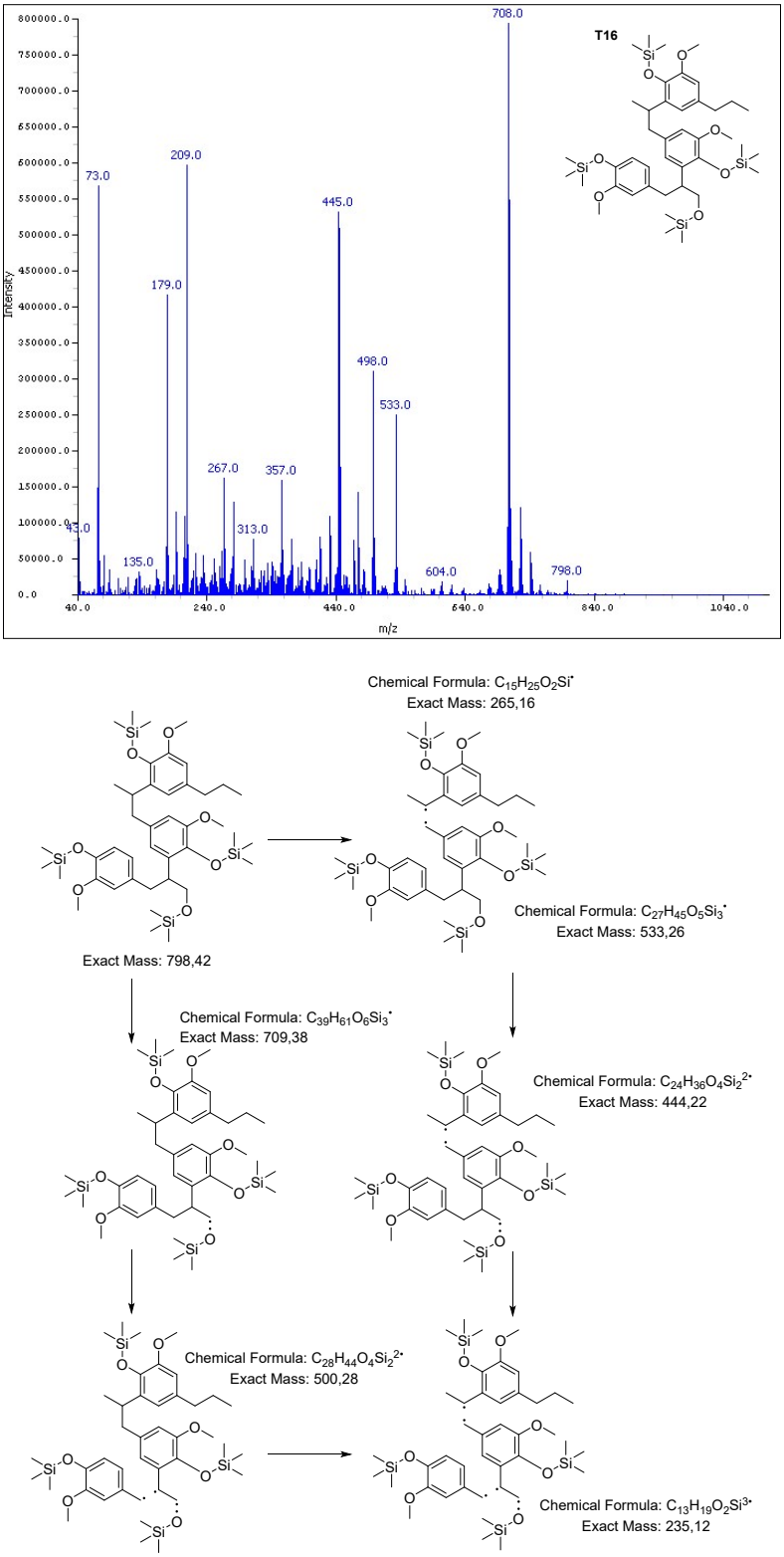

Figure S4.16. Mass spectrum and fragmentation pattern analysis of trimer **T16**.

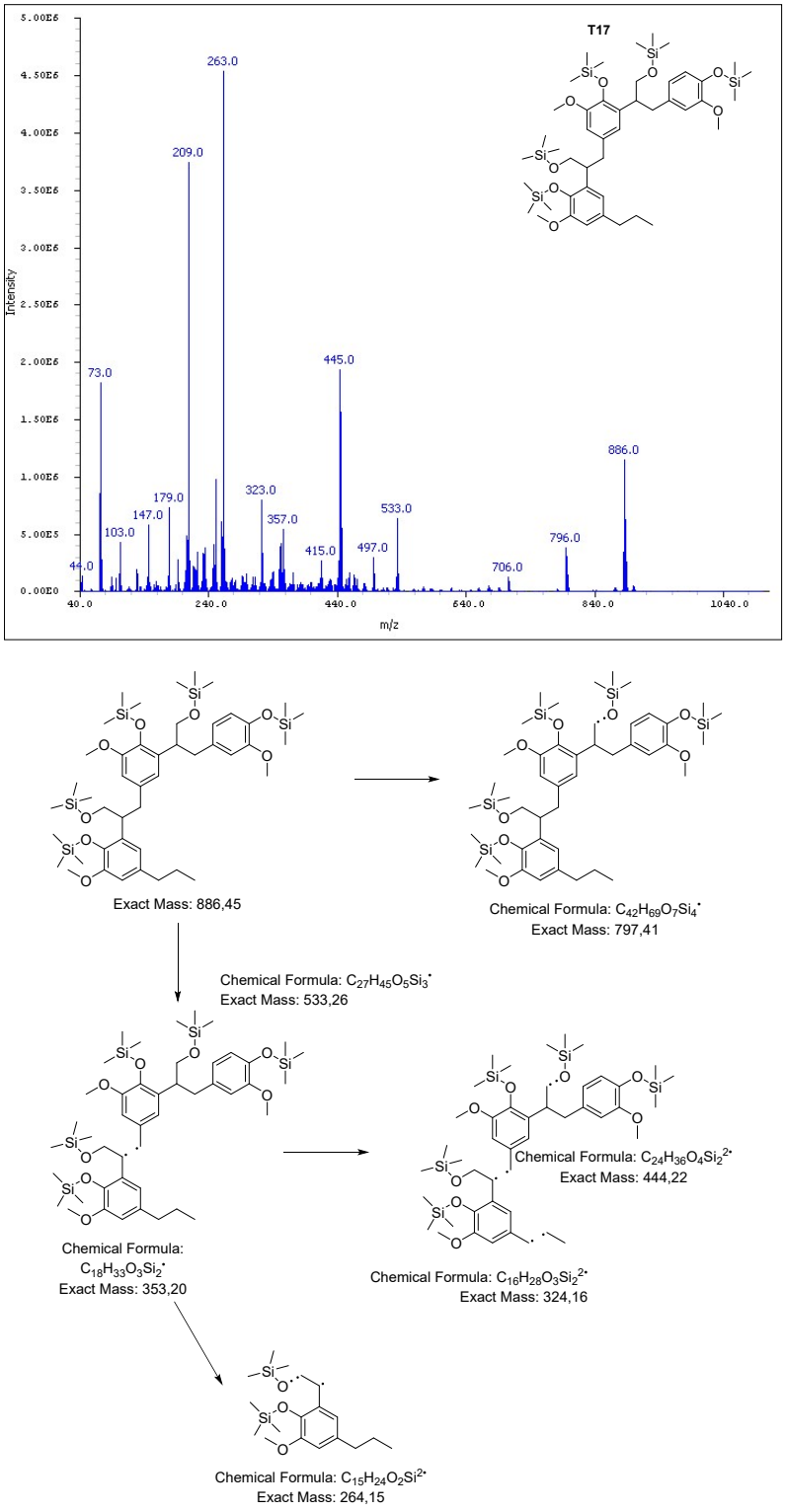

Figure S4.17. Mass spectrum and fragmentation pattern analysis of trimer **T17**.

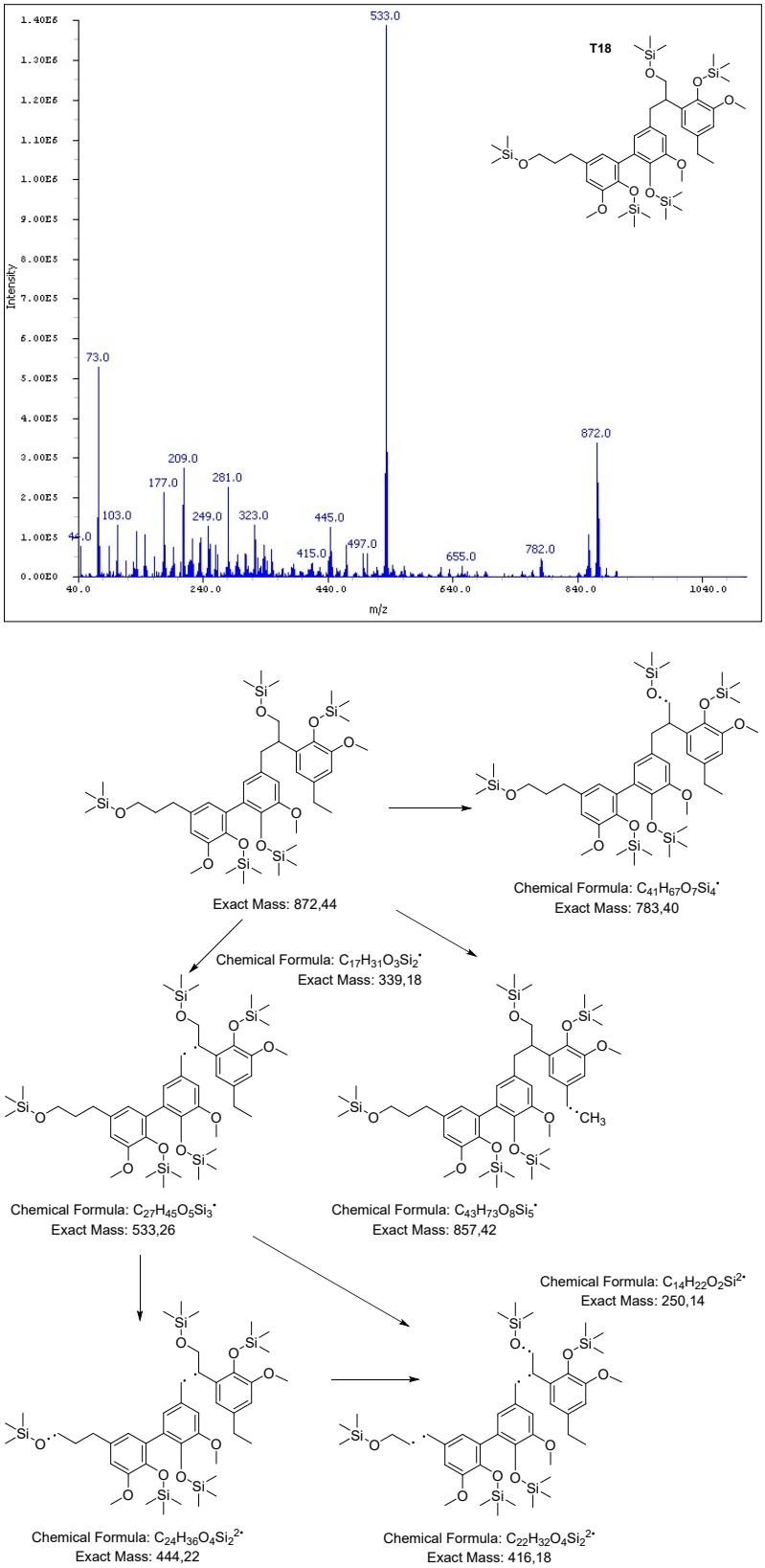

Figure S4.18. Mass spectrum and fragmentation pattern analysis of trimer **T18**.

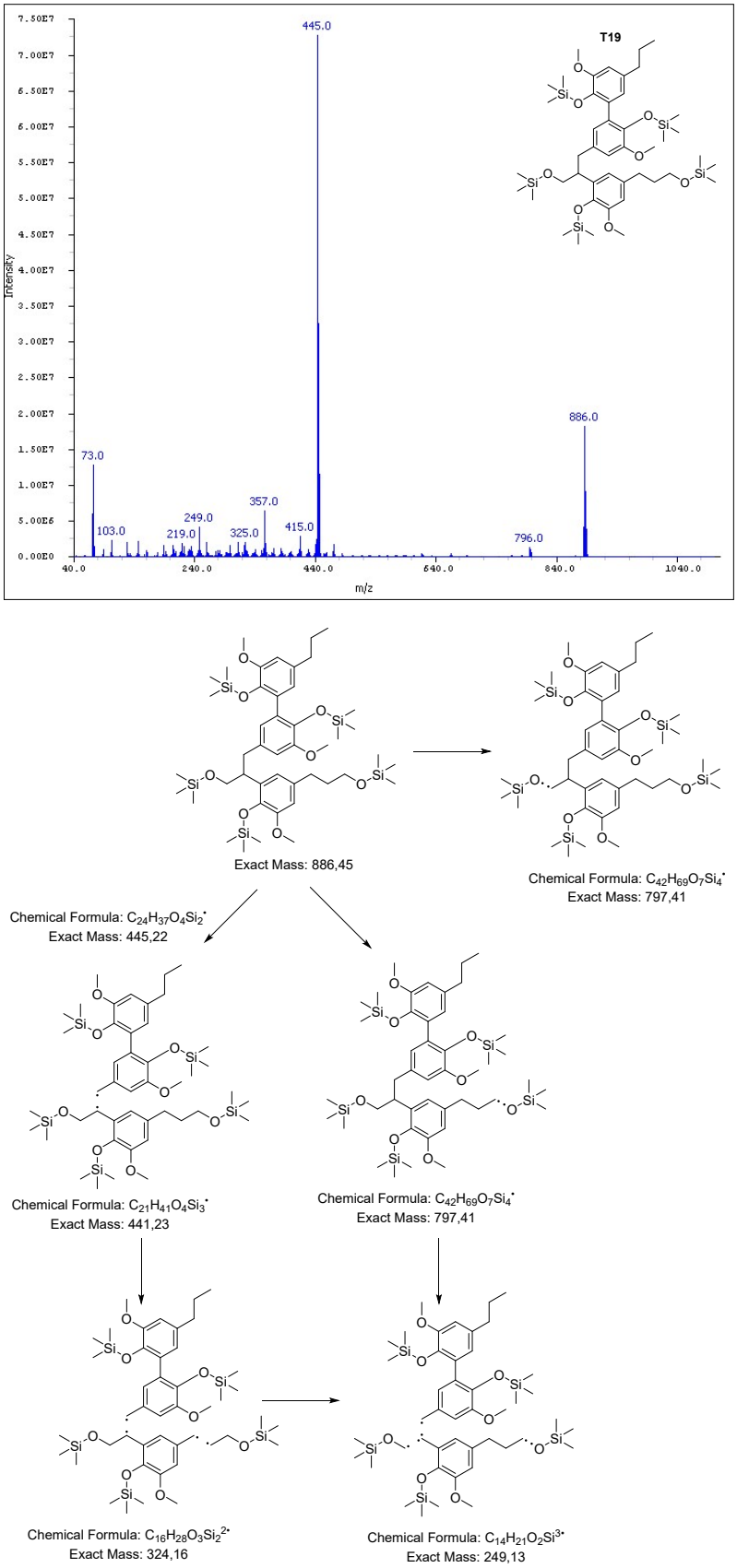

Figure S4.19. Mass spectrum and fragmentation pattern analysis of trimer **T19**.

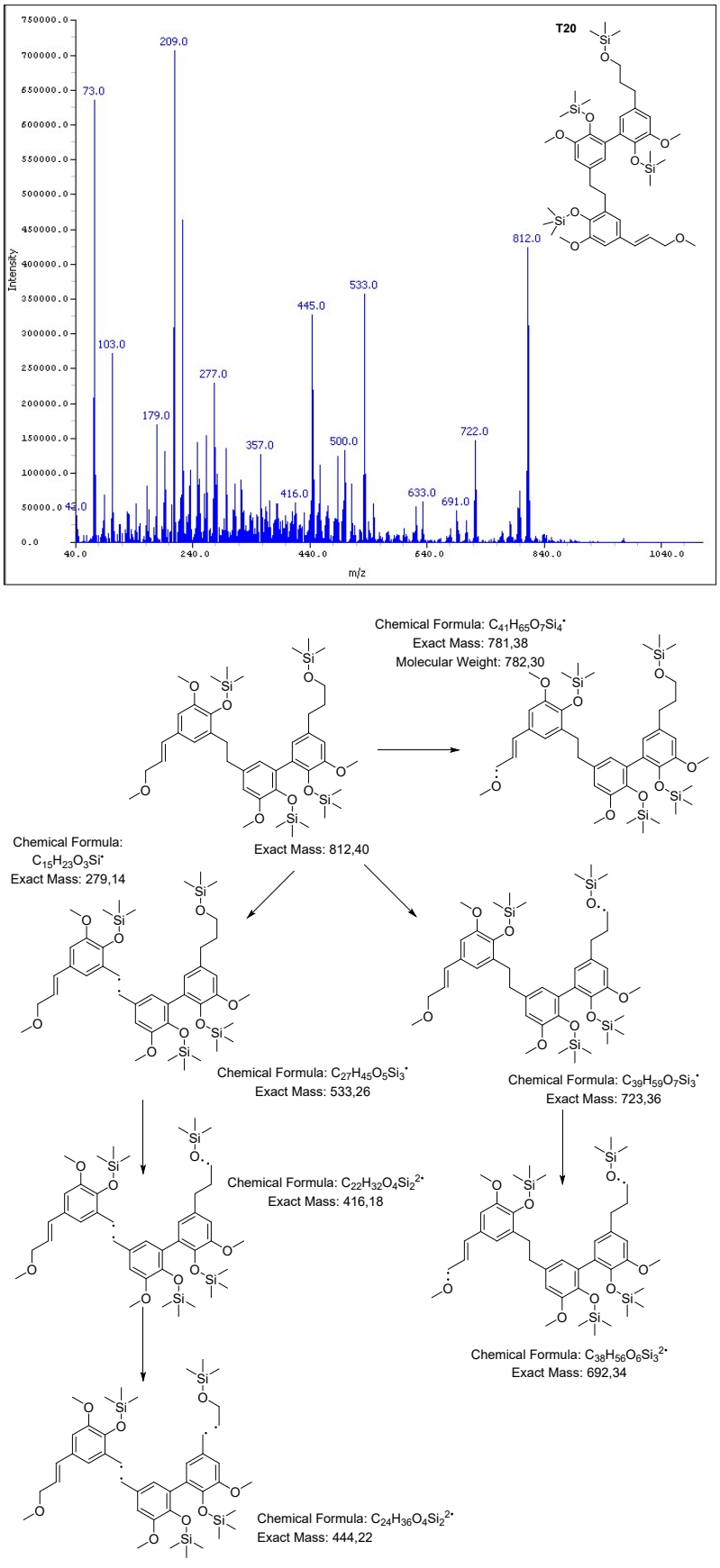

Figure S4.20. Mass spectrum and fragmentation pattern analysis of trimer **T20**.

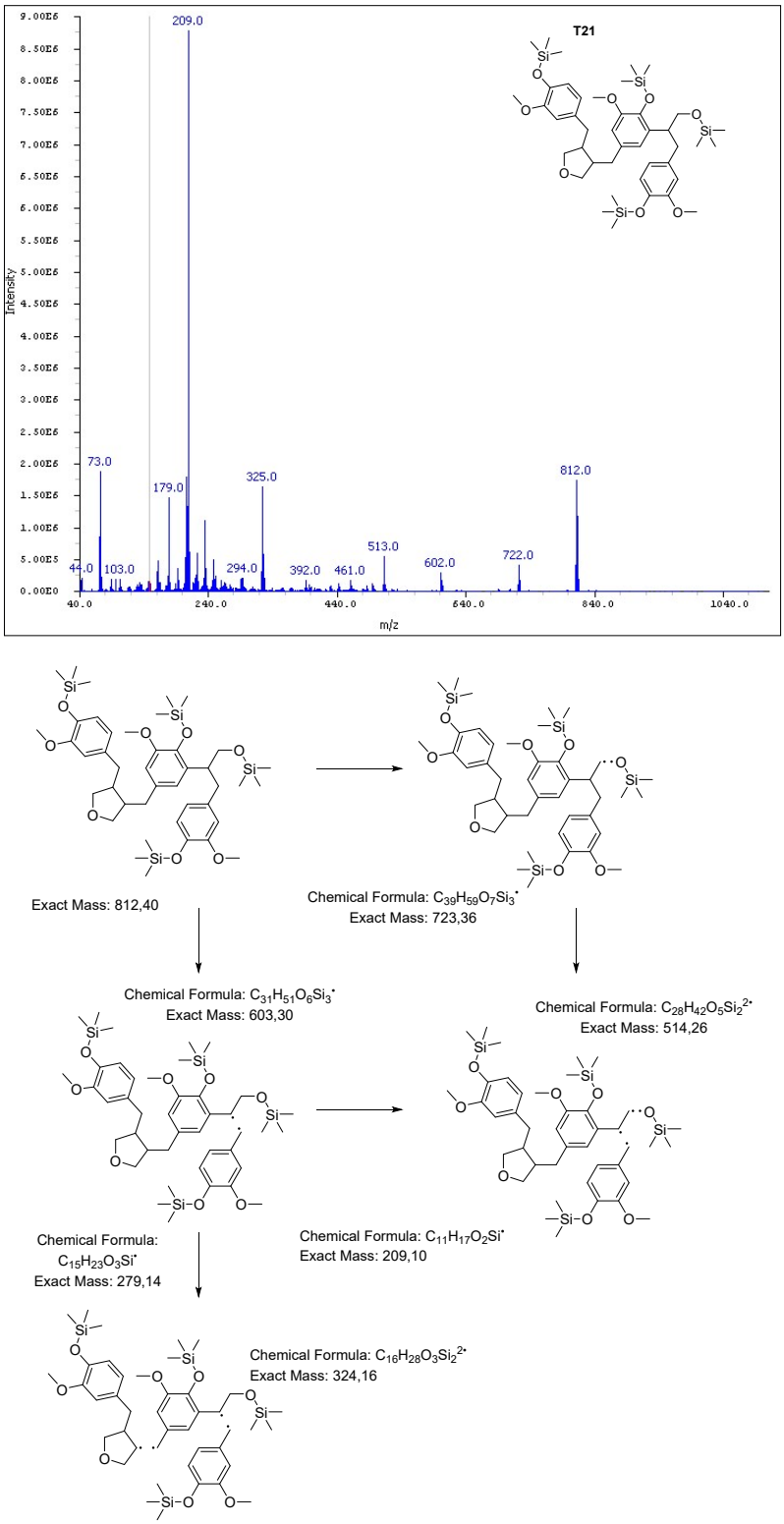

Figure S4.21. Mass spectrum and fragmentation pattern analysis of trimer **T21**.

S5. Comparison of the inter-unit linkage selectivity obtained by GC × GC and ^{1}H-^{13}C HSQC NMR Spectroscopy

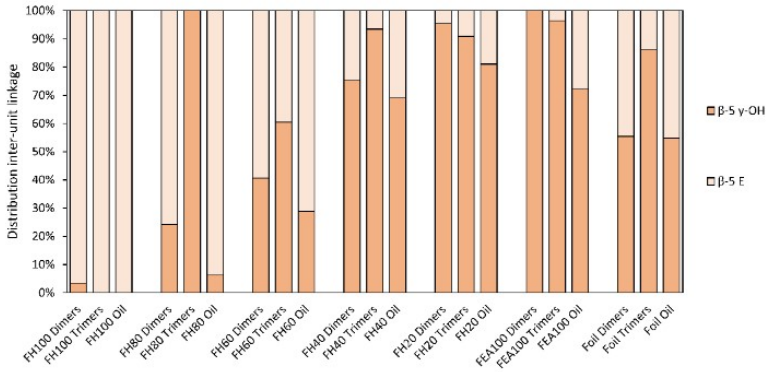

Figure S5.1. Comparison of distribution of β-5 inter-unit linkages in the different RCF lignin fractions.

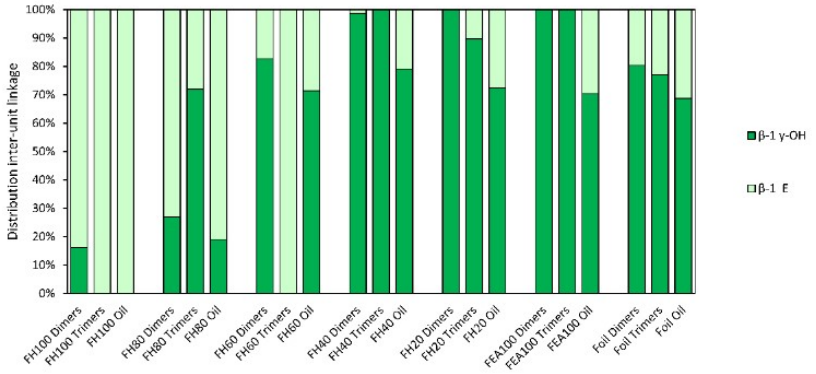

Figure S5.2. Comparison of distribution of β-1 inter-unit linkages in the different RCF lignin fractions.

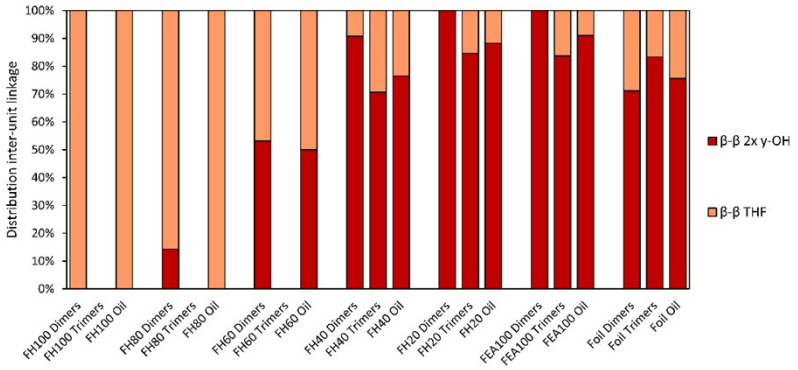

Figure S5.3. Comparison of distribution of β-β inter-unit linkages in the different RCF lignin fractions.

Note S5.4. The formulas used to recalculate the GC × GC results are as follows

$$\text{Monomers (vs G-units)} = wt\%\ monomers\ in\ fraction^{a}\ x \frac{mole\ monomer\ (n)}{total\ mole\ monomers\ in\ fraction}$$

$$\text{Dimers (vs G-units)} = wt\%\ dimers\ in\ fraction^{a}\ x \frac{\left(\sum_{n}^{m} \frac{mole\ dimer\ (n)}{total\ mole\ dimers\ in\ fraction}\right)}{2\ *}$$

$$\text{Trimers (vs G-units)} = \frac{wt\%\ trimers\ in\ fraction^{a}\ x\ \left(\sum_{n}^{m}\frac{mole\ trimer\ (n)}{total\ mole\ trimers\ in\ fraction}\right)}{3\ *}$$

With n = specific molecule bearing a specific molecular structure in the fraction and m the total amount of molecules bearing that specific molecular structure in that fraction.

*= correction for number of aromatics per molecule

[a]= assumption that 100% of a sample's mass = lignin

S6. Synthesis of lignin model compounds

General information for synthesis of model compounds

All chemicals and solvents were purchased from Sigma-Aldrich (St. Louis, MO, USA) and used without additional purification. Nuclear magnetic resonance (NMR) spectra were acquired on a Bruker AVANCE 400 MHz spectrometer equipped with a 5 mm BBO probe. Bruker's Topspin 3.6.2 software was used for data processing. Tetramethylsilane was used as an internal reference of 0 ppm for ^{1}H-NMR spectra, and solvent peaks were used for ^{13}C-NMR spectra (δ_C $CDCl_3$ 77.23, acetone-d_6 29.92 ppm). The acquisition parameters for ^{1}H-NMR spectra included a relaxation delay 1.0 s, an acquisition time of 4.09 s with 64 scans, and a 90° pulse width, a relaxation delay 2.0 s and an acquisition time of 1.1 s with 1024 scans for ^{13}C-NMR spectroscopy. The gradient correlation spectroscopy (gCOSY) and heteronuclear single quantum coherence (HSQC) were recorded using standard Bruker implementation.

Synthesis method

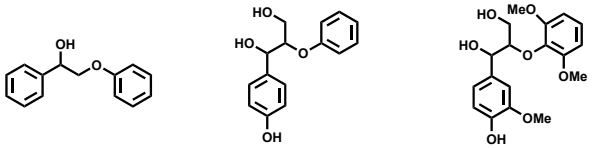

1 **2** **3**

2-Phenoxy-1-phenyl ethanol (**1**) and 1-(4-hydroxyphenyl)-2-phenoxy-1,3-propanediol (**2**), were synthesized as previously described.[8,9] 2-(2,6-dimethoxyphenoxy)-1-(4-hydroxy-3-methoxyphenyl)propane-1,3-diol (**3**) was prepared as follows (**Figure S6.1.**).

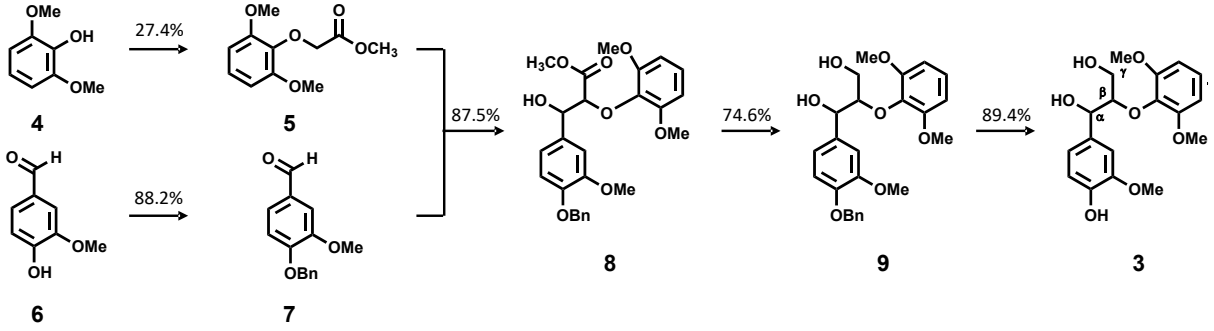

Figure S6.1. Synthetic route of 2-(2,6-dimethoxyphenoxy)-1-(4-hydroxy-3-methoxyphenyl)propane-1,3-diol (**3**).

Methyl 2,6-dimethoxyphenoxyl acetate (**5**)

To the solution of syringol (compound **4**, 7.71 g, 50.0 mmol), potassium carbonate (10.4 g, 75.0 mmol) and potassium iodate (0.83 g, 5.0 mmol) in acetone (100 mL), 2-methyl bromoacetate (5.23 ml, 55.0 mmol) was added at room temperature. After refluxing for 16 hours, excess K_2CO_3 was removed by filtration. The solvent in the filtrate was removed by rotary evaporation. The remaining syrup was diluted with H_2O (50 mL) and extracted with ethyl acetate (70 mL) three times. The organic layer was washed with brine two times and then dried over $MgSO_4$. Crude compound **5** (2.52g, 27.4 mol%) was obtained and used for following coupling reaction without purification.

Benzylated vanillin (**7**)

To the solution of vanillin (compound **6**, 6.50 g, 42.7 mmol) in DMF (5 mL), benzyl bromide (6.16 mL, 51.3 mmol), potassium carbonate (8.86 g, 64.1 mmol) and potassium iodate (0.71 g, 4.27 mmol) were added at room temperature. After stirring for 14 hours at room temperature, the reaction mixture was filtered and washed with ethyl acetate (50 mL) to remove excess K_2CO_3. The filtrate was diluted with H_2O (60 mL) and extracted with ethyl acetate (30 mL) three times. The combined organic layer was washed with brine two times and then dried over Na_2SO_4. Crude oil obtained was recrystallized from ethanol/hexane (1:1) to yield white powder (compound **7**, 7.94g) with 88.2 mol% yield.

β-Hydroxy methyl ester (**8**)

To the solution of diisopropylamine (1.88 mL, 13.4 mmol) in anhydrous THF (30 mL), *n*-butyllithium/n-hexane (2.5 M) (5.35 mL, 13.4 mmol) was added dropwisely at -78°C over 20 min. After stirring for 30 min, methyl-2,6-dimethoxy phenylacetate (compound **5**, 0.91 g, 3.73 mmol) in anhydrous THF (10 mL) was added dropwise over 1 hour at -78°C. After 30 min stirring, benzylated vanillin (compound **7,** 2.70 g, 11.2 mmol) was added dropwise over 1 hour. After 3 hours stirring, the reaction solution was heated from -78°C to room temperature, and the reaction was quenched by addition of ethyl acetate (150 mL) and H_2O (100 mL). The reaction mixture was extracted with ethyl acetate (50 mL) two times. The combined ethyl acetate layer was washed with brine and dried over $MgSO_4$. Crude oil was purified by a silica gel column to obtain of β-hydroxy methylester (compound **8**, 4.57 g, 87.5 mol%) with an erythro and *threo* isomer mixture. *Erythro* isomer (**8E**): ^{1}H NMR (400 MHz, $CDCl_3$) δ 7.43-7.26 (5H, m, Arom-H), 7.06-7.00 (2H, m, Arom-H), 6.83 (2H, s, Arom-H), 6.59 (2H, d, *J*=11.2Hz, Arom-H), 5.13 (2H, s, CH_2), 4.94 (H, d, *J*=5.0Hz, Hα), 4.71 (1H, d, *J*=5.1Hz, Hβ), 3.88 (3H, s, OMe), 3.83 (6H, s, 2xOMe), 3.56 (3H, s, CH_3COO-). ^{13}C NMR (100 MHz, $CDCl_3$) δ 169.4 (Cγ), 152.9, 149.6, 147.8, 137.4, 136.2, 132.1, 128.6, 127.9, 127.4, 124.6, 119.0, 113.8, 110.4, 105.4, 86.0 (Cβ), 73.5 (Cα), 71.1 (CH_2), 56.3 (OMe), 56.1 (OMe), 51.9 (*C*H_3COO-) ppm. *Threo* isomer (**8T**): ^{1}H NMR (400 MHz, $CDCl_3/D_2O$(9:1)) δ 7.42-7.26 (5H, m, Arom-H), 7.07-7.01 (1H, m, Arom-H), 6.91 (1H, s, Arom-H), 6.82-6.75 (2H, m, Arom-H), 6.59 (2H, d, *J*=11.2Hz, Arom-H), 5.13 (2H, s, CH_2), 4.95 (H, d, *J*=11.5Hz, Hα), 4.05 (1H, d, *J*=11.5Hz, Hβ), 3.86 (3H, s, OMe), 3.83 (6H, s, 2xOMe), 3.52 (3H, s, CH_3COO-). ^{13}C NMR (100 MHz, $CDCl_3/D_2O$(9:1)) δ 170.1 (Cγ), 152.7, 149.9, 148.2, 137.3, 130.8, 128.7, 128.0, 127.5, 124.8, 119.6, 113.9, 110.3, 105.3, 89.9 (Cβ), 75.5 (Cα), 71.1 (CH_2), 56.3 (OMe), 56.2 (OMe), 51.9 (*C*H_3COO-) ppm.

Benzylated β-O-4 dimer (**9**)

To a solution of the β-hydroxy methyl ester (compound **8**, 2.19 mg, 4.67 mmol) in methanol (7 mL), $NaBH_4$ (0.88 g, 23.4 mmol) was added at 0°C. After stirring for 4 days at room temperature, the reaction mixture was neutralized with 10% AcOH aq, diluted with H_2O (70 mL) and then extracted with ethyl acetate (70 mL) three times. The combined ethyl acetate layer was washed with brine and dried over $MgSO_4$. Residual solid was purified by a silica gel column chromatography with ethyl acetate/hexane (1:1, v/v) as an eluent to obtain pale yellow syrup (compound **9**, 1.53 g, 74.6 mol%, *erythro*/*threo* isomer mixture). ^{1}H NMR (400 MHz, $CDCl_3$) δ 7.40-7.21 (5H, m, Arom-H), 7.04-6.94 (2H, m, Arom-H), 6.84-6.76 (2H, m, Arom-H), 6.56 (2H, d, *J*=8.5Hz, Arom-H), 5.06 (2H, s, CH_2), 5.01 (H, t, *J*=3.2Hz, Hα), 4.30 (1H, d, *J*=3.2Hz, OH), 4.15 (1H, m, Hβ), 3.92 (1H, m, Hγ), 3.82 (3H, s, OMe), 3.75 (6H, s, 2xOMe), 3.51 (1H, m, Hγ), 3.37 (1H, m, OH). ^{13}C NMR (100 MHz, $CDCl_3$) δ 153.2, 149.4, 147.0, 137.0, 134.8, 132.9, 128.2, 127.5, 127.0, 124.1, 118.0, 113.6, 109.6, 105.1, 86.6 (Cβ), 72.2 (Cα), 70.7 (CH_2), 60.2 (Cγ), 55.8 (OMe), 55.7 (OMe) ppm.

2-(2,6-dimethoxyphenoxy)-1-(4-hydroxy-3-methoxyphenyl)propane-1,3-diol (Compound **3**)

To a solution of compound **9** (28.2 mg, 4.67 mmol) in methanol (3 mL), 5% Pd/C (30 mg) was added at room temperature. After stirring for 1.5 hours under H_2 atmosphere, the reaction mixture was filtered to remove Pd/C and then the filtrate was dried to yield a white powder (compound **3**, 20.4 mg, 89.4 mol%, *erythro*/*threo* isomer mixture). Acetylated compound **3**: ^{1}H NMR (400 MHz, $CDCl_3$) δ 6.92-7.02 (4H, broad, Arom-H), 6.53 (2H, d, *J*=8.4Hz, Arom-H), 6.16 (0.13H, d, *J*=6.3Hz, Hα), 6.11 (0.84H, d, *J*=5.0Hz, Hα), 4.63 (1H, q, *J*=5.2Hz, Hβ), 4.49 (1H, dd, *J*=12.0, 5.5Hz, Hγ), 4.26 (1H, dd, *J*=12.0, 3.6Hz, Hγ), 3.80 (3H, s, OMe), 3.74 (6H, s, 2xOMe), 2.29 (3H, s, CH_3CO-), 2.14 (3H, s, CH_3CO-), 1.98 (3H, s, CH_3CO-). ^{13}C NMR (100 MHz, $CDCl_3$) δ 171.1 (CH_3*C*O-), 169.7 (CH_3*C*O-), 169.1 (CH_3*C*O-), 153.6, 151.0, 139.6, 136.4, 135.4, 124.3, 122.6, 119.3, 111.6, 105.4, 81.0 (Cβ), 74.2 (Cα), 62.9 (Cγ), 56.13 (OMe), 56.06 (OMe), 21.3 (*C*H_3CO-), 20.93 (*C*H_3CO-), 20.85 (*C*H_3CO-) ppm.

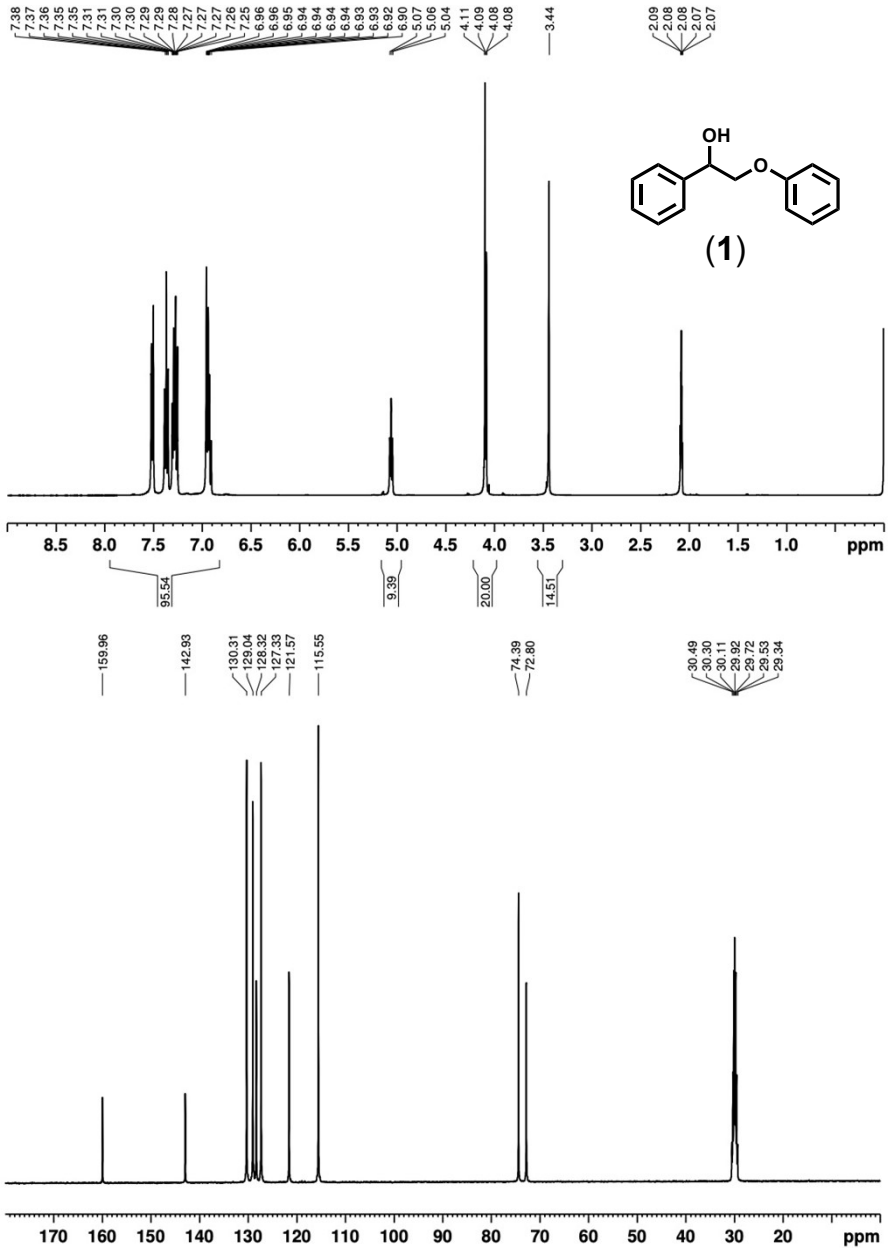

Figure S6.2. ^{1}H and ^{13}C-NMR spectra (Acetone-d_6) of 2-Phenoxy-1-phenyl ethanol (compound **1**).

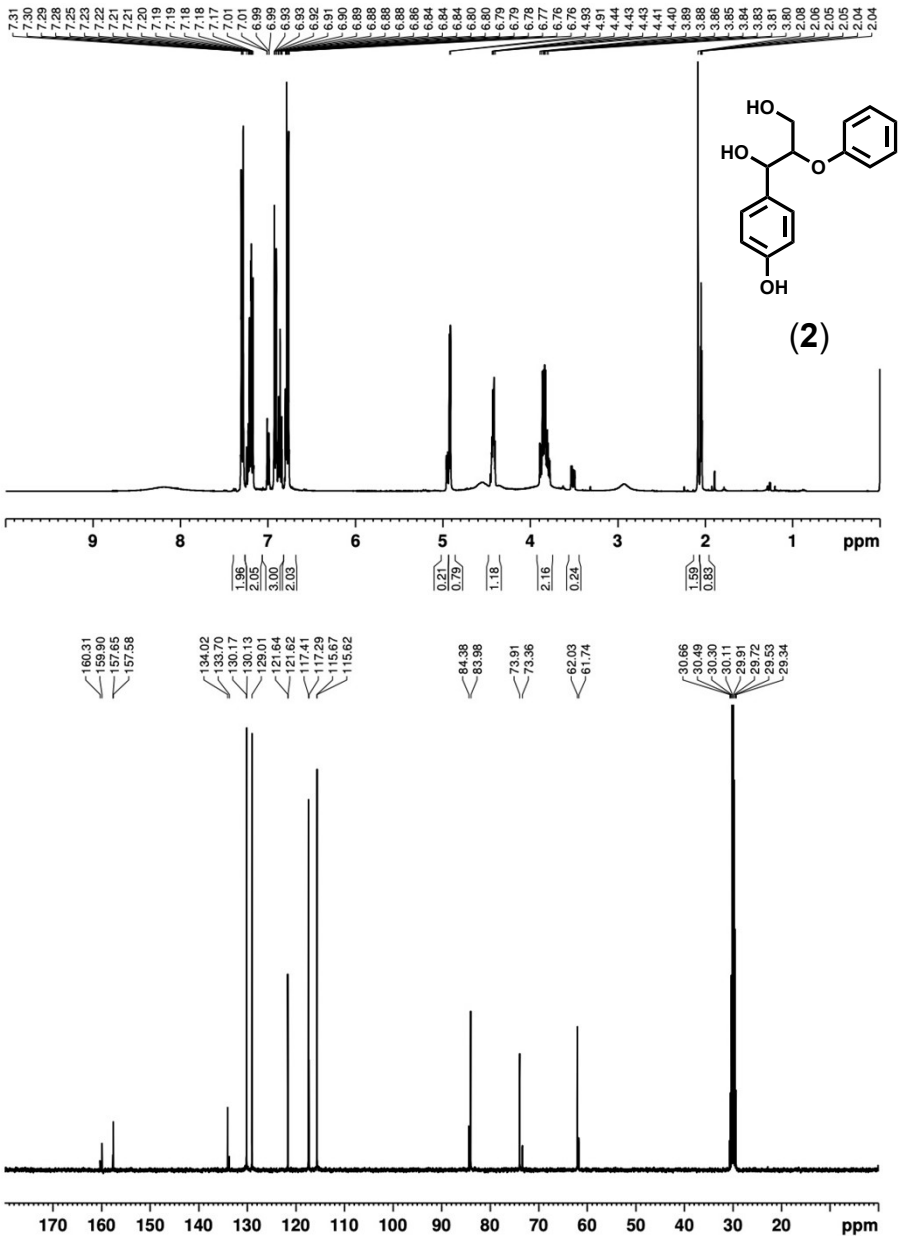

Figure S6.3. ^{1}H and ^{13}C-NMR spectra (Acetone-d_6) of 1-(4-hydroxyphenyl)-2-phenoxy-1,3-propanediol (**2**).

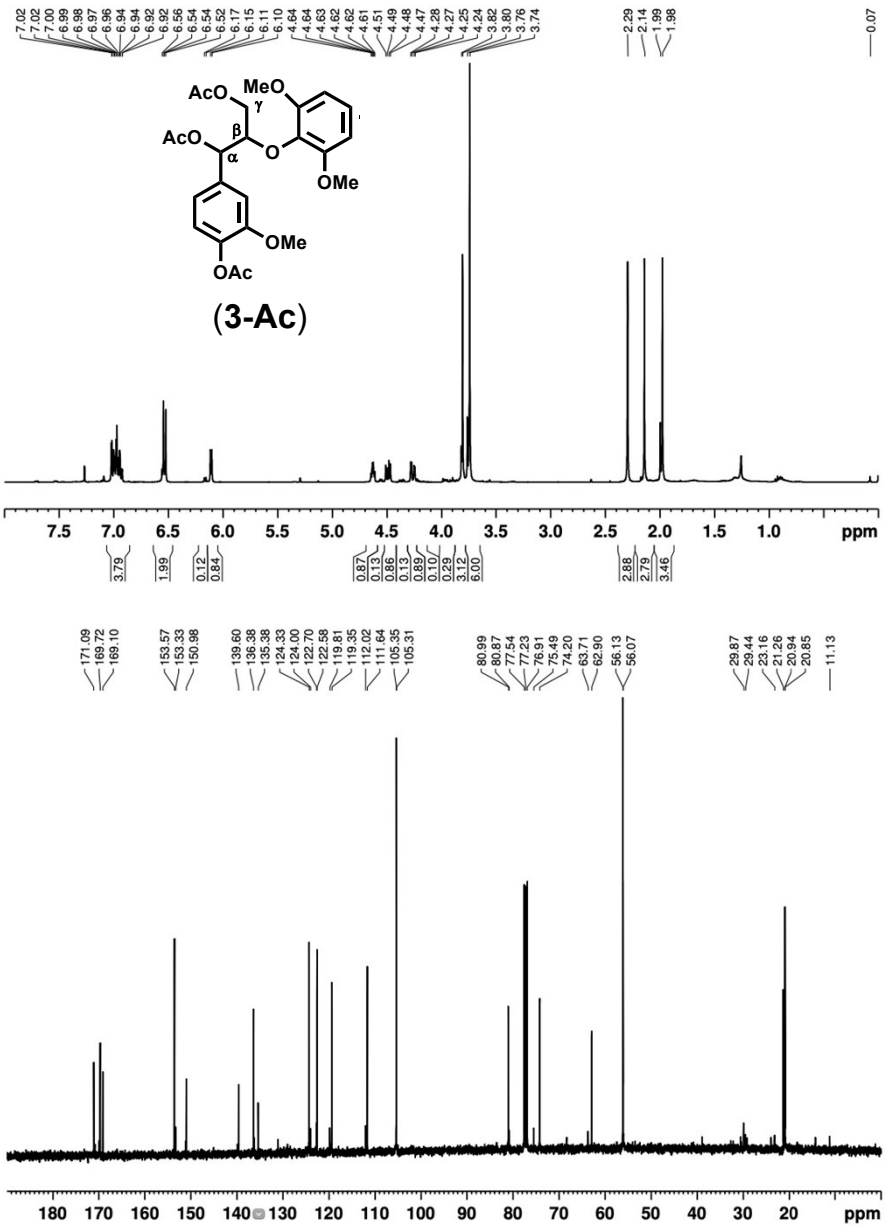

Figure S6.4. ^{1}H and ^{13}C-NMR spectra ($CDCl_3$) of acetylated 2-(2,6-dimethoxyphenoxy)-1-(4-hydroxy-3-methoxyphenyl)propane-1,3-diol (**3**).

Supplementary References

1. de Saint Laumer, J.-Y.; Cicchetti, E.; Merle, P.; Egger, J.; Chaintreau, A., (MRF)Quantification in Gas Chromatography: Prediction of Flame Ionization Detector Response Factors from Combustion Enthalpies and Molecular Structures. *Analytical Chemistry* **2010,** *82* (15), 6457-6462. DOI: 10.1021/ac1006574.
2. de Saint Laumer, J.-Y.; Leocata, S.; Tissot, E.; Baroux, L.; Kampf, D. M.; Merle, P.; Boschung, A.; Seyfried, M.; Chaintreau, A., Prediction of response factors for gas chromatography with flame ionization detection: Algorithm improvement, extension to silylated compounds, and application to the quantification of metabolites. *Journal of Separation Science* **2015,** *38* (18), 3209-3217. DOI: 10.1002/jssc.201500106.

3. Michailof, C. M.; Kalogiannis, K. G.; Sfetsas, T.; Patiaka, D. T.; Lappas, A. A., Advanced analytical techniques for bio-oil characterization. *WIREs Energy and Environment* **2016,** *5* (6), 614-639. DOI: 10.1002/wene.208.
4. Van Aelst, K.; Van Sinay, E.; Vangeel, T.; Cooreman, E.; Van den Bossche, G.; Renders, T.; Van Aelst, J.; Van den Bosch, S.; Sels, B. F., Reductive catalytic fractionation of pine wood: elucidating and quantifying the molecular structures in the lignin oil. *Chemical Science* **2020,** *11* (42), 11498-11508. DOI: 10.1039/D0SC04182C.
5. Anderson, E. M.; Stone, M. L.; Katahira, R.; Reed, M.; Muchero, W.; Ramirez, K. J.; Beckham, G. T.; Román-Leshkov, Y., Differences in S/G ratio in natural poplar variants do not predict catalytic depolymerization monomer yields. *Nature Communications* **2019,** *10* (1), 2033. DOI: 10.1038/s41467-019-09986-1.
6. Yue, F.; Lu, F.; Regner, M.; Sun, R.; Ralph, J., Lignin-Derived Thioacidolysis Dimers: Reevaluation, New Products, Authentication, and Quantification. *ChemSusChem* **2017,** *10* (5), 830-835. DOI: https://doi.org/10.1002/cssc.201700101.
7. Yamamoto, S.; Otto, A.; Simoneit, B. R. T., Lignans in resin of Araucaria angustifolia by gas chromatography/mass spectrometry. *Journal of Mass Spectrometry* **2004,** *39* (11), 1337-1347. DOI: https://doi.org/10.1002/jms.726.
8. Kruger, J. S.; Cleveland, N. S.; Zhang, S.; Katahira, R.; Black, B. A.; Chupka, G. M.; Lammens,T.; Hamilton, P. G.; Biddy, M. J.; Beckham, G. T., Lignin Depolymerization with Nitrate-Intercalated Hydrotalcite Catalysts. ACS Catalysis **2016**, 6 (2), 1316-1328. DOI: https://doi.org/10.1021/acscatal.5b02062
9. Sturgeon, M. R.; O'Brien, M. H.; Ciesielski, P. N.; Katahira, R.; Kruger, J. S.; Chmely, S. C.;Hamlin, J.; Lawrence, K.; Hunsinger, G. B.; Foust, T. D.; Baldwin, R. M.; Biddy, M. J.; Beckham, G. T., *Green Chem.* **2014**, 16, 824-835. DOI: https://doi.org/10.1039/C3GC42138D